D4.2 REPORT ON 6G-NTN RADIO CONTROLLER

First Version

Revision v.1.0

Work package	4
Task	T4.2
Due date	30/06/2024
Submission date	17/07/2024
Deliverable lead	CTTC
Version	1.0
Authors	Husnain Shahid, Miguel A. Vazquez (CTTC) Ji Lianghai, Karthik Anantha Swamy (QCOM), Riccardo Campana, Carla Amatetti, Alessandro Vanelli-Coralli (UNIBO) Li Zheng, Abdelhamed Mohamed Sayed Ahmed, Laurent Reynaud (ORA), NADARASSIN Madivanane (TAS-F)
Reviewers	Sorya Tong, Dorin Panaitopol (Thales SIX) Juan Bucheli (QCOM)
Abstract	This deliverable provides an initial report on 6G-NTN Radio Controller (RC) leveraging the AI/ML aspects to dynamically manage the resource allocation considering the user traffic information and other challenging conditions for the network. The contribution comprises proposing the AI/ML architecture incorporating AI/ML functionalities. Moreover, this report identifies four potential resource network functions to optimize in terms of resources using AI/ML. To accomplish this task, a detailed description of the NTN system is also extracted from D3.2, D3.3, D3.4 and D3.5, useful for system simulations. The utmost section formulates the detailed

Grant Agreement No.: 101096479
Call: HORIZON-JU-SNS-2022
Topic: HORIZON-JU-SNS-2022-STREAM-B-01-03
Type of action: HORIZON-JU-RIA

	problem statements, AI-enabled optimization algorithms and initial insights on optimized outcomes.
Keywords	Radio Resource Management (RRM), RAN Intelligent Controller (RIC), Artificial Intelligence (AI)

Document Revision History

Version	Date	Description of change	List of contributor(s)
V0.1	15/11/2023	ToC modifications	Miguel A. Vazquez (CTTC)
V0.2	18/01/2024	Network Function Defined and ToC Locked	Miguel A. Vazquez (CTTC)
V0.3	06/05/2024	Architecture modifications to make it as baseline	Husnain Shahid (CTTC) Karthik Anantha Swamy (QCOM)
V0.4	23/05/2024	Distributed Architecture Defined	Karthik Anantha Swamy (QCOM)
V0.5	10/06/2024	Release to review	Husnain Shahid (CTTC)
V0.6	20/06/2024	Reviews Received	Sorya Tong, Dorin Panaitopol (Thales SIX) Juan Bucheli (QCOM)
V0.7	26/06/2024	Reviews Addressed	Husnain Shahid (CTTC), Ji Lianghai (QCOM), Riccardo Campana (UniBo), Li Zheng, Laurent Reynaud (ORA), NADARASSIN Madivanane (TAS-F)
V1.0	08/07/2024	Final Reviews Received and Addressed	Carla Amatetti (UniBo) Husnain Shahid (CTTC)

DISCLAIMER

Co-funded by the European Union

6GSNS

Project funded by

Schweizerische Eidgenossenschaft
Confédération suisse
Confederazione Svizzera
Confederaziun svizra

Swiss Confederation

Federal Department of Economic Affairs, Education and Research EAER
State Secretariat for Education, Research and Innovation SERI

6G-NTN (*6G Non Terrestrial Network*) project has received funding from the **Smart Networks and Services Joint Undertaking (SNS JU)** under the European Union's **Horizon Europe research and innovation programme** under Grant Agreement No 101096479. Views and opinions expressed are however those of the author(s) only and do not necessarily reflect those of the European Union. Neither the European Union nor the granting authority can be held responsible for them. This work has received funding from the Swiss State Secretariat for Education, Research and Innovation (SERI).

COPYRIGHT NOTICE

Project co-funded by the European Commission in the Horizon Europe Programme		
Nature of the deliverable:	**Initial Report on 6G-NTN Radio Controller**	
Dissemination Level		
PU	*Public, fully open, e.g. web (Deliverables flagged as public will be automatically published in CORDIS project's page)*	✓
SEN	*Sensitive, limited under the conditions of the Grant Agreement*	
Classified R-UE/ EU-R	*EU RESTRICTED under the Commission Decision No2015/ 444*	
Classified C-UE/ EU-C	*EU CONFIDENTIAL under the Commission Decision No2015/ 444*	
Classified S-UE/ EU-S	*EU SECRET under the Commission Decision No2015/ 444*	

* R: Document, report (excluding the periodic and final reports)

DEM: Demonstrator, pilot, prototype, plan designs

DEC: Websites, patents filing, press & media actions, videos, etc.

DATA: Data sets, microdata, etc.

DMP: Data management plan

ETHICS: Deliverables related to ethics issues.

SECURITY: Deliverables related to security issues

OTHER: Software, technical diagram, algorithms, models, etc.

EXECUTIVE SUMMARY

D4.2 is one of the deliverables of the task T4.2 in work package (WP) 4 of 6G-NTN project which is set to provide an initial comprehensive report on the design of AI-enabled RAN Intelligent Controller (RIC) to effectively manage the resource allocation in Terrestrial Networks (TN) and Non-Terrestrial Networks (NTN). It is envisaged that efficient Radio Resource Management (RRM) has paramount significance in integrated TN-NTN networks to ensure Quality of Service (QoS) requirements and overall system optimization by dynamically allocating the available resources leveraging the challenges such as non-uniform user traffic demand and dynamic user densities as a function of time, and heterogeneous and unpredictable channel conditions etc., just to mention a few. In this context, the urge of adaptive resource allocation given such challenging conditions is significant both in non-Real Time (non-RT) and near Real Time (n-RT) scenarios in order to ensure global coverage, seamless connectivity, and ubiquitous communication requirements.

To this end, this report provides intuition regarding adaptive resource management and allocation where the solution proposed herein covers the broaden domains, spanning from identifying the prospective RIC resource network functions intended to be optimized, to discussing Artificial Intelligence/Machine Learning (AI/ML) architectural aspects. These aspects explore the AI/ML framework deployment scenarios corresponding to these identified network functions and subsequently the discussion expands towards the potential AI/ML optimization algorithms.

In essence, the overall document encompasses five critical elements,

- To be specific at first, the discussion delves into understanding the current AI/ML 3GPP activities. This helps to propose the effective high level architectural aspects to be incorporated in AI-enabled RIC in line with the architecture defined in D3.5.
- Afterwards, in the second element, the efforts are directed towards identifying the potential RIC resource network functions intended to optimize, in particular,
  - Traffic Off-Loading (TOL)
  - Fractional Frequency Reuse (FFR)
  - Traffic Prediction (TP) and NTN Radio Optimization
  - Link Quality Prediction (LQP)
- Considering these resource network functions, one of the sections of this report contributes towards the comprehensive state of the art (SoTA), defining the problem statements and the Key Performance Indicators (KPIs) to be optimized in order to enhance the system performances.
- The fourth element depicts the NTN system description aspects that include user traffic loads in NTN, user spatial distribution, mission definition of overall system. This information is critical and perquisite to train the potential AI-enabled optimization algorithms. The mentioned information is extracted from T3.1 of WP3 where the 3D multilayer NTN architecture is proposed and D4.3 of T4.2 focuses on open datasets.

- The fifth and ultimate element is about the preliminary insights on intended optimization algorithms for optimizing the KPIs of identified resource network functions and alongside offers some initial outcomes as well.

Since D4.2 provides the initial report on the design of AI- enabled RIC, a detailed study on the aspects provided here and the detailed implementation of optimization algorithms is intended to be provided in D4.6.

TABLE OF CONTENTS

LIST OF FIGURES

LIST OF TABLES

ABBREVIATIONS

3D	3 Dimensions
3GPP	3rd Generation Partnership
ABFN	Analogue Beamforming Network
ADRF	Analytics Data Repository Function
AF	Application Function
AI	Artificial Intelligence
AIS	Automatic Identification System
AMF	Access and Mobility Management
AnLF	Analytics Logical Function
APIs	Application Programming Interfaces
ARIMA	Autoregressive Integrated Moving Average
AS	Access Stratum
ASP	Application Service Provider
BER	Bit Error Rate
BFNs	Beamforming Networks
BH	Beam Hopping
BS	Base Station
C/I	Carrier to Interference
CN	Core Network
CNN	Convolutional Neural Network
CSI	Channel State Information
CU	Centralized Unit
DBF	Digital Beamforming
DCCF	Data Collection Coordination Function
DL	Deep Learning
DL	Downlink
DNN	Deep Neural Network
DQL	Deep Q Learning
DRA	Direct Radiating Arrays
DRL	Deep Reinforcement Learning
DU	Distributed Unit
eNA	Enhanced Network Automation
FedDA	Federated Dual Attention Function
FFR	Fractional Frequency Reuse
FL	Federated Learning
FML	Federated Meta-Learning
FR	Frequency Reuse
FR1	Frequency Range 1
FS	Feeder Satellites
FSPL	Free Space Path Loss
GEO	Geostationary Earth Orbit
GNN	Graph Neural Networks
GP	Gaussian Process
HetNets	Heterogeneous Networks
HPLMN	Home Public Land Mobile Network
H-RE-NWDAF	Home Roaming Exchange NWDAF
HO	Handover
IBO	Input Back-Off
ICIC	Inter-Cell Interference Coordination

ISD	Inter-Site Distance
IORs	Inner to Outer Ratios
IoT	Internet of Things
ISL	Inter Satellite Link
KPIs	Key Performance Indicators
LBEF	Load Balancing Efficiency Factor
LBSH	Load Balancing Satellite HO
LCM	Life Cycle Management
LEO	Low Earth Orbit
LMF	Location Management Function
LMMSE	Linear Minimum Mean Square Error
LOS	Line of Sight
LPP	Location and Positioning Protocol
LQP	Link Quality Prediction
LSTM	Long Short-Term Memory
LTE	Long Term Evolution
MADRL	Multi-Agents Deep Reinforcement
MAE	Mean Absolute Error
MDRM	Multi-Dimensional Resource Management
MDAS	Management Data Analytic Service
MDAF	Management Data Analytic Function
MEA	Minimum Elevation Angle
MEC	Mobile Edge Cloud
MEO	Medium Earth Orbit
MIMO	Multiple Input Multiple Out
ML	Machine Learning
MLP	Multi-Layer Perceptron
mmW	Millimeter Wave
MSE	Mean Square Error
MTLF	Model Training Logic Function
n-RT	Near Real Time
NAS	Non-Access Stratum
NEF	Network Exposure Function
NF	Network Function
NRF	Network Repository Function
NGSO	Non-Geostationary Orbit
NG	New Generation
NLOS	Non- Line of Sight
NOC	Network Operations Center
non-RT	Non- Real Time
NR	New Radio
NS-3	Network Simulator 3
NTN	Non- Terrestrial Networks
NW	Network
NWDAF	Network Data Analytics Function
OAM	Operation, Administration, and Maintenance
OFDMA	Orthogonal Frequency Division Multiple Access
OTT	Over-The-Top
PRB	Physical Resource Block
PDU	Protocol Data Unit
PPDR	Public Protection and Disaster Relief

PPO	Proximal Policy Optimization
PS-FFR	Partially Strict FFR
QoE	Quality of Experience
RAAN	Right Ascension of the Ascending Node
RAN	Radio Access Network
RATs	Radio Access Technologies
RE	Radiating Element
RF	Radio Frequency
RIC	RAN Intelligent Controller
RMa	Rural Macro
RNNs	Recurrent Neural Networks
RRC	Radio Resource Control
RRM	Radio Resource Management
RRUR	Radio Resource Utilization Ratio
RSRP	Reference Signal Received Power
RSRQ	Reference Signal Receiver Quality
RSSI	Received Signal Strength Indicator
SARSA	State Action Reward State Action
SD	System Description
S-FFR	Strict FFR
SFR	Soft Frequency Reuse
SNR	Signal to Noise Ratio
SINR	Signal to Interference and Noise Ratio
SLA	Service Level Agreement
SLB	Swap-Based Load Balancing
SMF	Session Management Function
SMS	Short Message Service
SoTA	State of the Art
SS	Service Satellites
TL	Traffic Load
TN	Terrestrial Networks
TOL	Traffic Off-Loading
TP	Traffic Prediction
TWTA	Travelling Wave Tube Amplifier
UDR	Unified Data Repository
UE	User Equipment
UMLB	Utility-Based Mobility Load Balancing
UP	Uplink
UP	User Plane
UPF	User Plane Function
USD	User Spatial Distribution
UTP	User Traffic Pattern
VPLMN	Visited Public Land Mobile Network
V-RE-NWDAF	Visitor Roaming Exchange NWDAF
WGS	World Geodetic System
WG	Working Group
WP	Work Package

1 INTRODUCTION

Before delving into the RAN Intelligent Controller (RIC) functions this deliverable proposes, at first a concise discussion about the overall 6G-NTN (6G-Non-Terrestrial Networks) project objectives that are expected to be accomplished throughout the project duration. This helps to better understand the context and the purpose of this deliverable which provides the initial contribution by designing the Artificial Intelligence (AI)-enabled RIC in the realm of integrated Terrestrial Network (TN) and NTN. Since the inputs are acquired from other work packages to fulfil the design requirements of RIC, this section further extends the discussion by identifying the interconnection of this deliverable with the tasks corresponding to other work packages in order to better understand the correlation among them. In essence, the interconnection is with the use cases already defined in D2.1 [1] and the corresponding open datasets provided in D4.3 [2] that would be utilized to train the AI networks in RIC. Subsequently, the overall organization of the document is illustrated.

1.1 GOALS OF 6G-NTN PROJECT:

The broad ambition of the 6G-NTN project is the full integration of NTN component into future 6G infrastructure which allows to meet consumer expectations in terms of performance and integrity enhancement, seamless connectivity in mobility, resilience in service corresponding to traffic variations etc. This part of the deliverable briefly discusses the potential goals and ambitions of 6G-NTN in a more technical way that are expected to be executed during the project duration. The potential objectives of the project are the following:

- The identification and proposal of use cases as potential candidates of 6G-NTN.
- Defining the user and technical requirements of 6G-NTN project.
- Designing 3D (multidimension) multilayered architecture comprised of interconnected terrestrial nodes, space nodes and airborne flying nodes.
- Designing more effective terminals in terms of cost, size and power consumption which would be compatible to operate with both TN and NTN access.
- Designing the flexible software defined payload intended to optimize the platform and payload resources.
- Designing and evaluation of flexible waveform using data-driven approaches. The flexibility is in terms of supporting terrestrial and non-terrestrial deployments and extends the capability of coverage into light indoor environment.
- Development of AI-enhanced RIC to provide effective Radio Resource Management (RRM) solutions, considering the multi-frequency, multi-constellation, and TN-NTN connectivity aspects to foster the high availability values and heterogenous traffic demand. D4.3 is one of the contributions to the critical design of RIC [2].
- Another aspect is evaluating the interference scenarios and their impact on radio access network. Based on the impact, spectrum management techniques will be proposed.
- Taking into account the latency requirements defined in Work Package 2 (WP2), another aim is to define the accurate and reliable Position and Timing solutions for 6G-NTN. In addition, it will define the enhanced NTN-UE positioning mechanism for regulated services.
- Providing virtualized and cloud native architectures for 6G core network. The objective is also to define the open interfaces and APIs to configure, monitor and orchestrate the NTN edge and core networks.

- In addition, based on the assessment of cybersecurity threats and vulnerabilities for 6G-NTN, there is a need to provide solutions to counter these vulnerabilities. In this regard, a goal is to propose solutions relying on cloud native architecture and open interfaces mainly focused on securing the communication scheme.
- The final objective is to develop solid strategic approaches for effective communication, dissemination and community building at European, national, and international levels. This includes the engagement and coordination with the target stakeholders from mobile, satellite and vertical industries having an interest in taking up the 6G-NTN technologies and concepts as developed.

1.2 CONTEXT

The efforts to efficiently utilize the resources in NTN are becoming a priority and requiring attention, both in non-Real Time (non-RT) and near Real Time (n-RT) scenarios. It is vitally important to enhance overall system performance while providing reliable and cost-effective services. The significance of this requirement arises for the multi-orbital and multi-band satellite integrated networks that introduce complexities due to the variability of satellite links, non-uniform user traffic demand, dynamic user densities with time, and heterogenous channel conditions etc. Classical and heuristic Radio Resource Control (RRC) approaches may struggle to adopt this heterogeneous nature effectively. Also, the system related constraints and the number of resources to manage at the larger scale, the classical methods exhibit limited efficacy in addressing these complexities, thus leading to sub-optimal solutions and degraded performance. In this context, AI-driven approaches hold significant potential as a key contributor to resource optimization process. Therefore, D4.2 is explicitly focused on providing the inputs to one of the objectives of 6G-NTN project in terms of performing the initial contribution on designing the AI enabled intelligent radio resource controller for the use cases, particularly: maritime, Public Protection and Disaster Relief (PPDR), and direct to handheld, identified as defined in D2.1[1]. The aim is to investigate the specific potential resource network functions in RIC to perform the resource allocation optimization, as described in later sections in detail.

1.3 PURPOSE

In point of fact that efficient RRM has paramount significance to ensure Quality of Service (QoS) requirements and overall system optimization by dynamically allocating the available resources considering the aforementioned challenges. Those QoS requirements become even more stringent particularly due to ever growing user demands, global coverage, seamless connectivity, and ubiquitous communication requirements. These requirements might be fulfilled to a great extent by the intelligent decision-making capabilities of RRC, capable of continuously analyzing network conditions, learning and identifying complex patterns and features to enhance overall network performance.

To this end, this deliverable provides an initial contribution towards AI- enabled RIC capable of optimizing the RMM in integrated TN-NTN framework. In particular, the focus relies on identifying the potential resource network functions, for instance,

- **Traffic Off-Loading (TOL):** to balance the load between TN and NTN depending on the dynamic user traffic i.e. by off-loading traffic to NTN. This impacts as increasing QoS during high network load conditions and a reduced TN energy consumption when the traffic request is lower.
- **Fractional Frequency Reuse (FFR):** FFR in multibeam satellite system aims to maximize the overall offered system capacity and the spectrum utilization. This

resource network function leverages the dynamic user traffic demand and density information as a function of time.

- **Traffic Prediction and NTN Radio Optimization:** Considering the full integration between TN and NTN and the latency constraints for many potential services, the future traffic volume and trends prediction in different sub-networks or geographical areas will facilitate the proactive planning for scaling the network infrastructure. This also involves optimizing the resources accurately by implementing AI/ML-based RRM leveraging the traffic information to cater for the diverse traffic demands and varying quality of service requirements in a real-time fashion.

➲ **Link Quality Prediction:** A distinguishing characteristic of NTN is the fast movement of Low Earth Orbit (LEO) satellites, which necessitates frequent satellite-switching by a UE. To serve the UE continuously during the switch, online radio measurement procedure in the legacy solution may cause certain inefficiencies and bottlenecks, such as power consumption, spectrum usage, potential service interruptions due to measurement gaps, early coordination at network side. Thus, to improve the efficiency during NTN mobility, an AI-based mechanism is considered to predict the UE's radio channel condition in the time-and-spatial domain to overcome the aforementioned inefficiencies.

The proposed resource network functions are set to be thoroughly investigated from the architectural aspects, to identify the appropriate AI-enabled algorithms in optimizing the overall resource management. Moreover, it is evident that the AI paradigm heavily relies on the availability of large and diverse data to effectively learn from the variable environment. Therefore, the real-world datasets offered in D4.3 [2] and some other datasets leveraging the realistic representation are utilized for training the AI algorithms in the aforementioned resource network functions.

1.4 D4.2 RELATION TO OTHER WORK PACKAGES IN 6G-NTN

The dependencies of all work packages (WP) on each other are illustrated in **Figure 1-1**. This deliverable is one of the tasks of WP4 related to 6G-NTN Radio Access Technologies (RATs). It requires to take inputs from the tasks of other WPs and similarly provides outputs to accomplish the other WPs.

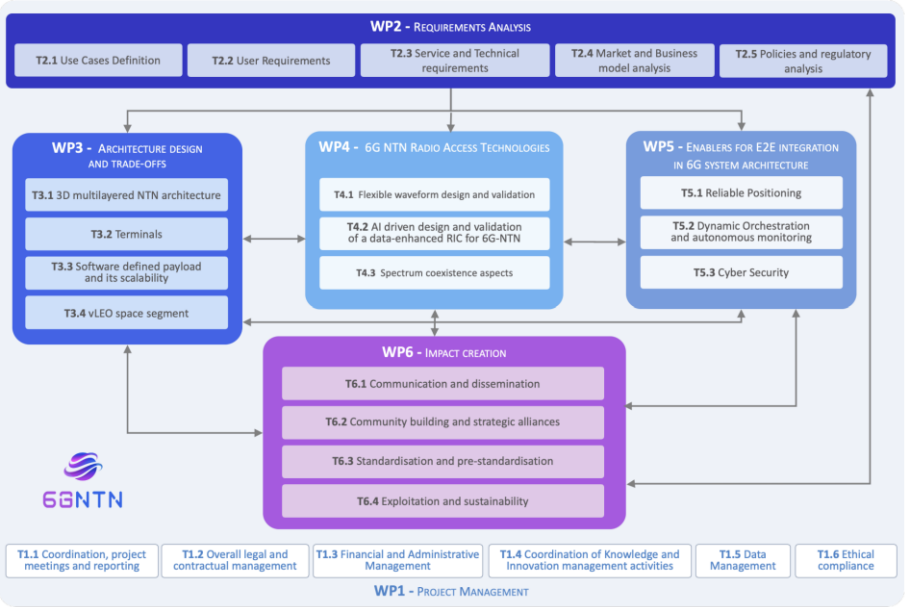

FIGURE 1-1: 6G-NTN OVERALL WORK PACKAGES ORGANIZATIONS AND THEIR DEPENDENCIES

The organization of deliverable D4.2 with other defined tasks are explicitly given as,

- D4.2 is dependent on the inputs from the task T2.3 of WP2 (Requirements Analysis), related to the provision of service and technical requirements. The T2.3 contributed with the User Traffic Pattern (UTP) values which would be utilized along with open datasets of D4.3 to perform the management of NTN resources for defined use cases.
- D4.2 might be incorporating 3D multilayered NTN architecture investigated in T3.1, specifically in D3.5 [3] in order to identify the options for deploying the NTN RIC and the overall system description.
- D4.2 would contribute to dissemination task T6.1 of WP 6 (Impact Creation) by publishing the work related to RIC in international conferences, workshops, and journals.
- A subset of the outcomes of D4.2 will be developed into a higher TRL in WP5.

The apparent connection of D4.2 with the tasks of other WPs can be seen in **Figure 1-2**.

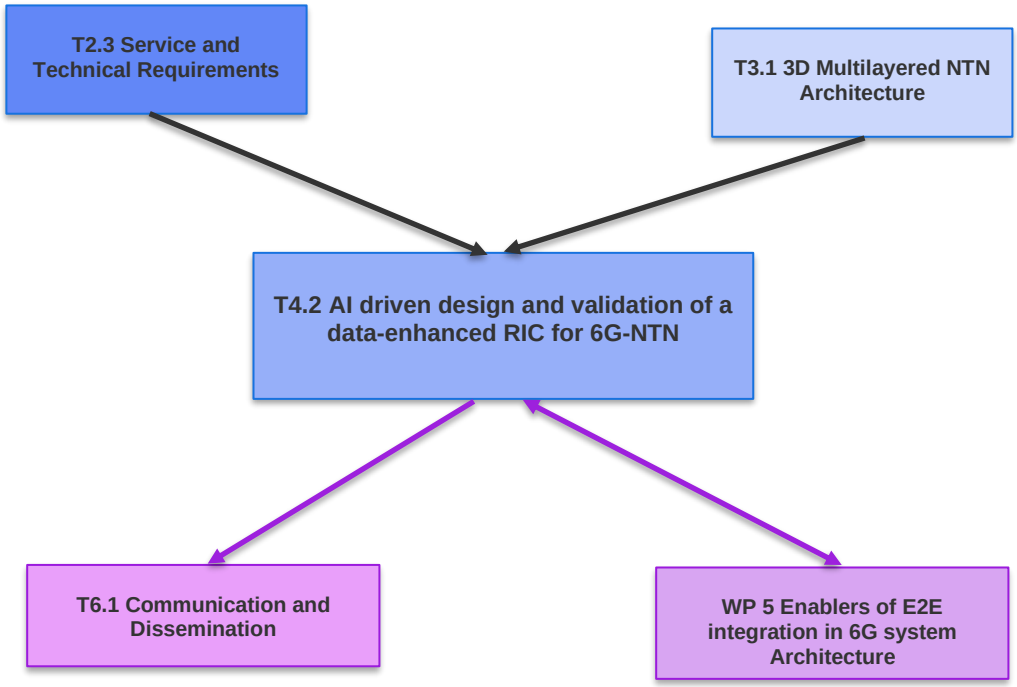

FIGURE 1-2: *THE ASSOCIATION OF TASK D4.2 WITH THE TASKS OF OTHER WPS IN 6G-NTN PROJECT*

1.5 ORGANIZATION OF THE DOCUMENT

The organization of this document is as follows:

Section 2 offers deep insights into the architectural aspects of data enhanced radio resource control. In this context, at first, it covers the broadened view of current 3GPP activities on AI/ML in the framework of TN. In particular, it comprises the discussion of AI/ML for air interface, AI/ML for Next-Generation Radio Access Network (NG-RAN), and AI/ML for 5G Core components. Afterwards, the discussion revolves on proposing a base AI/ML architecture to handle the AI functions. Following this, the efforts extend towards defining AI integrated architectural aspects for each identified network function individually that provide information about how and where the model training, testing and deployment of agents will be performed.

Section 3 details each resource network function, for instance, Traffic Off-loading, Fractional Frequency Reuse, Traffic Prediction and NTN Radio Optimization, and Link Quality Prediction. Primarily, the efforts are made on comprehensively discussing the state of the art (SoTA) for each network function. This requires identifying the gaps in the solution used in literature and then proposing robust solutions to bridge those gaps accordingly. In the following part, the importance is given to elaborate the problem statements and the KPIs for each function.

Section 4 is about the provision of System Description (SD) for NTN systems. In essence, NTN system description provides the antenna definition for C and Q/V bands, Traffic Load (TL) for direct to device or Public Protection and Disaster Relief (PPDR) use cases, and User Spatial Distribution (USD). The TL and USD are directly acquired from D4.3. This provided SD is primordial in simulating the system environment while enabling the AI-based RRM.

Section 5 provides an initial version of potential AI/ML based optimization algorithm intended to be utilized for optimizing each resource network function. This includes the initial insights on algorithm details and the corresponding initial outcomes.

Section 6 draws the conclusion of this deliverable.

2 ARCHITECTURE FOR DATA-ENHANCED RADIO CONTROL

This section initially presents a comprehensive overview of current AI/ML activities in 3GPP focusing on TN. It primarily focuses on the discussion of AI/ML for air interface, AI/ML for NG RAN, and AI/ML for 5G Core components. Alongside, the architectural aspects of network functions are presented, which provide the depiction about the data processing framework within the context of AI/ML. Then, we introduce a proposed evolved architecture for 6G-NTN, taking into account the recent architecture description in WP3 and the data-enhanced network functions which show promise for NTN. Finally, we describe these network functions.

2.1 CURRENT AI/ML ACTIVITIES IN 3GPP

In this subsection, we provide an overview of the 3GPP activities on AI/ML. It should be noted that the legacy 3GPP work has mainly focused on AI/ML for TN so far, i.e. not NTN-specific consideration yet.

2.1.1 AI/ML for Air Interface

3GPP Rel-18 studied AI/ML for NR air interface, e.g. to identify common notation and terminology for AI/ML related functions, procedures, and interfaces. This subsection provides a high-level summary on the study outcome captured in TR 38.843 [4].

2.1.1.1 Life Cycle Management

Different life cycle management (LCM)-related aspects of AI/ML have been studied in Rel-18, that include data collection, model training, functionality/model identification, model deployment, model inference, model monitoring, model updating, UE capability.

In particular, both model-ID-based and functionality-based LCM have been considered to ensure an aligned understanding of the considered model by the Network (NW) and UE, where the model-ID-based LCM relies on the model ID to identify an AI/ML model during LCM, e.g. to activate/deactivate/fallback/switch an AI/ML model, while the functionality-based LCM relies on the associated AI/ML-enabled feature enabled by configuration. It is noted that in the functionality-based LCM, NW may not be able to identify the AI/ML model used by the UE for the considered AI/ML functionality. In addition, the following aspects have been studied:

- The need for UE to report a subset of (updated) applicable functionality(es)/model(s) after functionality/model identification.
- An AI/ML model may be associated with specific configurations/conditions associated with UE capability of an AI/ML-enabled Feature and additional conditions (e.g., scenarios, sites, and datasets).
- How to handle UE's limitation/condition on AI operation, e.g. w.r.t. UE memory, battery, and other hardware limitations

It is noted that LCM can include scenarios for which the management decision (e.g., (de)activation, selection, switching, fallback, etc.) is taken by the network or by the UE. For network-side decision, this can be either network-initiated, or UE-initiated and requested to the network. While for UE-side decision, this can be either event-triggered as configured by the network and where the UE's decision is reported to the network, or UE-autonomous, with or without UE's decision being reported to the network.

Model Identification

The identification of an AI/ML model can be categorized based on if over-the-air signaling is needed for identifying the model. In one example, without over-the-air signaling, the model may be assigned with a model ID during the model identification, which may be referred/used in over-the-air signaling after the model identification, e.g. referred as Type A in Rel-18. In another example, model identification may take place with the over-the-air signaling during the model transfer from NW to UE, e.g. referred as Type B in Rel-18.

Additional Conditions

In Rel-18, additional conditions (e.g. scenarios, sites, datasets, dynamic conditions) refer to any aspects that are assumed for the training of the model but are not a part of UE capability, and it can be divided into NW-side additional conditions and UE-side additional conditions. The additional conditions have an impact on the applicable model. In Rel-18, different options have been proposed to be taken as the potential approaches to ensure consistency between training and inference regarding NW-side additional conditions for the UE-side model inference.

Scenario/Configuration-specific models

To achieve a good AI/ML performance, there may be a need for generalizing AI/ML models, e.g. by considering different scenarios and/or different configurations.

If a single model cannot generalize well to multiple scenarios/configurations/sites for an AI/ML use case, it may be beneficial to consider scenario/configuration-specific models:

- This approach may require model delivery/transfer to the UE, e.g. if the UE has limited storage.
- It may also require switching a scenario/configuration-specific AI/ML model, such that the particular scenario/configuration can be properly handled.
- An alternative to model delivery/transfer for scenario/configuration-specific models is to consider on-device fine-tuning/retraining/updating.

Data Collection

Data collection is considered as needed for different procedures/purposes in AI/ML, e.g. model training, model inference, model monitoring, model selection, model update. However, it is noted that different latency requirements may be imposed regarding the data collection for different purposes. In one example, a low latency may be needed for model inference and (real-time) performance monitoring, but not for offline model training.

Though the AI/ML algorithm is not to be specified by 3GPP, the corresponding procedures to collect the necessary data for different LCM purposes should be considered by 3GPP with potential spec impacts. The corresponding specification impact may include, e.g.:

- Measurement configuration and reporting.
- Content, type and format of data, e.g. model input or ground truth.
- Assistance information for categorizing the data, and the corresponding signaling procedure for data collection.

It is noted, the study outcome in TR38.843 [4] also includes a table listing the existing data collection methods with some related details, where the existing data collection methods may be re-used for data collection by the corresponding NW entity in a considered AI/ML use case.

For NW-side data collection, certain aspects have to be considered:

- UE to support data logging.
- UE to report the collected data periodically, event-based, and on-demand.
- The UE memory, processing power, energy consumption, signaling overhead.
- Which entity to manage the data collection procedure, e.g. to initiate/terminate the data collection procedure from the other entities.

For UE-side model training, different data collections have been proposed during Rel-18:

- UE collects and directly transfers training data to the Over-The-Top (OTT) server.
- UE collects training data and transfers it to Core Network. Core Network transfers the training data to the OTT server.
- UE collects training data and transfers it to Operation, Administration and Maintenance (OAM). OAM transfers the needed data to the OTT server.

Collaboration Levels

During Rel-18 study, the collaboration between UE and NW is categorized into three levels:

- Level x: No collaboration i.e. referring to implementation-based only AI/ML algorithms without any specification impact.
- Level y: signaling-based collaboration without model transfer. In one example, model delivery in Level y can be done in an over-the-top manner.
    - Note: this level includes cases without model delivery
- Level z: signaling-based collaboration with model transfer. More specifically, compared to Level y, the model delivery over the air interface in Level z is done in a non-transparent manner to 3GPP signaling.

In addition, the model delivery aspect has also been studied in Rel-18, such as:

- The format used for model delivery, the storage location of the model, and the corresponding location.
- Impact of transferring a model with known structure vs. unknown structure.
- Usage and advantage of offline compiling and testing.
- Impact of multi-vendors.

Functional Framework

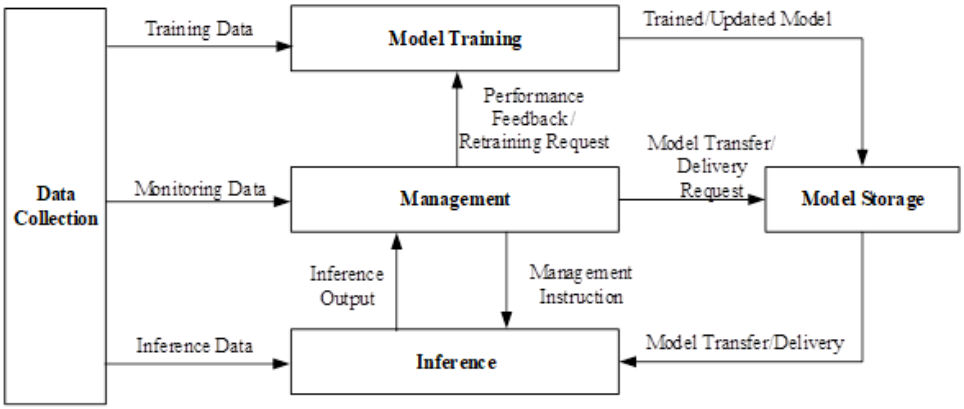

FIGURE 2-1: FUNCTIONAL FRAMEWORK FOR AI/ML FOR NR AIR INTERFACE [4].

The functional framework concluded in Rel-18 is shown in **Figure 2-1**, with more illustration details of each functional block and the data flows captured in TR 38.843 [4]. Please note that this figure does not pose any restriction on the actual deployment location of a functional block in the practical system.

Model Transfer/Delivery

It should be noted that, per Rel-18 study, there is no conclusion regarding the need for standardized solution(s) to transfer/deliver AI/ML model. However, following solutions have been considered:

- Solution 1a: gNB can transfer/deliver AI/ML model(s) to UE via RRC signaling.
- Solution 2a: Core Network (except location management function (LMF)) can transfer/deliver AI/ML model(s) to UE via non access stratum (NAS) signaling.
- Solution 3a: LMF can transfer/deliver AI/ML model(s) to UE via location and positioning protocol LPP signaling.
- Solution 1b: gNB can transfer/deliver AI/ML model(s) to UE via User Plane (UP) data.
- Solution 2b: Core Network (except LMF) can transfer/deliver AI/ML model(s) to UE via UP data.
- Solution 3b: LMF can transfer/deliver AI/ML model(s) to UE via UP data.
- Solution 4a: OTT server can transfer/deliver AI/ML model(s) to UE (e.g., transparent to 3GPP).
- Solution 4b: OAM can transfer/deliver AI/ML model(s) to UE.

The different solutions have been analysed in Rel-18, by accounting for their impacts on limitation on model transfer/delivery size, continuity of model transfer/delivery (e.g. considering UE mobility across gNBs), NW controllability on model transfer/delivery, and QoS.

2.1.1.2 Use Cases

In Rel-18, three use cases are proposed as an initial set for being considered to study and develop a comprehensive AI/ML framework, which may be reused or considered as a foundation for supporting other potential AI/ML use cases in future:

Channel State Information (CSI) Feedback

- Sub use case 1: Spatial-frequency domain CSI compression to reduce the overhead for transmitting the CSI feedback from UE to NW
    - Two-sided AI model is used, which includes an AI/ML-based CSI generation part to generate the CSI feedback information and an AI/ML-based CSI reconstruction part which is used to reconstruct the CSI from the received CSI feedback information.
    - At least for inference, the CSI generation part is located at the UE side, and the CSI reconstruction part is located at the gNB side.
    - Different options for the considered AI/ML model training collaboration in the two-sided model listed below and their corresponding pros and cons are discussed in Rel-18
        - Type 1: Joint training of the two-side model at a single side/entity, e.g., UE-side or Network-side.
        - Type 2: Joint training of the two-side model at network side and UE side, respectively.
        - Type 3: Separate training at network side and UE side, where the UE-side CSI generation part and the NW-side CSI reconstruction part are trained by UE side and network side, respectively.

- Sub use case 2: Time domain CSI prediction to avoid outdated CSI,

    - Focusing on the UE-side model in Rel-18.

    - Inference input includes the UE's historical CSI measurements, while the output includes a prediction of future CSI information.

Beam Management

Following sub use cases have been considered to mitigate the problems experienced in the legacy beam management procedure, e.g. to reduce the amount of transmitted reference signals and/or to reduce the latency of finding a suitable beam (pair) by the UE:

- Sub use case 1: Spatial-domain Downlink beam prediction for Set A of beams based on measurement results of Set B of beams, where Set B can either be different from Set A or be a subset of Set A
- Sub use case 2: Temporal Downlink beam prediction for Set A of beams based on the historic measurement results of Set B of beams. In this sub use case, Set A and Set B can be different, or Set B can be a subset of Set A, or Set B can be the same as Set A.

In the beam management sub use cases described above, Set B is a set of beams whose measurements are taken as inputs of the AI/ML model. It is noted that there may be different alternatives to be considered as the output of the AI/ML model inference, e.g. Layer-1 (L1) Reference Signal Received Power (RSRP) prediction of one or multiple top predicted beams, IDs of one or multiple top predicted beams. In addition, the model training and the model inference in this use case can be performed at UE or NW. In case the model inference takes place at NW side, the UE has to send its (historical) measurements over Set B of beams to the NW.

Positioning

This use case aims at improving the accuracy of positioning. It can be noted that with the legacy 5G NR positioning technology, the accuracy of the geometry-based positioning mechanisms highly relies on the availability of the line-of-sight path. Thus, in scenarios with heavy non-line of sight (NLOS) conditions (e.g. indoor factory), the positioning accuracy may degrade, and AI/ML can be used for improvement.

Along with the Rel-18 study, two sub use cases have been selected:

- Direct AI/ML positioning, which generates UE location as the AI/ML model output.
  - AI/ML model output: UE location.
  - AI/ML model input example: fingerprinting based on channel observation.
- AI/ML assisted positioning:
  - AI/ML model output: new measurement and/or enhancement of existing measurement.
  - AI/ML model input example: LOS/NLOS identification, timing and/or angle of measurement, likelihood of measurement

2.1.1.3 Standards Impact

The work in Rel-18 also points out the aspects that may potentially have specification impact, which will be discussed and standardized in future releases, e.g. different procedures on LCM, dataset collection for training/validation/test, collaboration specifics such as signaling, assistance information, model identification/transfer/applicability, measurement configuration/report, and feedback. Some details are listed below on the specific impact considerations:

Data collection

- Which data is needed for AI/ML operation, e.g. input, output, feedback?
- New measurement configuration and report procedure/content for data collection.
- Data collection at UE side may be either requested by UE or indicated by NW. Note: assistant information may be needed during data collection for categorizing the data.
- At NW, for NW-side AI ML model inference, different data can be considered and collected, e.g. either by NW itself or from UE.
- How to reduce the overhead for NW side data collection, e.g. selection or compression of the collected data?
- For NW-side data collection, which entity initiates and terminates the data collection procedure via which procedure/protocol?
- For UE-side model training, how does the UE transfer its collected data to the OTT server.
- The association between data collection and additional conditions. In one example, additional conditions may need to be considered for the positioning use case.
  - Which aspects should be considered as conditions/additional conditions?

- In beam management use case, if and how NW indicates the association between beams in Set A and beams in Set B to the UE for UE-side AI/ML model.
- Transfer of the assistance information between NW and UE, e.g.
  - Transfer UE-side assistance information for NW-side AI/ML model inference:
    - UE location.
    - UE moving direction.
    - UE Rx beam shape/direction.
  - Transfer NW-side assistance information for UE-side AI/ML model inference:
    - NW-side beam shape information.
- How to generate and collect the ground-truth label, e.g. in the positioning use case.

Performance Monitoring

- How to perform monitoring of an active model/functionality, e.g. based on what information, and which entity should perform the monitoring?
- In some cases, legacy behavior may be used as a reference, where intermediate and/or system KPIs can be considered as a metric for evaluation.
- For performance monitoring, an association between AI/ML scheme and the reference scheme may be included.
- For performance monitoring, consider to select/define/configure proper performance metric(s), a proper reference mechanism for comparison, and the corresponding signaling/configuration/measurement/report
  - Note: There can be multiple performance metrics and reference mechanisms that can be considered as alternatives for a considered use case
- How to support the following performance monitoring types and the corresponding impacts, e.g. on configuration and procedure, performance metric, UE report type:
  - **Type 1:** UE monitors and determines functionality fallback/switch/activation/deactivation/selection based on NW configuration.
  - **Type 2:** NW monitors and determines functionality fallback/switch/activation/deactivation/selection based on UE data reporting.
  - **Type 3:** UE monitors but NW determines functionality fallback/switch/activation/deactivation/selection based on UE reporting performance.

- In a considered use case, an indication/request/report from UE to gNB may be considered for performance monitoring, wherein the indication/request/report triggers NW to configure the UE for performance monitoring and/or reporting.

LCM

- How to assess the performance of an inactive model/functionality and what is the information needed for that purpose, e.g. in order to determine a model for activation/selection/switching?
- Which entity should make the LCM decision, e.g. model/functionality activation/ deactivation/updating/switching, based on the performance monitoring?
- How to support co-existence and fallback between AI/ML approach and the legacy non-AI/ML approach.
- Signaling procedures for LCM, for different scenarios where the management decision may be taken by either NW or UE.
- Dataset delivery from UE/NW to NW/UE during the separate sequential training with the two-side model, in the CSI compression use case.
- The relation between the CSI configuration from NW and the CSI payload in the report from UE, in the CSI compression use case.
- Alignment between the UE-side model and the compatible NW-side model, in the CSI compression use case.
- The approach to support model transfer/delivery.
- UE capability report, e.g. to indicate the UE's supported AI/ML-enabled feature/feature group.
- UE reporting/indicating the relevant information of its supported AI/ML model/functionality to NW, where the relevant information may indicate, e.g. under which condition(s) a model/functionality is applicable/suitable, or whether model(s)/functionality(ies) are (non)applicable under the current context.

2.1.2 AI/ML for NG-RAN

3GPP Rel-17 studied the essential enhancements and high-level principles needed to improve RAN intelligence by AI/ML, and the study item output is captured in TR 37.817 [5]. Later on, based on the study item, corresponding enhancements are further discussed, developed, and specified in 3GPP Rel-18. In this subsection, a brief overview is provided.

It is noted, this work is sometimes referred to as AI/ML for NG-RAN in 3GPP RP-220635 [6] , and the work is largely conducted by 3GPP RAN3 Working Group (WG).

2.1.2.1 Relevant scope

In the Rel-18 normative work, 3GPP has specified data collection enhancements and signaling support over current NG-RAN interfaces and architecture for the following reference RAN functions:

- Load Balancing

- Mobility Optimization
- Network Energy Saving

The above-listed reference RAN functions can benefit from the capabilities of AI/ML, e.g. to take account of more data inputs, to achieve a system level solution, and to obtain predictions.

It is noted, both the split architecture (e.g. gNB DU-CU split) and non-split architecture were under the initial plan for Rel-18 investigation. However, at the end of Rel-18, only the non-split architecture has been specified for supporting AI/ML in NG RAN.

2.1.2.2 Functional Framework

Figure 2-2 illustrates the functional framework defined in 3GPP for AI/ML in NG RAN, where the detailed definition of each functional block is provided in TR 37.817 [5].

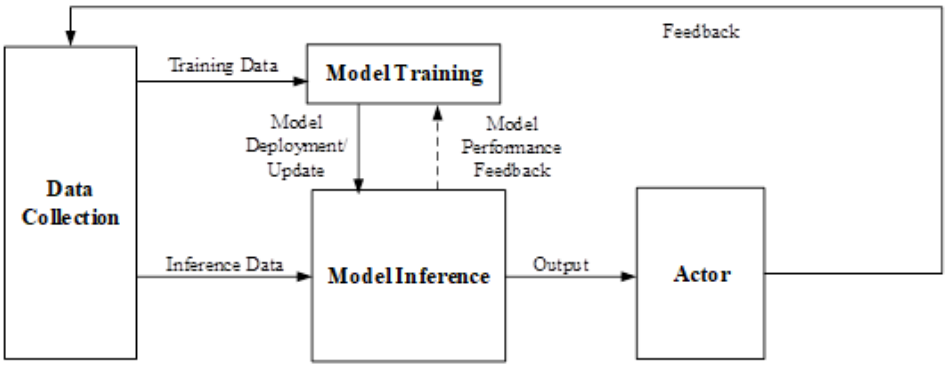

FIGURE 2-2: FUNCTIONAL FRAMEWORK DEFINED IN TR 37.817 [5]

It should be pointed out that the AI/ML algorithm/model itself is not specified by 3GPP and should be implementation specific. As mentioned before, one focus of 3GPP's work is how to enable data collection and exchange among the different functional blocks, where the data can be composed of different data types such as input data (e.g. data used for model training/inference), output data (e.g. the output of model inference) and feedback (e.g. feedback data).

By mapping the AI/ML functional block to different NW entities properly, Rel-18 has considered a distributed architecture as well as a centralized architecture, based on where the inference and training take place:

- Distributed architecture
    - Inference in NG-RAN
    - Training in either OAM or NG-RAN
- Centralized architecture
    - Training and inference in OAM

It is noted, in one example, that an NG-RAN node may be a gNB, which is interacted with and managed by the OAM entity. In addition, the distributed architect has been the main focus of the 3GPP in RAN3 so far, compared to the centralized architecture that will be mainly studied in SA5.

2.1.2.3 Standards Impact

The data collection and corresponding signaling is performed between two NG-RAN nodes, e.g. between two gNBs via Xn interface. In details, two procedures have been specified to enable an NG-RAN node to collect either one shot or periodic reporting from the other NG-RAN node in TS 38.423 [7]:

- Data collection reporting initiation procedure - used by an NG-RAN node to start information reporting or to stop information reporting from another NG-RAN node, in order to support AI/ML in NG-RAN.

- Data collection reporting procedure – used by an NG-RAN node to report information accepted by the NG-RAN node following a successful Data Collection Reporting Initiation procedure.

It is noted, the procedures above are data type-agnostic. In other words, the same procedure can be used to collect data, no matter whether the data is considered as input data, output data, or feedback data. In the signaling/message supporting these procedures, the data type of the collected data (i.e. the intended use of the data) will not be explicitly indicated and, thus, it is up to implementation regarding how such a collected data should be used. In one example, a collected data may be considered as both an output data (e.g. inference output from one AI/ML algorithm for generating prediction) and an input data (e.g. inference input for another AI/ML algorithm by using the generated prediction). Since AI/ML is promising in prediction, the collected data from the reporting NG-RAN node can be a prediction data associated to a prediction time, which is indicated in the data collection request message by the collecting NG-RAN node, e.g. during the data collection reporting initiation procedure.

2.1.2.4 Solutions for the Investigated Use Cases

It is noted, the high-level procedures and signaling flows for the three reference use cases are captured in TR 37.817 [5], with respect to both the distributed and centralized architecture options. Here, only the signaling flows for the distributed architecture are cited in **Figure 2-3**, **Figure 2-4**, and **Figure 2-5**, as the examples for illustration. Please refer to TR 37.817 [5] for additional information on Rel-17 study item outcome. It is further noted, 3GPP did not specify the NW actions to be taken based on the AI/ML model inference output, and the corresponding NW actions in practice will be implementation specific.

Load Balancing

The task of load balancing is to balance the load among neighboring RAN nodes, such that the (potential) traffic congestion in a particular node can be mitigated. In one example, a congested RAN node may decide to hand over a UE and its traffic to another neighboring RAN node.

As seen from **Figure 2-3**, in AI/ML-based load balancing, a RAN node may need to collect certain measurement data from the UE to derive its own condition/statistics as well as certain input data from another neighboring NG-RAN node. According to the current 3GPP design, the data collection from the UE can leverage any legacy UE report procedure(s) such as Minimal Driving Test (MDT), while the data collection from another neighboring NG-RAN node can be performed by using the data collection procedures described in section **2.1.2.3**. In more details, the following information at cell level have been agreed by 3GPP, and they may be collected from their own cell as well as the neighbor cell(s) and used by an AI/ML functional block for load balancing:

- Predicted Radio Resource Status.
- Predicted Number of Active UEs.
- Predicted RRC connections.
- Average UE Throughput Downlink (DL).
- Average UE Throughput Uplink (UL).
- Average Packet Delay.
- Average Packet Loss.

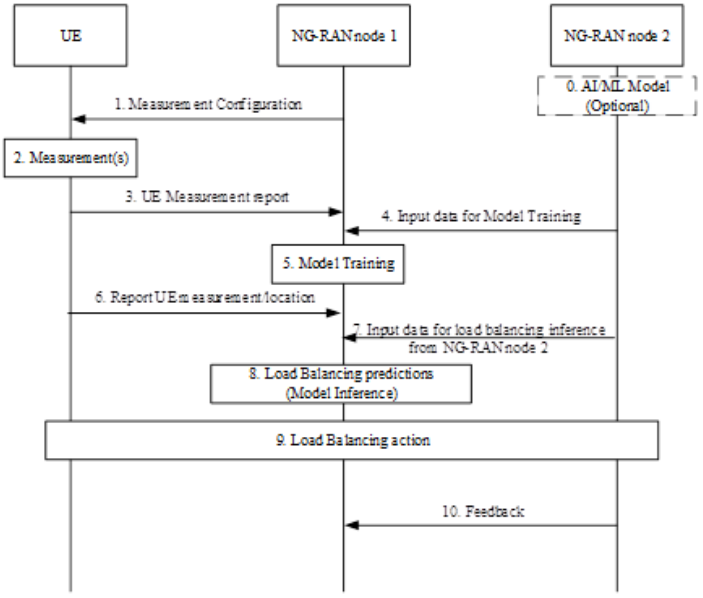

FIGURE 2-3: LOAD BALANCING WITH BOTH MODEL TRAINING AND MODEL INFERENCE IN NG-RAN, DEFINED IN TS 37.817 [5].

Mobility Optimization

Mobility optimization can be used to improve the UE performance during the UE's movement, e.g. to optimize the handover procedure (e.g. to select proper (candidate) target cell(s)) and to avoid a handover failure.

As seen from **Figure 2-4**, the signaling flow is very much similar to the load balancing solution shown in **Figure 2-3**. In addition, all the information listed for the load balancing solution are also available and applicable for collection and use by AI/ML for mobility optimization. However, 3GPP introduced some additional information to be considered for mobility optimization:

- Predicted UE trajectory, which contains a list of NG-RAN cells where the UE is predicted to connect.
- Predicted time duration that the UE is expected to stay in the predicted cell.
- Feedback for UE trajectory prediction after the UE's mobility event (e.g. handover), such as a list of cells in which the UE actually moved and the time that a UE stayed in the cell

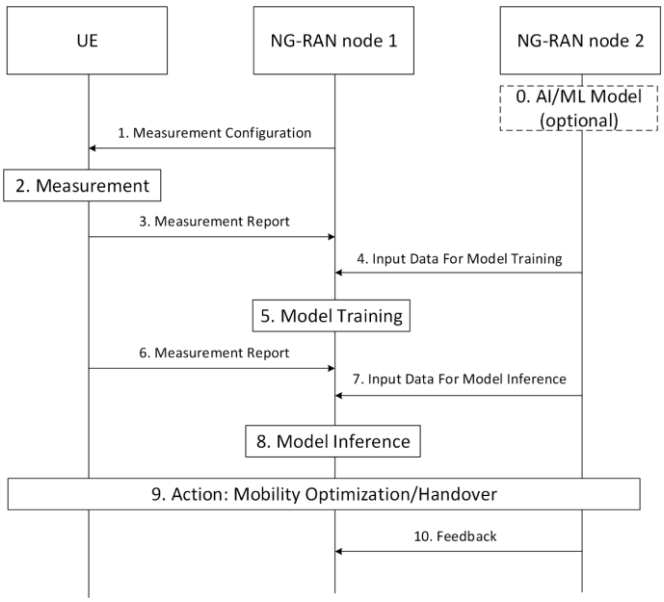

***FIGURE 2-4**: MOBILITY OPTIMIZATION WITH BOTH MODEL TRAINING AND MODEL INFERENCE IN NG-RAN, DEFINED IN TS 37.817 [5].*

Network Energy Saving

This technology targets at reducing network energy consumption, e.g. by offloading UE(s) to another cell and/or activating/deactivating a cell.

Regarding the parameters/information used for network energy saving, energy cost is the only metric that is specific for this use case, on top of the other metrics introduced for load balancing and mobility optimization. It is noted that the energy cost is a NG-RAN node level information, instead of cell level information. The signaling flow is shown in **Figure 2-5**

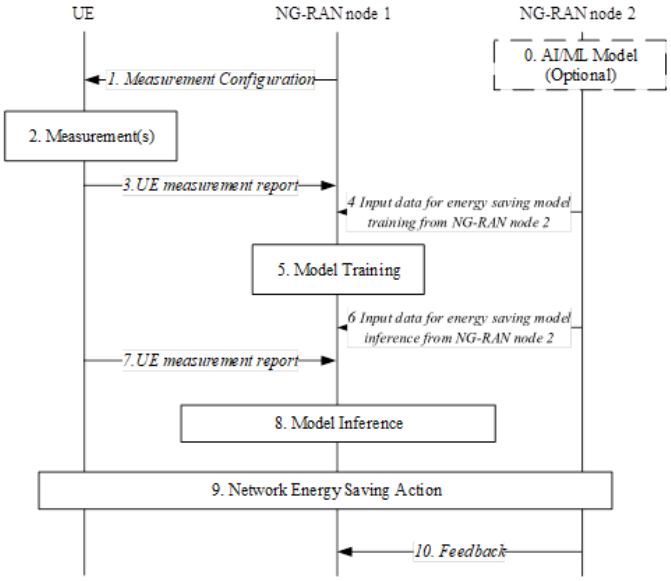

***FIGURE 2-5**: NETWORK ENERGY SAVING WITH BOTH MODEL TRAINING AND MODEL INFERENCE IN NG-RAN, DEFINED IN TS 37.817 [5]*

2.1.3 AI/ML in 5G Core

2.1.3.1 enhanced Network Automation (eNA)

This work is sometimes referred to as enhanced Network Automation (eNA) in 3GPP, and it is mainly conducted by 3GPP SA2 WG. The fundamental architecture can be summarized below:

- Network Data Analytics Function (NWDAF) is used to host analytics and model training for other Network Functions (NFs), e.g. to generate statistical data about the past or future.

- Data used by NWDAF may be collected and provided by NFs of 5GC (e.g. AMF, SMF. UDR, NEF), AF, OAM and data repository.

- NWDAF exposes its analytic service and the service outcome to NFs of 5GC, AF, and OAM, in an on-demand fashion. Based on the analytics outcome exposed from NWDAF, the NF can adapt its behavior to optimize the performance of communication network.

It is noted that NWDAF was first introduced in 3GPP Rel-15 to be responsible for operator-managed NW analytics with a limited number of supported use cases (e.g. to analyze network slice load level), which are further extended in the later releases of 3GPP.

Moreover, based on the 3GPP design in Rel-17, analytics and model training in NWDAF may contain two logical functions:

- An Analytics Logical Function (AnLF), which performs inference and exposes its analytics services.

- A Model Training Logic Function (MTLF), which trains ML models and exposes the training services to an AnLF.

Thus, based on the implementation choice, an NWDAF may contain an AnLF, an MTLF, or both AnLF and MTLF. And an NWDAF containing AnLF may discover an NWDAF containing MTLF by using Network Repository Function (NRF).

To avoid duplicated data (e.g. raw data or analytics data) transmission in the 5GC, Data Collection Coordination Function (DCCF) can be deployed and used to coordinate the data requests (e.g. from multiple data consumers) and avoid collecting the same data from the same data source for multiple times. Thus, a data consumer may send its request for data to DCCF instead of data source, and the DCCF determines if the requested data has been collected before and arranges the data delivery accordingly.

Rel-17 design also allows the network to collect relevant UE data for AI/ML operation. In a bit more details, the UE may set up a Protocol Data Unit (PDU) session to the data collection Application Function (AF) located in the operator's network, wherein the PDU session can be used to collect the UE's data via user plane. This user plane solution would require a Service Level Agreement (SLA) between the operator and the Application Service Provider (ASP), such that the ASP can interact with the UE for configuring the data collection from the UE to the operator's data collection AF. With the collected UE's data, NW may optimize its behaviour to better support the UE's communication service(s), correspondingly.

In Rel-18, 3GPP further studies and specifies additional enhancements on the AI/ML operation in 5GC, e.g.:

- To improve the correctness of NWDAF analytics, e.g. by collecting and leveraging analytics feedback.
- Data and analytics exchange in roaming case, e.g. by allowing an NF in the HPLMN/VPLMN to collect data from VPLMN/HPLMN, respectively, via H-RE-NWDAF in HPLMN and V-RE-NWDAF in VPLMN.
- To enhance Data collection and Storage, e.g. to enable ML model storage, removal, and retrieval by Analytics Data Repository Function (ADRF).
- To enhance trained ML Model sharing, e.g. by introducing an ML Model Interoperability indicator for a considered NWDAF containing MTLF, wherein the ML Model Interoperability indicator comprises a list of NWDAF providers (vendors) that are allowed to retrieve ML models from this NWDAF containing MTLF.
- To support Federated Learning in 5GC, where multiple NWDAFs can perform federated learning in a decentralized manner without exchanging or sharing their local data set.
- To support NWDAF to interact with Management Data Analytic Service (MDAS)/Management Data Analytic Function (MDAF) for obtaining management data analytics generated by MDAS/MDAF

The corresponding outcome of Rel-18 study is captured in TR 23.700-81[8].

2.1.3.2 System Support for AI/ML-Based Services

It is noted that 3GPP in Rel-18 has also worked on how to support application-layer AI/ML services. Comparing to other AI/ML studies/work in 3GPP to improve NW automation and communication performance, the AI/ML services in this work considers how the 5GS supports the transmissions of AI/ML-based services over the application layer (such as download, upload, updates, etc.) and identifies traffic characteristics of the AI/ML model distribution, transfer and training for various applications. The intent of this study is to focus on 5GS architectural and functional extensions so that service providers can leverage 5GS as the intelligent transmission platform to support AI/ML-based services SP-220071[9].

The corresponding study outcome is capture in TR 23.700-80 [10], which covers multiple key issues, such as:

- To enable the AF to require QoS for a list of UEs within a multi-member AF session and to monitor their QoS performance, e.g. for federated learning operation.
- To support external parameter provisioning, e.g. from AF to NF, such as application-specific expected UE behavior parameters.
- To enable application AI/ML traffic transport, such as for AF to negotiate with NW for a Planned Data Transfer with QoS requirements (PDTQ).

- And to support federated learning operation, e.g. such that NW may derive and indicate a list of candidate UEs that are suitable for federated learning to the corresponding AF.

2.2 6G-NTN ARCHITECTURE ASPECTS

After the profound discussion on current AI/ML activities in 3GPP, this section primarily extends the analysis by proposing a high-level architecture design incorporating AI/ML aspects in 6G-NTN to support the network functions. The idea herein is to propose a baseline architecture model ensuing the architecture insights from D3.5 [3] and then integrating the deployment of an AI/ML-friendly architecture to manage the different AI/ML functions, for instance, data collection, model training, model storage, model inference, and management etc. Afterwards, following the baseline paradigm, each resource network function defines their own architecture requirements and characteristics on deploying the AI/ML building blocks depending on the network function instance.

2.2.1 Architecture Design for AI/ML in 6G-NTN

2.2.1.1 Conventional Architecture

The AI/ML architecture framework designed in Rel-18 AI/ML for air interface, as shown in **Figure 2-1**, is taken as the baseline to design the AI/ML conventional architecture (term used in D3.5). Additional details are provided subsequently.

In this context, it is proposed to deploy an AI/ML server to manage the different AI/ML functions e.g. data collection, model training, model storage, model inference, and management. In this case, the interaction between the UE and the AI/ML server can be performed over the U-plane. In one example, a PDU session can be established between the UE and the AI/ML server for an interactive AI/ML procedure as shown in **Figure 2-6** and, such as:

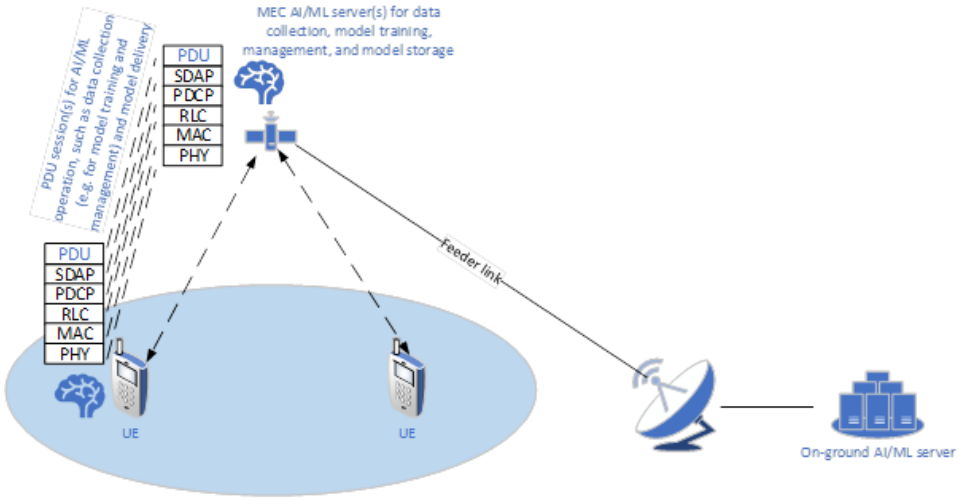

FIGURE 2-6: ILLUSTRUTION OF HOW THE UE CAN INTERACT WITH THE MEC AI/ML SERVER IN U-PLANE

- Collecting data from the UE by the AI/ML server as a data repository, e.g. for model training/retraining, and performance monitoring

- In principle, the data collection function may be considered and designed as a general function in 6G NTN, where AI/ML operation is only one place to use the collected data. Thus, the collected data can be also used by other non-AI/ML operations in 6G NTN, e.g. a NW node may request data from the data collection server, in order to adjust the NW's behavior and configuration without using AI/ML.

➲ Transferring/delivering a trained/retrained model from the AI/ML server to the UE.

➲ Configuring the UE to perform model inference by the AI/ML server.

➲ Sending management/LCM instruction from the AI/ML server to the UE, e.g. to activate/deactivate/switch an AI/ML model.

It is noted, instead of using one single AI/ML server, multiple servers may be implemented and used for different AI/ML functions, where each server handles a particular AI/ML function and interacts with other servers based on the need. For example, the data collection function and the model training function can be managed by two different servers, where the model training server can fetch its needed model training data from the data collection server. In addition, in this example, the UE may set up multiple PDU sessions towards different servers, where different PDU sessions handle different AI/ML functions. Alternatively, the UE may use a single PDU session to connect to a single logic server or a server proxy, which is responsible for distributing/aggregating the different UE's flows to/from different physical servers, where the different UE flows may correspond to the data for different AI/ML functions.

It is further noted, besides interacting with the UE, the AI/ML server can also be used to interact with a NW node such as a gNB or a CN entity, e.g. for collecting data from the NW node, for transferring model and sending management/LCM instruction to the NW node.

In addition, to reduce the traffic transmitted over the feeder link as well as the additional latency caused by the feeder link for running certain AI/ML procedures, it is proposed to deploy Mobile Edge Cloud (MEC) AI/ML server(s) onboard satellite(s) for different AI/ML functions, e.g. data collection, model training, management, and model storage. In case multiple onboard MEC AI/ML servers are used, each of them can handle a particular function. In this proposal, to support deploying an MEC AI/ML server onboard the satellite, at least the complete U-plane protocol stacks may be required to be deployed in-space. As one example, **Figure 2-6** illustrates how the UE and the MEC AI/ML server can interact with each other via a PDU session. As shown in the same figure, the satellite needs to be equipped at least with the complete Access Stratum (AS) U-plane protocol stacks of a gNB, a User Plane Function (UPF), as well as the MEC AI/ML server. The established PDU session is also used for the connection between the UE and the on-ground AI/ML server, though it is not shown in the figure for simplicity.

It is noted that an AI/ML server can also be deployed on the ground, where the on-ground AI/ML server can communicate and collaborate with the MEC AI/ML server(s) onboard the same or different satellites. For example:

➲ The MEC AI/ML server can be used for managing an AI/ML function in a local area covered by the associated satellite, e.g. by interacting with the UEs served by the associated satellite and the NW nodes carried in the associated satellite.

➲ The on-ground AI/ML server may coordinate multiple MEC AI/ML servers and the corresponding operation of their AI/ML function(s). In addition, the on-ground AI/ML server may also act as an interface to interact with other on-ground NW nodes.

In addition, an AI/ML function managed and coordinated by the on-ground AI/ML server and/or the MEC AI/ML server may be designed to involve other physical entities, e.g. UE, NW. For example:

- A collected data from the UE/NW may be generated and stored locally at the UE/NW, without being transferred to a central AI/ML server.
- A model may be trained at the UE/NW, based on the configuration/instruction from the AI/ML server. In one example, to protect the privacy of the UE/NW and/or offload the computation at the AI/ML server, the UE/NW may perform model training based on the local stored data.
- Model inference may be configured by the AI/ML server to be performed at the UE/NW, e.g. based on the local generated data, to speed up the inference procedure.
- After a trained/updated model is received from the model storage entity by the UE/NW, the UE/NW may store it, even after the model is deactivated. This allows the UE/NW to reuse the stored model in the future, without the need to download it from the model storage entity again.
- UE/NW may be configured to perform model management by the AI/ML server. For example, the UE/NW may be configured to monitor the model performance based on the data generated in real time, such that a fast LCM procedure can be achieved if needed.

More details for this proposal are provided below for the proposed MEC AI/ML server(s) to handle different AI/ML functions. It is also worth noting that satellite mobility needs to be accounted in this proposal, since switching between satellites for continuously serving a considered area may imply a relocation of the onboard MEC AI/ML server from one satellite to another, e.g. as shown in **Figure 2-7**. In **Figure 2-7**, the outgoing satellite and the incoming satellite correspond to the satellite stops serving the considered area and the satellite starts serving the considered area, respectively, due to the movement of satellites.

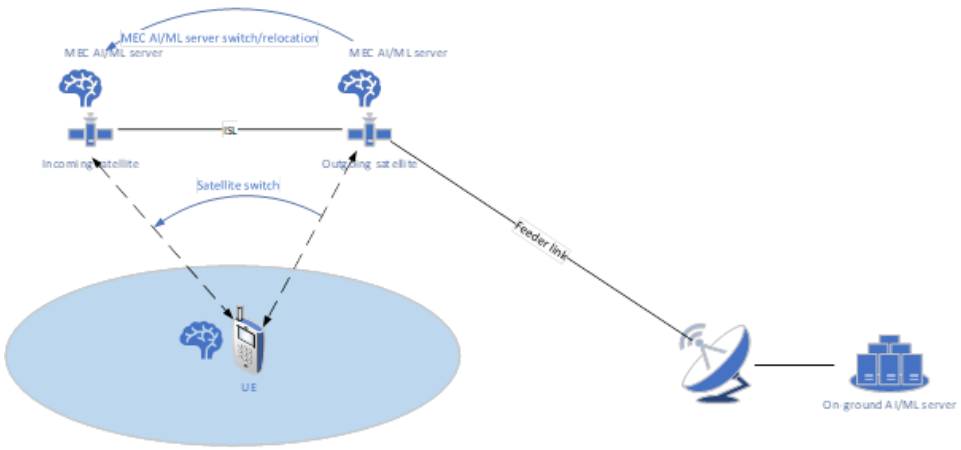

FIGURE 2-7: SWITCHING THE SERVING SATELLITE FOR A CONSIDERED AREA IMPLIES A RELOCATION OF THE MEC AI/ML SERVER FOR THE CONSIDERED AREA

Thereupon, AI/ML functions specified according to the proposed architecture are studied as,

- On data collection function:
  - UE's data can be collected by the MEC AI/ML server directly from the UE via service link in U-plane via a PDU session and the collected data can be used at least for local optimization. For the purpose of reducing traffic load of feeder link, it is preferred not to transmit some collected data, e.g. model training data, to the ground NW, e.g. to the on-ground AI/ML server. In this case, the data can be processed onboard the satellite by the MEC AI/ML server.
  - For the data collected from a NW node such as gNB:
    - If the data is generated from the ground segment (e.g. the satellite information generated by the space control center), the on-ground AI/ML server can be used to collect the data. Afterwards, depending on if the data is needed by the MEC AI/ML server, the on-ground AI/ML server can push the data towards the MEC AI/ML server, which can further forward the data to other MEC AI/ML server(s) located in other satellite(s) via Inter Satellite Link (ISL).
    - If the data is generated in the space, e.g. by the satellite(s) and its onboard gNB(s), such as handover performances by using the AI/ML-based channel estimation/prediction, the data can be collected by the MEC AI/ML server directly from the in-space NW node. Furthermore, if needed, the collected data can be shared/transferred to the on-ground AI/ML server or the MEC AI/ML server in another satellite, e.g. the incoming satellite.
  - Collected data may be stored in the UE and/or the NW. In this case, the UE/NW may be configured by the AI/ML server to initiate the data collection procedure as well as to inform the AI/ML server regarding the data collection status, e.g. if the data has been collected and stored in the UE/NW. Furthermore, MEC AI/ML may instruct data transfer from the UE/NW to an AI/ML function, e.g. Model training/inference/monitoring.
  - In order to handle the satellite mobility, the collected data and the corresponding data collection context can be transferred from the MEC AI/ML server in the outgoing satellite to the MEC AI/ML server in the incoming satellite, e.g. via ISL, such that they are always available and managed by the MEC AI/ML server serving the corresponding data collection area.
- On model training:
  - A model can be trained/retrained/updated locally at the MEC AI/ML server and optionally at the UE connected to the MEC AI/ML server, which avoids sending the training data to the on-ground AI/ML server.
  - The model trained by the MEC AI/ML server onboard a satellite may be considered and used as a location-specific AI/ML model. Thus, different MEC AI/ML servers with different serving areas may apply different location-specific AI/ML models for the same AI/ML function. In this case, there may be a need for switching the model by LCM, e.g. when a high mobility UE moves from one area to another.
  - If a model is needed for being applicable in a global/larger area, e.g. in an area covered by multiple satellites and the associated multiple MEC AI/ML servers, federated learning may be applied where each of the multiple MEC AI/ML servers trains its local model and sends the trained model to the on-ground AI/ML server for creating the global model. In this way, a global model can be obtained without the need of transferring the in-space data to the on-ground AI/ML server.
  - Due to satellite mobility, the context for AI/ML model training function and the trained model(s) for a considered local area may be transferred from the

outgoing satellite to the incoming satellite, e.g. via ISL, such that the model training function is always maintained in the satellite and its onboard MEC AI/ML server that serves the considered local area.

- On management:
  - It is proposed to move at least part of the management function from the on-ground AI/ML server to the MEC AI/ML server. For example, a particular management procedure may require a low latency, in order to achieve a fast action/adaptation and ensure the system performance. Thus, with the management function running at the edge, it can generate management instructions in a faster manner compared to the on-ground AI/ML server. As one example, if an abnormality is detected by the MEC AI/ML server and/or the UE based on the monitoring data, the UE and/or the NW can be immediately configured to fall back to the legacy solution or to switch to another AI/ML model. In another example, if a management function only uses the data generated and stored locally in the MEC AI/ML server, it may be also preferred to consider the MEC AI/ML server for that management function.
  - It is noted, gNB may need to interact with the UE closely in some cases, e.g. in the proposed AI/ML-based channel estimation/prediction mechanism where gNB may need to know if and which AI/ML model is applied. Thus, there is at least a need for gNB to be aware if and when the AI/ML model is activated/deactivated/switched. In this case, if the management function is handled by the MEC AI/ML server, it would be preferable to have the gNB's RRC entity onboard the satellite, such that the MEC AI/ML server can communicate with the gNB's RRC entity located in the same satellite directly, to reduce latency of the management procedure.
  - To handle satellite switch caused by mobility, the context of management function needs to be transferred from the MEC AI/ML server in the outgoing satellite to the MEC AI/ML server in the incoming satellite.
- On model storage:
  - A trained/retrained model by the model training entity can be stored at the onboard model storage entity managed by the MEC AI/ML server(s). Thus, the model storage entity can be constructed by the AI/ML management function to transfer/deliver the trained/retrained model to a UE over the service link directly. It is noted, the proposed AI/ML server for AI-related management and model storage enables the use of a multicast/broadcast PDU session to multicast/broadcast the trained/retrained model to a group of UEs over the service link, which can further reduce the NTN resource usage for transferring/delivering the model to multiple UEs.
  - In addition, the trained model can be further transmitted from the MEC AI/ML server to the on-ground AI/ML server. In this case, the on-ground AI/ML server may use the models obtained from different MEC AI/ML servers to obtain a global model by federated learning. Moreover, the on-ground AI/ML server may also store the trained model, which can be fetched by MEC AI/ML server(s) if needed, e.g. by the incoming satellite and MEC AI/ML server if ISL is not available.
  - The trained model from one MEC AI/ML server can also be transmitted to other MEC AI/ML server(s) located on other satellite(s), e.g. the incoming satellite via ISL. This would allow to maintain the model trained by using the data obtained from a local geographic coverage area in the satellite and in the corresponding MEC that are responsible for the servicing of the local area.
- On inference:
  - The MEC AI/ML server can configure the model inference. In one example, the MEC AI/ML server can determine whether the model inference should take

place in the UE, a NW node, at the MEC AI/ML server itself, or a combination thereof. In another example, the MEC AI/ML server can also determine and configure to activate or deactivate model inference at the corresponding entity(s). In case multiple AI/ML models exist for an AI/ML feature, the MEC AI/ML server can also determine which particular AI/ML model to use based on the instruction generated by the management function.

Thus, as mentioned before, in order to handle the satellite mobility in NTN, a virtual MEC AI/ML server concept is proposed to keep the AI/ML context (e.g. collected data, trained model, management/LCM policy, etc.) locally above a considered area, by transferring the local AI/ML context (e.g. data, model, management) from the outgoing MEC AI/ML server to the incoming MEC AI/ML server, e.g. via ISL and/or feeder link. One important task for the on-ground AI/ML server is to coordinate different in-space physical infrastructures for realizing the virtual MEC AI/ML server concept. As illustrated, the proposed architecture allows an AI/ML vendor to implement an AI/ML feature over the top of the 3GPP network in 6G NTN.

2.2.1.2 Distributed Architecture: Initial Insights

In a satellite network with distributed-architecture (term used in D3.5), the satellites are categorized into service satellites (SS) and feeder satellites (FS). A SS is devoted to UE-connectivity and does not a have a feeder-link. On the other hand, a FS contains a feeder link, but not a service link. Up to 4 SSs connect to a single FS, and FSs are inter-connected. Typically, there are fewer FSs, on a possibly different constellation, than SSs. This way, link-capacity on service and feeder sides are expected to be de-coupled to a certain degree as proposed in D3.5 [3] which provides further details on this architecture.

This architecture offers greater flexibility in the design of the corresponding AI/ML operations in this system. For instance, while the MEC-servers may still be associated with SSs, their AI/ML functionality can be made very lean by restricting it to essentials such as UE data-collection, model-transfer, and UE-configuration triggers. More intensive functionality such as inference and storage may well be handled by AI/ML servers on the FSs. Partial functionality of the ground-servers may also be shifted onto the FSs. These aspects could be optimized based on location-specific demands and other network capacity constraints.

Furthermore, if the FSs are designed to be at a higher altitude than the SSs, their relative slowness can be effectively used during context transfer between outgoing and incoming satellites via the FSs. Model inference may even be improved in the distributed architecture because a FS connects to multiple SSs and simultaneous fusing of location-specific user-data would be valuable for network optimization.

Disclaimer: Further detailed insights into the analysis and design of AI/ML aspects for the distributed architecture are planned to be detailed in D4.6, which is dedicated to focus on the final report on 6G-NTN RIC.

Thereafter, the resource network functions intended to be optimized are proposed. On an individual basis, these network functions explicitly provide the operational descriptions and define their own AI/ML architecture within the aspects of deploying AI/ML server following the baseline AI/ML architecture design proposed in **Section 2.2.1** for 6G-NTN. The potential resource network functions in this initial report are as follows.

2.3 6G-NTN RIC NETWORK FUNCTIONS

2.3.1 Traffic Off-Loading

2.3.1.1 High-Level Description

In modern mobile cellular systems, a dense network of cells is deployed to provide connectivity to a demanding number of users. However, the mobility of User Equipment (UE) leads to a disparity in the load across the network cells, affecting the Quality of Service (QoS) for UEs and resulting in inefficient resource utilization. Additionally, the demand for high data rates by UEs and the non-uniform distribution of UEs exacerbate resource overutilization in certain cells. To address these challenges, it is necessary to distribute the workload evenly across cells, thereby ensuring efficient resource utilization. To this aim, different cell-load balancing techniques are developed in terrestrial networks, which aims to equally distribute the load among cells to maintain a satisfactory end-user experience and efficient network operation.

In some scenarios, UEs may be unable to transition to neighboring cells due to resource scarcity and limited coverage. This constraint impedes efficient load balancing among cells and diminishes the quality of service for users. Leveraging NTN, the load can be balanced not only between TN cells, but also between TN and NTN, adding a second plane of load balance optimization. In this context the quality of service of TN can be enhanced by off-loading some traffic to the NTN, increasing the overall network throughput and resource exploitation. The optimal assignment of UEs to TN or NTN is a demanding task that must be performed in a centralized entity based on the network status information collected from UEs and cells.

2.3.1.2 Architectural Aspects

The reference architecture for the traffic off-loading network function is shown in **Figure 2-8** The reference architecture for the Traffic-Offloading network function is described below. TN is composed of a set of three-sector cells. The NTN is composed of a satellite generating a single NTN beam with overlapped service area with TN and complementing its service. TN and NTN are served by the same core network and by the same AI/ML server. The data that must be collected by the AI/ML server to perform model training and inference is listed in **Table 1**.

Due to the coordination nature of this network function, training, storage, and inference of the AI/ML service should reside in centralized AI/ML servers that can be either located in the same or in different nodes of the network. From **Table 1**, it is clear that the majority of the data that must reach the AI/ML server is produced on-ground. Thus, to minimize the average latency of the delivery of the data in the system and the load on the transport network the AI/ML servers should be located on-ground.

More precisely, the traffic off-loading network function should manage the AI/ML functions in the following ways.

Model Training:

- The model training/retraining/updating for AI/ML-based load balancing should take place in an on-ground AI/ML server exploiting collected data.
- The AI/ML models are trained on data originating from the same area where they are going to be deployed, learning the optimal behavior for the specific location, and supporting the location specific A/ML model functionality. The trained model can be shared and transferred to multiple AI/ML servers located in different areas to be exploited for retraining.

- A model could be trained to gain global applicability exploiting offline federated learning and gathering data from the complete network.
- Online model retraining or updating can be a valuable strategy, particularly for scenarios where dynamic information that wasn't captured during offline training needs to be incorporated, or when the model needs to adapt to evolving environmental conditions. This approach involves refining an initial AI/ML model that was trained through offline methods, enabling it to accommodate real-time changes and adjustments.
- The AI/ML server can apply offline training to obtain an initial AI/ML model based on the data collected from the network.

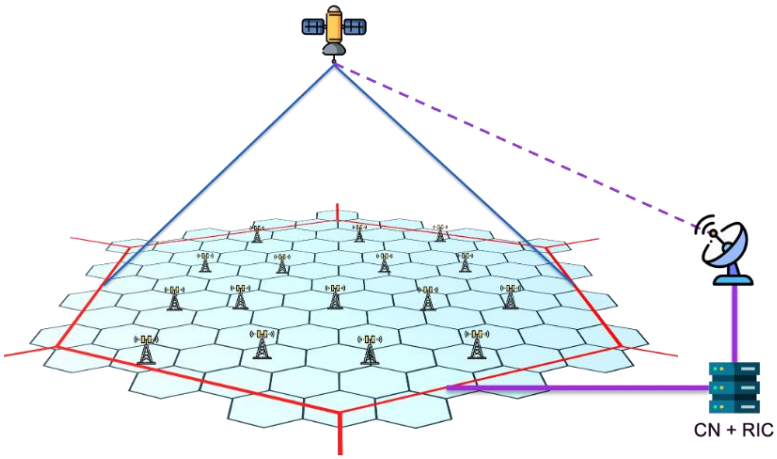

FIGURE 2-8 THE REFERENCE ARCHITECTURE FOR THE TRAFFIC-OFFLOADING NETWORK FUNCTION

Model Storage

For traffic off-loading network function, the model will be stored in the AI/ML servers located on-ground and near to the location for which the model has been trained and in which it will be exploited. A network trained for global applicability could be stored also in a geographically centralized AI/ML server.

Model Inference

The model inference will be performed at the on-ground AI/ML server. Indeed, the majority of the input data is produced in the ground network and the majority of RAN nodes using the inference output are on-ground. Moreover, the inference of a large AI/ML model is a computationally intensive task that is not easily deployable on a resource limited satellite.

Data Collection

The data listed in **Table 1** is explicitly being considered to support AI/ML model training and inference for traffic off-loading network function.

TABLE 1. INPUT DATA TO PERFORM MODEL TRAINING AND INFERENCE IN TRAFFIC OFF-LOADING

Collected data	Source	Distribution network	Usage
UEs SINR measurements	UE	Ground network	

UE's location	UE	Ground network	Input to training input to management
UE's service requirements	UE	Ground network	
TN cells resource allocation	TN cell	Ground network	
NTN cell resource allocation	Satellite	Feeder link	
Satellite ephemeris	Satellite	Feeder link	

2.3.2 Fractional Frequency Reuse in NTN

2.3.2.1 High-Level Description

The ever-growing demand for communication services is coming up with the immense challenge of utilizing the limited spectrum resource efficiently in both terrestrial and non-terrestrial networks.

One major challenge in satellite communication is inter-beam interference, which appears when a certain frequency bin is reused among the coverage area. Taking this constraint into account, it is very likely that the users end up using the same frequency bands in adjacent cells or beams which results in co-channel interference. In essence, this results in complications to meet the quality of service (QoS) requirements. In order to combat these challenges at network level, a variety of Inter-Cell Interference Coordination (ICIC) solutions have been developed for terrestrial networks.

Firstly, from the perspective of terrestrial cellular networks, Frequency Reuse (FR) schemes have been widely adopted especially in Heterogeneous networks (HetNets) where different cells overlaid within the main cell and utilize different frequency resources to mitigate the co-channel interference. These have been found as viable solutions to enhance the overall system performance. In the context of FR-n, where n = {1,2,3…N} is the frequency color scheme in FR, for instance, when n=3, each of the three adjacent cells utilizes frequency bands orthogonal to the frequency bands of each other. Although this can alleviate the intercell interference, it comes with the cost of extreme spectral inefficiency since the available bandwidth is not being fully utilized and thereby impacts the system throughput. Considering that problem, FR can be further categorized as Fractional Frequency Reuse (FFR) where further different orders of FR schemes are used within different regions of each cell. However, FFR framework when split into higher orders arises with a trade-off, for instance, using the higher order of FFR further increases the interference but utilizes the available spectral resources in a better way, whereas using the lower order FFR reduces the interference but with the cost of system spectral resources. To be specific, the popular FFR techniques being reported are the Strict FFR and Soft FFR as shown in **Figure 2-9**.

The strict FFR utilizes the FFR-1 in the central region of cells and for instance FFR-3 at the cell edge since the cell center users (near the Base Station) are not severely impacted by the interference due to strong desired signal. Thus, it is more advantageous for cell center users to share the bandwidth with other cell center users in the adjacent cells. In contrast, users in

cell edge region are exposed to more interference, hence use FFR-3 where three adjacent cell-edge regions use orthogonal frequency resources as shown in **Figure 2-9** (left). On the contrary, to better utilize the bandwidth resources, Soft FFR could be used which uses FFR-3 or more in the cell edge region as in Strict FFR, while the cell center shares the frequency bands from the adjacent cell edge regions instead of using totally orthogonal frequency resources. This leaves more bandwidth to be utilized by cell edge users as shown in **Figure 2-9** (right).

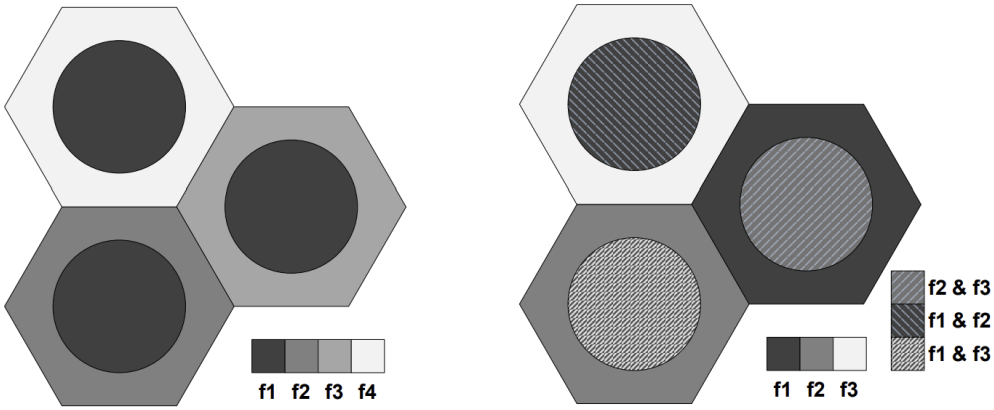

FIGURE 2-9 STRICT FFR (LEFT), SOFT FFR (RIGHT) WITTH CELL EDGE FR=3 [11]

However, while FFR has been envisaged for wide adoption in traditional TN to address such challenges, it has not yet been extensively explored in NTN due to constraints posed by legacy satellite payloads constructed by array-fed reflectors. In the forthcoming broadband satellite missions, direct radiating arrays (DRA) will enable flexible operation of the beams, allowing irregular deployments and mimicking the FFR schemes. Therefore, the idea herein is to investigate FFR in NTN to interplay with the beamwidths of inner and outer beams by dynamically adjusting the inner to outer beamwidth ratio depending on users' existence in serving beam. Moreover, the switching between multiple FFR schemes depending on traffic distribution at any given time, for instance, switching between strict and soft FFR to balance the spectral efficiency and interference minimization tradeoff, may optimize the overall system performance.

2.3.2.2 Architecture Aspects

Considering the architectures described in D3.5 [3] and adhering to the proposed AI/ML high-level in Section **2.2.1**, **Figure 2-10** depicts the high-level AI/ML architectures under consideration for FFR network function. The provided configurations are herein relevant for scenarios 1) where the entire gNB is onboard the satellite and perceive connection with on-ground networks 2) when the gateway might be inaccessible such as during periods when NTN payload cannot establish a connection with the ground network, for instance, when the satellite moves to a remote area or when connectivity is required in the middle of an ocean or during a natural disaster when on-ground infrastructure is severely compromised. It is important to emphasize that in both normal and direct-to-device scenarios, the architecture follows the configuration of regenerative satellite payload with at least a full gNB on-board. Since it is envisaged to place the gNB on-board and, in addition, to explicitly investigate FFR function herein for Direct-to-device scenario, the AI/ML server would benefit from being deployed on-board as well in order to support the latency-free use cases.

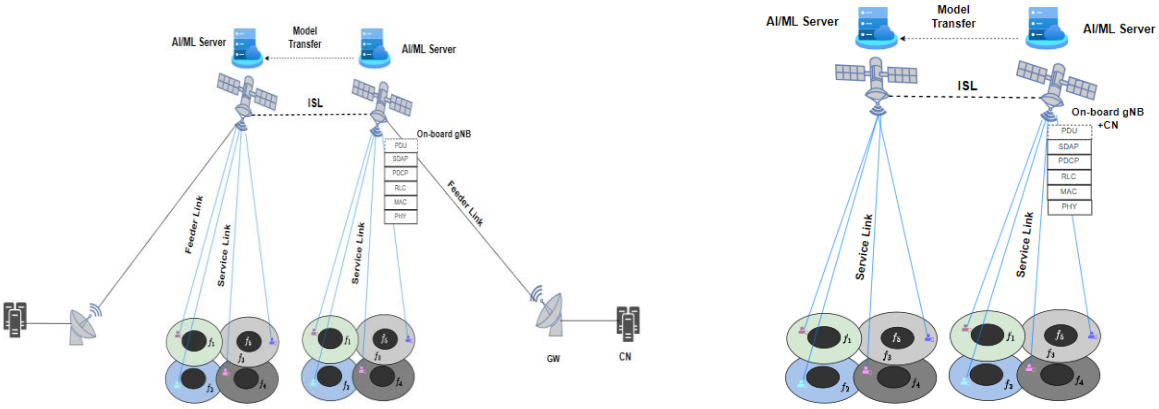

FIGURE 2-10 *AI/ML USER PLANE ARCHITECTURE ASPECTS FOR FFR. NORMAL SCENARIO (LEFT), DIRECT TO DEVICE SCENARIO (RIGHT)*

In essence, this network function would manage the AI/ML functions in the following ways.

Model Training:

- The model training for AI/ML based FFR is intended to be performed at on-board MEC AI/ML server.
- AI/ML server can make use of data collected by UEs being served in each beam, for instance, at high level: UE geocoordinates, channel state information (CSI), distance from beam center at given time and traffic density in order to mimic the FFR framework.
- Inspired from the baseline architecture in Section **2.2.1**, this network function intends to support the location-specific AI/ML model functionality. Since exploiting the dynamic FFR relies on traffic density, the location specific AI/ML model could be applied to optimize resource allocation in the region. For instance, serving the Mediterranean region and remote areas represents different environmental conditions, user behavior and infrastructure. Therefore, the location-specific AI/ML models tailored to local conditions may ensure optimized system performance. To do so, the datasets provided in D4.3 [2] for maritime and direct to cell relevant to remote areas are intended to provide the insights to train such location-specific AI/ML models.
- After a time *t,* if there is one or more additional beams that need to be activated to serve users in a region or under other evolving environmental conditions, a cooperative learning method such as an online training approach is worth considering during the training of the model. This allows to reduce the computation burden at onboard AI/ML server where the new adjustments in the network could be learnt over the existing trained network onboard.

Model Storage

For FFR network function, the model will be stored on-board AI/ML server, whereas the action of model transfer in **Figure 2-10** is meant to support the satellite mobility at a specific region so that the model training function remains specific to location.

Model Inference

Likewise, as in model training and storage, model inference will take place onboard the AI/ML server since the dynamic radio resource allocation and adjustment of beamforming characteristics are preset onboard the satellite as well. The model inference would utilize the relevant information collected by the UE within the serving beam and allocate the dynamic FFR and radio resources accordingly.

Data Collection

The data information listed in **Table 2** is intended to use to support AI/ML model training and inference for the FFR network function to dynamically adjust the inner beamwidth and adaptive resource allocation.

TABLE 2. *DATA INFORMATION FOR AI/ML MODEL TRAINING AND INFERENCE FOR FFR NETWORK FUNCTION*

Collected Data	Source	Usage
UE Geocoordinates	UE	Input to training and inference model onboard
UE distance to beam Center	NW	Input to training and inference model onboard
UE traffic density in each beam	NW	Input to training and inference model onboard
Outer Beamwidth	NW	Input to training and inference model onboard
Inner & Outer Beam Resource Allocation	NW	Output from inference
Inner Beamwidth	NW	Output from inference
UE Channel Measurements	UE	To evaluate the system performance

2.3.3 Traffic Prediction and NTN Radio Optimization

2.3.3.1 High-Level Description

In traffic prediction and RRM, our proposal centers around AI-based RRM, leveraging the capabilities of traffic prediction and reinforcement learning to optimize the allocation of radio resources to users based on their specific demands and latency requirements.

Our focus is on two key functions:

- Predicting future traffic patterns in a geographical area and identifying the volume and the trend for each type of traffic in RT or non-RT.
- Implementing AI/ML-based RRM to cater to diverse traffic demands and varying quality of service requirements.

2.3.3.2 Architectural aspects

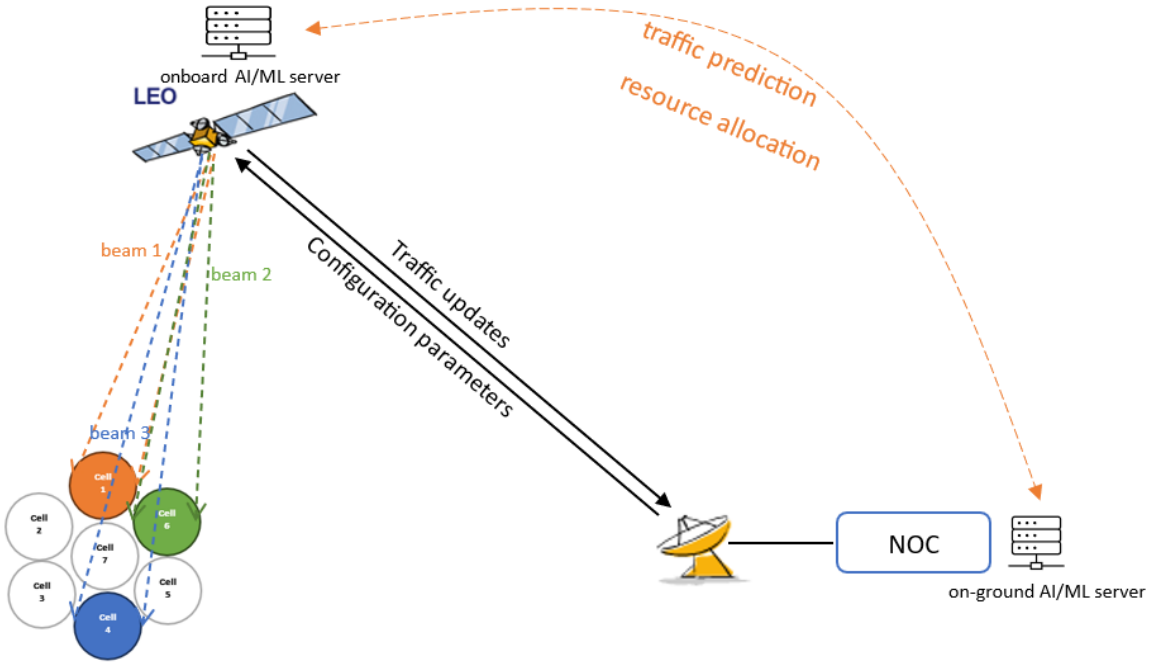

FIGURE 2-11 REFERENCE ARCHITECTURE FOR THE TRAFFIC PREDICTION FUNCTION

The reference architecture for the traffic prediction and resource management function is shown in **Figure 2-11**. In that architecture, the NTN segment is composed of a satellite generating B beams and N cells, assuming that at any given time, those B beams may not be sufficient to serve all N cells. Moreover, a prominent objective for this function is the optimization of how the satellite defines an appropriate beam hopping framework for beam selection (e.g., based on the determination of optimized flexible power and bandwidth resources for each beam to accommodate the requested user data traffic). Therefore, this framework, in its current definition, does not involve the TN access segment.

Similarly to the other 6G-NTN RIC network/management functions presented in this section, this LCM may take advantage of multiple AI/ML servers at different locations for the sake of optimization. The rest of this section proposes an early description of the rationale to prefer hosting such building blocks in either satellite or ground AI/ML servers, among other details. Please note this description will be further detailed in the subsequent deliverable.

Data Collection

Both the traffic prediction function and the beam-hopping resource management require user data initially acquired onboard the satellite. As shown in **Table 3**, such user data encompasses user position information (including UE geocoordinates and derived data such as angle to the beam center and distance to satellite), as well as user traffic demand (including traffic type, allowing to sort near real-time (n-RT) and non-RT traffic requests, and requested number of resource blocks).

Since this data is generated onboard the satellite, it may be collected by the MEC AI/ML server directly from the in-space NW node, for performance purposes (e.g., to limit the additional overhead on the feeder link specifically due to the data collection function).

TABLE 3.DATA INFORMATION FOR AI/ML MODEL TRAINING AND INFERENCE FOR THE USER TRAFFIC PREDICTION

Collected Data	**Source**	**Usage**
UE Geocoordinates	UE	Input to training, input to inference.
UE distance to beam Center	NW	Input to training, input to inference.
UE Distance to the satellite	NW	Input to training, input to inference.
User Traffic Type	UE	Input to training, input to inference.
Requested number of resource blocks	UE	Input to training, input to inference.
Other UE measurements	UE	Input to management

Model Training

The AI/ML traffic prediction function needs to be trained on a comprehensive dataset for the sake of accuracy, and computational power is therefore an important criterion in this case. As a result, two different requirements (i.e., proximity to the aforementioned data collection points to avoid large data transfers on the one hand, said computational power requirements on the other hand) support conflicting arguments about where to train the AI/ML model(s). In effect, the first requirement points to a satellite AI/ML MEC for the sake of low-latency due to data collection proximity. On the contrary, a ground AI/ML server, e.g. on an OAM node running on a centralized Network Operations Center (NOC) system, would be preferred to appropriately address the computational needs for that type of model training. This observation is further complexified when considering the general case of an NTN segment made of multiple satellites, whereby each satellite may need to train a local traffic prediction model (with locally collected data). In the next period, we intend to analyze a federated learning approach, in which each satellite sends its trained model from its AI/ML MEC towards the ground AI/ML server, which in turn will be able to train a global model. As a result, this architectural approach of federated onboard satellite(s) plus ground AI/ML training will be considered in more details in the next deliverable, and compared to centralized ground-only approach, performance-wise.

Model Inference

Regarding AI/ML server location to perform inference, the main argument relates to the need to collocate both model training and beam-hopping resource management function on the satellite itself, since meeting the objectives of this RRM function (i.e., to adeptly respond to transient variations in traffic demands, short-term variations, by refining the subchannel and power allocation protocols implemented on the satellite) requires very short delays between both model training and RRM function.

In addition, a particular care shall be given to the handling of non-geostationary satellite mobility in NTN. Since in such case, the service cell will be handoff from a setting satellite to a rising satellite, thereby requiring the transfer of the cell-related AI/ML context from the outgoing, setting satellite, MEC AI/ML server to the incoming, rising satellite, MEC AI/ML server, e.g. via ISL and/or feeder link. Similarly to the other considered 6G-NTN RIC network/management functions, the impact on all AI/ML building blocks and, in particular, on traffic prediction model inference shall be investigated, as well as the perspective to rely on the aforementioned concept of virtual MEC AI/ML server to keep local AI/ML contexts in case of non-geostationary satellite mobility.

Management

As introduced in this section, the user traffic prediction function aims at supporting the optimization of the associated beam-hopping RRM function. This function helps the satellite defines an appropriate beam hopping framework for beam selection based on multiple criteria including the determination of optimized flexible power and bandwidth resources for each beam to accommodate the requested user data traffic. Consequently, for the sake of performance, at least part of the management entity shall be hosted on the onboard MEC AI/ML server.

2.3.4 Link Quality Prediction in NTN

2.3.4.1 High-Level Description

To handle the issues listed in upcoming Section **3.4** and improve the efficiency during NTN mobility, an AI-based mechanism is proposed for the UE to estimate and predict its radio channel conditions towards different NTN satellites/cells in the time-and-spatial domain. For instance, the proposed mechanism may estimate the radio channels towards different satellites/cells at different time instances, thereby reducing the dependence on reference-signals for measurements and mitigating the issues listed above.

It is noted that, theoretically, the proposed AI/ML-based NTN channel estimation and prediction can be applied at either the UE or the NW, as long as the required information for model inference is available at the corresponding entity. However, in this work, we prioritize to consider the UE-side model inference unless stated otherwise, such that:

- For a UE in RRC_CONNECTED state, the UE may transmit the channel conditions estimated/predicted by using AI/ML to NW for optimizing NW's operation, e.g. to prepare and determine a proper handover (HO).
- For a UE in RRC_IDLE or RRC_INACTIVE state, the UE may leverage its estimated/predicted channel conditions to optimize its own operation, e.g. to (re)select a proper satellite/cell to camp on.

As one additional benefit of running the model inference at the UE-side, it enables to obtain real-time outcomes while capturing the UE dynamics, e.g. UE's movement/rotation, with no additional latency related to data collection. In the following, details on architecture framework, model training, model inference, performance monitoring, and LCM will be provided.

2.3.4.2 Architecture Aspects

In the following, more specific details are described and illustrated, by considering the proposed AI/ML-based NTN channel estimation/prediction. Please note, the following description is obtained based on an initial investigation, and it is subject to future changes which may be added in the next deliverable.

Model Training

The model training for AI/ML-based NTN channel estimation/prediction can take place in the (MEC) AI/ML server:

- The (MEC) AI/ML server can use the data collected from multiple UEs for model training/retraining/updating. This may speed up the procedure for model training/retraining/updating.
- The trained model can be shared and transferred to multiple UEs located in the considered area, e.g. via multicast/groupcast.
- Offline training can be applied by the (MEC) AI/ML server at least for obtaining an initial AI/ML model, based on the data collected from multiple UEs at multiple time instances.
- (Online) model retraining/updating may be considered, e.g. based on an initial AI/ML model obtained via offline training, in order to account for dynamic-and-micro information not captured in the offline model training. It is noted, in some cases, online model retraining/updating may be configured by the (MEC) AI/ML server to be performed at the UE, e.g. to generate a UE-specific model.

Model Storage

Depending on the applicability of a model, it may be stored in different locations:

- Trained model via offline training with local data managed by the MEC AI/ML server may be stored at the MEC AI/ML server.
- Trained model aiming for a global applicability, e.g. by using offline federated learning, may be stored at the on-ground AI/ML server.
- A retrained/updated UE-specific model may be stored at the corresponding UE.
- If not stored in the UE, a model can be delivered to one or multiple UEs for model inference, e.g. via groupcast or multicast.

Model Inference

As mentioned before, this work prioritizes running model inference at the UE. Thus, at least the UE needs to perform model inference to generate channel estimates for one or multiple satellite(s) at a set of time instances, which is the output of the AI/ML model.

It is noted, the need for the NW to run part of the AI/ML model for generating certain intermediate results is still under investigation, which will be considered the input to the AI/ML inference at the UE side. It will become clearer later, along with the progress of this work.

Performance Monitoring and LCM

Two potential approaches are under consideration for the management function to monitor the performance of the AI/ML-based channel estimation/prediction and the corresponding AI/ML model:

- Comparing the AI/ML-generated channel estimation/prediction to UE measurements.
- Investigating relevant system level performance, which may be impacted by the AI/ML-based channel estimation/prediction, e.g., HO and/or cell (re)selection performance.

Data Collection

The information listed in **Table 4** is considered for data collection to support the proposed AI/ML-based NTN channel estimation/prediction. As mentioned previously, it is noted that the (MEC) AI/ML server may configure the UE to store some data locally.

TABLE 4: *DATA COLLECTION FOR AI/ML-BASED CHANNEL ESTIMATION/PREDICTION*

Collected data	Source	Usage	Details/Comments
UE radio measurements	UE	Input to training, input to management	It may include UE measurements for multiple satellites in the same and different orbits, wherein the measurements for a considered satellite may take place at multiple time instances.
UE location	UE	Input to training, input to inference	Location associated to one or a set of collected UE measurements or estimations/predictions.
Timing	UE	Input to training, input to inference	Timing instance associated to one or a set of collected UE measurements or estimations/predictions
Satellite identity info	UE	Input to training, input to inference	Satellite information associated to one or a set of collected UE measurements or estimations/predictions, e.g. satellite/cell ID
NW-side assistance information	NW (e.g. SCC)	Input to training,	Detailed satellite information associated to the satellite/cell ID, such

		input to inference	as satellite location/ephemeris, satellite antenna information
UE-side assistance information	UE	Input to training, input to inference	UE-specific information related to UE conditions and to specific UE implementation aspects, such as UE-orientation information, UE antenna information
Additional condition	UE and/or NW	Input to training, input to inference	Any additional information that may have an impact on the AI/ML model, such as weather and/or NW configuration
AI/ML-based UE channel estimation/prediction	UE	Output from the inference, input to management	The AI/ML-generated channel estimation/prediction between the UE and the satellite indicated by the associated satellite identity information at the associated UE location and at the associated timing instance
Relevant system performance (to be further investigated later)	UE and/or NW	Input to management	System performance, which may be impacted by applying the AI/ML-based channel estimation/prediction

3 RADIO INTELLIGENT CONTROL NETWORK FUNCTIONS

This section comprises two vital components. The primary component is dedicated to comprehensively discuss the SoTA relevant to each RIC network function as identified in Section **2.3**, while the secondary component is to elaborate the corresponding problem statement and the KPIs being considered to optimize using AI-enabled robust algorithms.

3.1 TRAFFIC OFF-LOADING

3.1.1 State-of-the-art

The optimization of traffic off-loading is crucial for enhancing the performance of cellular networks. The traffic off-loading task is often addressed with a load balancing approach that involves the optimal allocation of resources, management of handovers, interference, and balancing the load between multiple cells and carriers [12]. This is especially challenging in the context of 5G and 6G networks, where the efficient allocation of radio resources is essential. To address these challenges, various innovative approaches have been proposed.

One approach involves the use of Machine Learning (ML) and Artificial Intelligence (AI) based load balancing algorithms running on Open RAN RIC (RAN Intelligent Controller). In this context, [13] discusses the implementation of the traffic steering xApp in a hierarchical and modular fashion. The results presented emphasize the advantages of this modular approach, illustrating how AI/ML tools can intelligently manage the functioning of the xApp and consequently enhance overall system performance. The authors in [14] leverage Deep Reinforcement Learning (DRL) and Graph Neural Networks (GNN) to achieve up to 10% gain in throughput, 45-140% gain in cell coverage and 20-45% gain in load balancing compared to baseline greedy techniques. Additionally, proactive approaches using multi-agent reinforcement learning and deep deterministic reinforcement learning algorithms have been explored to maximize UE throughput and improve handover decisions based on local channel measurements. Furthermore, the use of GNN and deep Q-learning approaches have been proposed to learn Q-functions from cell and UE deployment instances, providing scalable and effective solutions for connection management. In [15], an algorithm for Radio Access Technology (RAT) allocation predicated on Federated Meta-Learning (FML) is introduced, thereby facilitating the expeditious adaptation of RICs to dynamically evolving environments. A simulation environment has been devised, featuring LTE and 5G NR service technologies. Within this simulation framework, the primary aim is to satisfy UE demands within prescribed transmission deadlines, thereby enhancing the delivery of heightened Quality of Service (QoS) values. To enhance the collection of realistic data for xApp training, in [16], *ns-O-RAN* is introduced. It is a software framework that integrates a real-world, production-grade near-RT RIC with a 3GPP-based simulated environment on ns-3, enabling at the same time the development of xApps and automated large-scale data collection and testing of DRL-driven control policies for the optimization at the user-level.

Several works focus on the optimization of the load in small-cells deployments. In [17], a load balancing technique based on network segmentation and adaptive sleep scheduling for 5G-IoT networks is proposed. This technique involves the formation and grouping of sub-segments for each network segment to process IoT applications with different Quality of Service (QoS) requirements. Additionally, adaptive dynamic sleep scheduling is executed by each small cell base station based on its load level. The load balancing policy involves the transfer of overloaded traffic from small cell base stations to the macro cell when the average load of any small cell base station surpasses that of the macro cell. Simulation results validate the

proposed technique, demonstrating higher success probability, power efficiency, reduced energy consumption, and packet drops of small cell base stations compared to existing techniques. In addition, the research by Addali, [18], [19], focuses on addressing the challenges of unbalanced load distribution in 5G small-cell networks through the introduction of a Utility-based Mobility Load Balancing algorithm (UMLB) and a Load Balancing Efficiency Factor (LBEF). The UMLB algorithm considers both operator and user utility, aiming to achieve efficient load transfer from overloaded cells to under-loaded neighboring cells. The study emphasizes the importance of accurately adjusting handover parameters to prevent inefficient resource usage and degradation of QoS. Additionally, the research discusses the impact of user mobility on the algorithm and evaluates the performance through computer simulations. The proposed algorithm demonstrates promising results in improving network performance and user satisfaction by effectively balancing the load distribution in small-cell networks. In [20], an extreme Swap-based Load Balancing (SLB) algorithm between APs, which minimizes the load imbalance at cell edges is proposed. The experimental setup uses a dataset contributed by Irish mobile operators.

Recent literature has explored the application of controller and machine learning algorithms to assist self-optimizing and proactive schemes in making load balancing decisions. However, the authors in [21] argue that these algorithms often lack the ability to forecast upcoming high traffic demands, particularly during popular events, leading to cold-start problems and low convergence speed in hotspots with skewed load distribution. To address these challenges, three contributions are proposed. Firstly, it introduces urban event detection using Twitter data to forecast changes in cellular hotspots, enabling context-awareness. Secondly, it simulates a proactive 5G load balancing strategy considering the prediction of skewed-distributed hotspots in urban areas. Finally, it optimizes this context-aware proactive load balancing strategy by forecasting the best activation time.

Research work has timidly focused also on load balancing for non-terrestrial networks. In [22], the authors propose a novel load balancing algorithm designed specifically for a multi-RAT (radio access technology) network that encompasses both NTN and TN. To address this gap, the authors introduce the concept of a Radio Resource Utilization Ratio (RRUR) as a common load metric to assess the cell load of each RAT. This metric is utilized in conjunction with an adaptive threshold to identify overloaded cells. The proposed algorithm comprises two key steps: intra-RAT load balancing and inter-RAT load balancing. In the first step, the algorithm redistributes the load by offloading edge UEs from overloaded cells to neighboring underutilized cells based on the RRUR of each cell. If a cell's RRUR remains above a predefined threshold, the algorithm proceeds to the second step, which involves offloading delay-tolerant data flows of UEs to a satellite link as a form of inter-RAT load balancing. Additionally, the algorithm incorporates an estimation of the impact of load redistribution on the target cell load to minimize unnecessary load balancing actions. The effectiveness of the proposed algorithm is demonstrated through simulation results, which indicate that it not only achieves more even load distribution across terrestrial cells but also enhances network throughput and the number of quality-of-service satisfied UEs compared to previous load balancing algorithms. Additionally, in [23] the challenge of efficiently utilizing limited beam resources to serve users in Non-Geostationary Orbit (NGSO) communication systems are addressed. To enhance spectrum utilization, the authors propose a multi-satellite beam hopping algorithm that integrates load balancing and interference avoidance. The algorithm decomposes the multi-satellite beam hopping problem into three subproblems: multi-satellite load balancing, single-satellite beam hopping pattern design, and multi-satellite interference avoidance. Simulation results demonstrate that the proposed method significantly reduces the load gap among satellites and improves the average traffic satisfaction rate. Additionally, it exhibits superior performance in terms of unmet capacity compared to other benchmarks, thereby achieving better alignment between offered and requested data. Finally, [24] introduces a decentralized Load Balancing Satellite Handover (LBSH) strategy based on multi-

agent reinforcement Q-learning, implemented within the Network Simulator 3 (NS-3) software. The LBSH strategy aims to minimize the total number of HOs and the blocking rate while ensuring a balanced distribution of load among satellites. The results demonstrate the superiority of the proposed LBSH method over existing approaches, with a significant reduction in the average number of HOs per user and the blocking rate, thereby showcasing its potential to optimize satellite handover management and enhance network performance in LEO satellite constellations within the context of 5G and beyond technologies.

3.1.2 Problem Statement

TN deployed in rural areas experience varying levels of user traffic throughout the day, resulting in high load for base stations during peak periods and underutilization during off-peak periods. With the NTN component, the load can be balanced between the TN and NTN cells, off-loading part of the terrestrial base stations' traffic. This technique brings an increased QoS during high network load conditions and a reduced TN energy consumption when the traffic request is lower. Considering the case of overloaded TN, an AI component can gather information on the network's status and use it to optimize the amount of traffic to be handed over to NTN. The AI's goal is to maximize the overall Signal to Interference and Noise Ratio (SINR) of TN while accounting for the capacity limitation and high dynamicity of NTN. Indeed, due to the limited throughput and increased latency of NTN, not all users are suitable for off-loading from TN. The AI must be able to predict future user traffic and the capabilities of the NTN to ensure that only users with traffic requests compatible with the NTN's performance are handed over. The final goal is to maximize the overall throughput of the network.

The output KPIs intended to be optimized include:

- SINR
- Overall throughput capacity

3.2 FRACTIONAL FREQUENCY REUSE IN NTN

3.2.1 State-of-the-art

In the literature, FFR schemes have evolved over the years from basic to heuristic and towards AI-enabled approaches to identify the near optimal and optimal solutions. In essence, comparisons among different FFR schemes in the multicellular scenario are performed in [11] and [25]. The former studied the performance analysis of a Strict and Soft FFR in OFDMA system for uniformly distributed users and compared the performance with the system without FFR. Also, it analyzed multiple KPIs including outage probability, network sum-rate and SINR in inner and outer cells to evaluate performance. The study in [25] compared Strict and Soft FFR schemes in a hotspot scenario and applied an AI-enabled algorithm based on Q-learning to further improve the system performance. The comparison outcomes in the literature showed that FFR in cellular networks is a viable and effective solution to mitigate the inter cell interference to optimize system performance.

However, during the literature review, it is worth noting that applying FFR techniques in non-terrestrial networks are not widely studied, even though interference in NTN is more concerning than in terrestrial cellular networks due to prolonged signal propagation characteristics and the limited availability of spectrum resources. The aforementioned challenges make efficient spectrum management, resource allocation and interference mitigation even more challenging.

Therefore, the idea is to map those traditional FFR techniques used in HetNets into the paradigm of multibeam satellite systems where the main satellite beams are composed of smaller beams and would use different frequency resources in order to reduce inter-beam interference. This may also have some implications in improving the NTN performance as well. Taking this into account, a heuristic approach is formulated in [26] which maps the coloring node problem commonly used in graph theory to FR allocation problem in satellite broadband communication networks. In this problem, each connected node is of a different color representing a cell using different frequency resources. However, this work is limited to FR rather than FFR. On the other hand, a couple of studies on FFR schemes for ICIC in multibeam satellite can be found in [27] and [28] for uplink scenario. The former work focused on deriving the theoretical formulation of uplink interference and then comparing the different FFR schemes to analyze the performance. On the other hand, the work in [28] reviews the FFR based static, semi-static and dynamic ICIC techniques and proposes a scheduling-based algorithm in frequency domain to maximize the minimum Carrier to Interference (C/I) ratio. Based on another brief study of FFR, an analysis in order to optimize the FR in multibeam satellite system is provided in [29] which adopts a non-uniform beam layout pattern assuming that different regions require different frequency reuse patterns. The region with crowded beams requires a higher FFR order than the regions with fewer ones.

However, as the complexity increases, especially under time-varying network or heterogenous user traffic-like conditions, one-shot optimization algorithms are no longer appropriate solutions to the FFR allocation problem in multibeam satellite systems as they are unable to achieve the performance requirements due to static allocation of the resources throughout. Therefore, it is enormously needed to introduce AI/ML algorithms which are able to adapt to flexible network conditions and allocate the resources dynamically by interacting with the environment. Since the direct contribution towards FFR in multibeam satellite system is limited, and one of the reasons may be its applicability in the practical scenarios due to the limitations of digital beamforming technologies in applying FFR, particularly due to constraints posed by legacy satellite payloads constructed by array fed reflectors. Therefore, the literature is focused on indirectly optimizing the system capacity by reducing the inter-beam interference either by scheduling the resource allocation to users or dynamically allocating the bandwidth, power or frequency resources taking full frequency reuse into account. In this context, and within the framework of multibeam satellite system [30], a TDMA-based time slot scheduling process with full frequency reuse is discussed for downlink scenario which, instead, schedules the power and frequency resources to minimize the co-channel interference. The latency introduced to the joint scheduling and resource allocation in this scheme is further optimized by employing the reinforcement learning algorithm as a Markov decision process, while adopting a proximal policy optimization (PPO) to maximize the system long term revenue.

From another perspective, a variety of AI/ML algorithms have been utilized for resource allocation in heterogenous traffic, which can be directly mapped into the domain of FFR in multibeam satellite system. In this context, a learning-based Q-learning algorithm is used in [31] when traffic is time varying, and users coexist using the same frequency band. The algorithm controls the SINR threshold, while taking into account the interference as the state-space to be used as one of the components in the Q-learning-based optimization. Referred to as *Cooperative Learning*, it incorporates the new users to initialize their Q-learning table by averaging the Q tables from the existing users in the environment. This algorithm could also be adapted for use in the context of FFR in multibeam satellite systems, given the fact that the traffic is dynamically changing with time and the newer beams come into action to serve the users. Also, the utilization of adaptive bandwidth can directly influence the system throughput in multibeam satellite systems. Therefore, a similar work based on comparison between on-policy and off-policy approaches such as State Action Reward State Action (SARSA) and Q-learning, respectively to allocate the flexible bandwidth in satellite communication networks is

provided in [32]. Although it does not directly consider the inter-beam interference, the AI/ML framework can still be employed within the FFR framework as Joint bandwidth and frequency allocation optimization problem to enhance the throughput and reducing the inter-beam interference, respectively.

3.2.2 Problem Statement

In the realm of NTN, the multibeam satellite system emerges as a powerful paradigm due to its profound ability to generate focused beams. This enables high capacity and efficient resource utilization ensuring the QoS. As discussed in the previous section, a significant challenge hinders its full potential due to the presence of inter-beam interference, which becomes even more challenging for the highly heterogeneous characteristics of user traffic or channel conditions. As highlighted above, and since the traditional Digital Beamforming (DBF) technology poses restrictions on the use of the flexible beam parameters (especially when designing the flexible inner-beam radius), DRA will enable adaptive operation of the inner beams in the forthcoming satellite missions. In essence, DRA allows irregular deployments to provide high flexibility to adapt to the heterogeneity of user traffic and channel conditions, and then to modify the inner beam characteristic and resource allocation accordingly.

Taking the above into account and given the traffic and channel information, the objectives herein are to optimize the overall system capacity and spectral efficiency by minimizing the inter-beam interference and identifying the appropriate FFR scheme, respectively. This optimization can be done by identifying the appropriate inner to outer beamwidth ratio corresponding to each beam at which the maximum system throughput can be achieved, which is based on learning the dynamic nature of the environment.

To conclude, the time varying inner to outer beamwidth ratios and flexible resources allocation, for instance bandwidth and power, based on user traffic are potential objective functions to improve the overall system performance.

The output KPIs intended to be optimized include,

- Signal to interference and noise ratio (SINR)
- Overall throughput capacity
- Maximum spectral efficiency

3.3 TRAFFIC PREDICTION AND NTN RADIO OPTIMIZATION

3.3.1 Traffic prediction: State-of-the-art

Anticipating wireless traffic is crucial for overseeing high dynamic and low latency communication networks, particularly within the context of 6G wireless networks. From the operator's point of view, long-term network traffic prediction can facilitate the long-term planning for upgrading and scaling the network infrastructure. The concept of traffic prediction is mainly based on finding and exploring the potential dependencies involved in historical network traffic for assessing future traffic volume and trends. Proactive resource allocation and eco-friendly green communication strategies hinge on accurate predictions of future traffic states. An illustration of this is the potential to achieve adaptive channel assignment by forecasting wireless traffic, mitigating the risk of traffic congestion [38].

Cellular traffic prediction problems can be classified into two main types: temporal and spatial-temporal. The temporal prediction problem only considers temporal dependencies for

predicting the traffic flow of a base station, based solely on its own historical traffic data. The spatial–temporal prediction problem takes into account both spatial and temporal dependencies in traffic data and aims to predict the traffic data series of multiple network elements embedding spatial dependencies.

A common practice in the industry is to analyse the historical traffic data to calculate the network traffic's potential growth rate, which is not a scalable approach especially with the new services. In the literature, many statistical time series models and analysis methods have been proposed for wireless traffic prediction. Existing time series prediction methods generally fall into two categories, conventional models and deep learning models or linear and nonlinear models.

Most conventional models, such as α-stable distribution [33] , Autoregressive Integrated Moving Average (ARIMA) [34], HoltWinters [35] [36] [37] [38], covariance function [39] and entropy theory [40] are built with some insight into the time series and rely on manually tuned parameters to fit the time series, which impedes their application in large-scale prediction scenarios. The linearARIMA model has been used to model the short-term correlation in network traffic [41]. The Seasonal ARIMA (SARIMA) models are adopted to improve the ARIMA-based models on long-term traffic correlation modeling [42]. Wang *et al.* [43] proposed the sinusoid superposition model to describe both the short-term and long-term traffic patterns. The famous Facebook model called Prophet [44], uses a hand-crafted nonlinear module but it needs help to easily model non-stationary time series.

The pattern of cellular traffic is actually very complex due to various factors, e.g., user mobility, arrival pattern and diverse user requirements. It becomes increasingly clear that those linear models are not suitable for such kind of applications. The development of the deep learning method has emerged to solve the dilemma of inefficient performance, due to the nonlinear and complex nature of the traffic patterns, and the large number of parameters to be tuned in order to improve the accuracy of the prediction. The multiple layers feature of deep learning models can be exploited to recognize deep latent patterns and features at a more abstract level in time series.

Recurrent Neural Networks (RNNs) and Transformer networks are two main deep learning forecasting frameworks.

RNN-based models [45] [46] feature a feedback loop that allows models to memorize historical data and process variable-length sequences as inputs and outputs, which calculates the cumulative dependency between time steps to capture the temporal dependencies. Nevertheless, it fails to capture multi-scale variations within non-stationary time series. Qiu *et al.* [47] exploited the Recurrent Neural Network (RNN) to predict wireless traffic based on certain spatial-temporal information. The authors in [48], established a strategy combining an auto-encoder.

Long Short-Term Memory (LSTM) is a special kind of Recurrent Neural Networks (RNN), capable of learning long-term dependencies. LSTMs have an advantage over RNNs in that they are designed to avoid the long-term dependency problem [49]. The convolutional neural network (CNN) is adopted to capture the spatial correlation [50].

Transformer-based models [51] utilize a global self-attention mechanism rather than feedback loops to enhance the network's ability to capture longer dependencies and interactions within series data, thus, bringing exciting progress in various time series applications. The sparse self-attention mechanism is proposed for more efficient long-term time series processing [52][53].

A deep learning model proposed in [54] to forecast 5G network traffic, Diviner, incorporates stationary processes into a well-designed hierarchical structure and models non-stationary time series with multi-scale stable features.

In recent developments, the Gaussian Process (GP) model, classified as a Bayesian nonparametric machine learning model, has been suggested for the modeling and analysis of spatial-temporal data [55]. The GP incorporates domain/expert knowledge into the kernel function and explicitly refines hyperparameters using Bayesian theorems [56], yielding results that are inherently explainable. Consequently, it holds significant promise for enhancing interpretability and prediction accuracy.

Federated Learning (FL) has emerged successfully, as highlighted in references [57] [58], enabling predictive solutions while maintaining data locally. In the FL framework, numerous clients such as mobile devices and Base Stations (BSs) can cooperatively train a prediction model under the coordination of a central server. Notably, only intermediate model parameters derived from local training, rather than the raw data, are transmitted to the central server. The authors in [59] proposed a Federated Dual Attention (FedDA) framework for wireless traffic prediction. A federated learning applied to raw base station LTE data for time-series forecasting was also proposed in [60].

3.3.2 Radio Resource Management: State-of-the-art

The deployment of 5G and beyond involves the integration of TN-NTN, and satellite communication is set to play a crucial role in future networks. Addressing the substantial traffic demand and accommodating new potential services necessitates efficient radio resource utilization and dynamic traffic demand matching. Various approaches, including conventional optimization methods, heuristic algorithms, and deep learning, have been proposed to tackle these challenges.

The next generation of satellite communication, SATCOM, embraces a flexible (regenerative) payload satellite architecture. In the SATCOM context, RRM involves configuring key resources such as power, bandwidth, and beamwidth through optimization processes facilitated by the regenerative payload.

Practically speaking, achieving flexible power allocation entails utilizing a Travelling Wave Tube Amplifier (TWTA) with Input Back-Off (IBO). Moreover, a flexible payload should possess the capability to segregate frequency bands and reorganize them to attain flexible bandwidth. This is achieved by employing an onboard channelizer to identify the frequency plan (color assignment by frequency and polarization).

To enhance flexibility, reconfigurable Beamforming Networks (BFNs) are employed instead of output multiplexers. This halfway solution enables the synthesis of any beam and the selection from a set of configurations for the same coverage.

The beam hopping (BH) concept is proposed for SATCOM to adapt to the time varying communication demands which dynamically changes with time mobility and weather conditions. Through generation of multiple small beams and reuse of the same spectrum enormous times cross the coverage area, BH allows to increase the satellite capacity significantly.

Deep learning (DL) can help to identify the best optimal beam hopping pattern within the large search space, as the number of the patterns to explore increases exponentially with the number of the beams. The existing BH-related works aim to compose the beam switching and jointly optimize beam pattern illumination mechanism with power/spectrum allocation and precoding/beamforming design.

Lei et. al. investigated in [61] a Deep Learning method for Beam Hopping optimization to predict the number of elements in the beam pattern for Beam Hopping, as well as speeding up the process of Beam Hopping pattern selection and allocation. In [62], the same authors have explored a joint learning-and-optimization approach to provide an efficient, feasible, and near-optimal solution.

In [63], the authors investigated the optimal fairness policy for beam hopping in DVB-S2X satellite regarding two main goals: minimizing the delay of real-time services transmission and maximizing the throughput of non-instant services transmission.

A dynamic beam pattern and bandwidth allocation scheme based on deep reinforcement learning (DRL) is also exploited in [64], where a dynamic beam pattern and bandwidth allocation scheme flexibly uses three degrees of freedom: time, space and frequency. Considering that the joint allocation of bandwidth and beam pattern will lead to an explosion of action space, a cooperative Multi-Agents Deep Reinforcement Learning (MADRL) framework is presented in this paper, where each agent is only responsible for either the illumination allocation or the bandwidth allocation of one beam. The agents can learn to collaborate by sharing the same reward to achieve a common goal, which refers to maximizing the throughput and minimizing the delay fairness between cells.

Traditional satellites utilize a multibeam footprint with uniform power allocation per beam to provide connectivity for users. However, this approach becomes inefficient when faced with non-uniform demand distribution. Beams with low demands may allocate excessive power, while those with high demands may be allocated insufficient power, potentially leading to unmet user demands. Consequently, implementing an advanced power allocation algorithm is imperative for the next generation of satellite communication systems to ensure efficient power management [65] [66] [67] [68]. Various machine learning (ML)-based approaches have been proposed to address these issues:

In [69] and [70], the authors present a classification algorithm that determines the power required for each beam, minimizing the error between offered capacity and demand.

The authors in [71] employ a Convolutional Neural Network (CNN) to minimize the difference between offered capacity and per-beam demand while conserving unused satellite resources. However, this algorithm relies on training data, which must be updated in the event of changes to the traffic-demand pattern.

A power allocation algorithm leveraging Deep Reinforcement Learning (DRL) to maximize system transmitted data is explored in [72]. Here, the satellite functions as an agent, with the traffic between beams acting as the environment. The DRL state encompasses buffered data among beams, power allocations, and beam geographical distributions, allowing the agent to optimize power allocation to maximize data transmission.

Contrastingly, [73] proposes DRL for continuous power allocation in flexible high throughput satellites, aiming to minimize overall unmet system demand and power consumption. This DRL model is further utilized in [74] for comparison with metaheuristic techniques, revealing DRL as the most suitable option when time is critical and a quick solution is essential. Additionally, [75] investigates the performance of an extended multi-agent DRL method, dynamically allocating payload resources to meet the traffic demand of each beam.

Heuristic algorithms are also considered. In [76], the simulated annealing algorithm is employed with state-of-the-art satellite processors, achieving full power, frequency, and beamforming flexibility. Furthermore, a modified version of the simulated annealing algorithm is applied in [77] to solve the Multi-Dimensional Resources Management (MDRM) optimization problem with

full payload flexibility, accompanied by a detailed complexity analysis. For rapid convergence, [78] combines simulated annealing and Monte Carlo algorithms to establish a dynamic resource scheduling scheme.

3.3.3 Problem Statement

Our objective is to provide a highly efficient radio resource management framework to support UEs with different traffic demands and with different requirements of QoS by utilizing multi-dimensional communication resources in a flexible way. Accordingly, we maximize the achievable throughput of non-RT services transmission and ensure minimizing the delay for RT services while satisfying various resource constraints. The throughput of the non-RT services is defined as the sum of the throughput of non-RT packets in all the selected cells to be illuminated, while the delay of the RT services is defined as the average of instant packets delay. The MDRM problem is formulated as a tradeoff between two objective functions, for instance P1 and P2. The non-RT data throughput maximization is defined by the objective function P1 while P2 represents delay minimization of RT data. A weighted sum method is used to formulate a single objective function.

The expected outputs of this framework include:

- The expected traffic for each user in the following period according to the predefined time granularity.
- The plan for resource assignment is based on the users' positions and the available resources.
- A beam hopping plan for serving different cells.

3.4 LINK QUALITY PREDICTION IN NTN

3.4.1 State-of-the-art

This section describes some scientific literature related to the link quality estimation and prediction problem that we propose to solve using AI/ML paradigm. Meanwhile, the state-of-the-art on AI/ML in the 3GPPliterature has been described in Chapter 2.

AI-based solutions at the physical layer have primarily focused on channel-modeling, ionospheric scintillation detection, and remote-sensing [79]. Path-loss prediction, as applicable to channel-modeling, has been studied using approaches such as state-vector machines, neural-networks and decision trees. Urban and sub-urban environments in terrestrial network (TN) have been the major focus of these studies; this is understandable since the wireless channel in urban environments is typically challenging to model owing to the diverse topography and deep "wireless holes" in such scenarios. Furthermore, a notable feature in the NTN-channel is its greater bias to encompass a LOS path. From field-measurement experiments conducted in an urban-macrocell scenario reported in [80], it is shown that learning-based approaches all have good performance and outperform the conventional log-distance model. Further, in a comparative study, it was also shown that random-forest-solution has the best performance in the measured scenario followed, in order, by support-vector regression, back-propagation neural network and log-distance model.

A deep convolutional neural network (CNN) based approach to estimate channel parameters (specifically, path loss exponent and standard deviation of shadowing) directly from 2D satellite images, as an alternate to 3D-model based ray-tracing approaches, is proposed in [81]. Such CNN-based prediction from satellite-images have been reported to obtain gains in the order of 1-4.5 dB over 3D ray-tracing models and conventional empirical models [82]. The foregoing approaches were generalized to pathloss histogram prediction in urban and sub-urban areas in [83]. In [84], satellite-images in a Deep Neural Network (DNN) were shown to achieve improved prediction of NR signal quality metrics such as RSRP, Reference Signal Receiver Quality (RSRQ) and SINR. In another case, Recurrent Neural Network (RNN)-based link quality prediction (Received Signal Strength Indicator (RSSI) and Signal to Noise Ratio (SNR)) was proposed and studied for improving the reliability of service transmission in 5G smart grid network in [85]. It is to be noted that such prediction of signal quality at unseen locations using position-based measurements and satellite information, albeit closely connected with the problem that we shall delve into, is largely focused on TN. It is expected that their generalization to NTN is not straightforward since the satellite-user-environment geometry is rapidly varying, even for a stationary UE.

AI/ML based channel estimation has also been studied in the context of massive-Multiple-Input Multiple-Output (MIMO) TN network. For example, [86] presented a DL-based CSI estimation technique for massive MIMO antenna arrays. The proposed DNN uses two hidden MultiLayer Perceptrons (MLP) layers and a linear output layer to jointly perform the task of OFDM demodulation and CSI matrix generation for massive-MIMO downlink transmission. The authors reported substantial improvement in the end-to-end system performance, achieving up to 5 and 2 orders of magnitude reduction in Bit Error Rate (BER) with respect to practical LS and optimal Linear Minimum Mean Square Error (LMMSE), respectively. See [87] and references therein for CNN-based solutions to mmWave massive MIMO channel estimation.

In [88], the authors proposed a method of estimating channel excess attenuation in mmW satellite links using DNN. Using real measurements of weather and satellite-signal data (Q-band) for training and performance evaluation, it was shown that real-time estimation of the atmospheric fading can be obtained at a high degree of accuracy. The significance of this work lies with the opportunities it raises to deliver the real-time fading estimations using low-cost weather sensors combined with feedback on the channel state from the return link, which can be used in the deployment of propagation impairment mitigation techniques.

Among other related PHY-layer topics that have adopted AI-based solutions in NTN is Doppler-prediction [89]. This specifically targets IoT, low-power devices that can avoid conventional computation methods, which can be a burden in terms of complexity and power.

We note here that the problem that we intend to solve, as discussed in the following section, implicitly attempts to achieve ephemeris-less prediction, while aiming at a measurement quality comparable to that of conventional methods. In this context, such a study would be a valuable addition to the NTN AI/ML literature.

3.4.2 Problem Statement

An important feature of NTN, especially in relation to LEO-satellites, is the fast movement of satellites. For example, a satellite cannot be expected to be visible to a stationary ground UE beyond a few (< 20 min) minutes, depending on the orbital height. Thus, maintenance of a seamless service forces an NTN UE to experience frequent satellite-switch. Note that this applies even for a stationary UE, a characteristic not seen in TN; therefore, the average rate of handovers in NTN is expectedly higher than in TN. In order to support RRM, e.g. mobility,

the NTN UE has to perform more frequent measurements on serving cell and neighbor cell(s), based on NW configurations. However, increased (unnecessary) measurements may cause:

- Additional power consumption for satellite to transmit and for the UE to measure.
- Resource waste for transmitting reference signals, and
- Service interruption, e.g. due to scheduling restriction and/or measurement gap, depending on the UE type/capability.
- Further, online measurement has limited capability to support early coordination/preparation.

Therefore, to handle the above issues, we propose an AI/ML-based spatiotemporal NTN channel measurement estimation and prediction to:

- Estimate the channel with a satellite at a location.
- Predict channels for a satellite at a set of future time instances.

UE-side model inference is prioritized over the NW-side model inference. RRC_CONNECTED UE may transmit the channel conditions estimated/predicted by AI/ML to NW for optimizing NW's operation, e.g. HO. RRC_IDLE/INACTIVE UE may use the estimated/predicted channel conditions for optimizing the UE's own operation, e.g. cell (re)selection.

Towards this goal, we plan to create an AI/ML simulation framework for the study of the effectiveness of the approach. An important study-item shall be to understand the effects and interplay of UE-mobility, environment, satellite motion and geometry, and the prediction time-window that affects the quality of the predicted measurements. The key KPI that we shall target includes, but is not restricted to, measurement-reporting quality.

Outputs include:

- ID and time duration of satellites relevant of consideration for UE mobility, e.g. target cell for UE's handover, or UE's cell (re)selection and time duration.
- Radio measurement predictions with a satellite based on AI/ML.
- A reduced set of real measurements to be performed by the UE.

4 SYSTEM DESCRIPTION

This part of the document is devoted to the description of the 6G NTN system for the implementation of the AI/RIC management of the present task. The system definition is given in D3.5 of Task 3.1 [3]. This chapter refers to WP 3 and WP 4 which formalize and synthetize the data for ease of implementation of the partial 6G NTN model. The present task will focus on the LEO constellations of the NTN and more particularly on the two LEO constellations defined in Task 3 of 6G-NTN: one in C-band and a second one in Q/V band. These constellations and their associated payload are issued from a trade-off presented in [90] [91] [92].

4.1 NTN DESCRIPTION

4.1.1 Objective

As mentioned in the objective of this work in Section 1, it is necessary to have a model of NTN in order to be able to implement the algorithms for the identified AI/RIC network functions. The following chapter will give the necessary information and model in such a way to be usable in an accurate enough way.

More precisely, the objective is to provide the essential parameters allowing the implementation of an antenna model in order to drive the AI/RIC management in conjunction with the TN. In other words, there is a need for a model able to simulate the entire system that could be used to define how the system as a whole can be implemented effectively.

The 6G system is made up of the NTN and the TN from its initial definition, each with a specific role and mission. NTN aims to cover all areas, with priority given to those not covered by TN, while TN will be limited to terrestrial coverage. In addition, it should be noted that NTN, as its acronym indicates, is a system comprising several types of elements evolving above the earth surface, ranging from drones, haps or constellations of satellites (i.e., LEO, MEO and GEO). In our case, we will first define the mission assigned to the NTN ensured by LEO constellation and propose a methodology for simulating their coverage in terms of radiation and localization. The element of information constitutes a model for implementing and testing the most advanced algorithm in resources management.

4.1.2 Mission Definition

The mission definition for the NTN is issued from the request of NTN to cover all the earth surface composed of earth fixed cells. The coverage is ensured by a multibeam antenna covering these fixed cells. To fulfill the mission, 2 LEO constellations have been defined, one in C band and one in Q/V band. These two-frequency bands are envisaged as future candidates for the 6G NTN system. For more details, please refer to previous 6G-NTN deliverables with work begun in [94] and completed in [91]. The constellations parameters have been resumed below in Table 5 [92]:

TABLE 5. *CONSTELLATION PARAMETERS*

Parameters	Unit	Value
Number of Planes		27
Number of Satellites per Plane		47

Right Ascension of the Ascending Node (RAAN) per Orbit	(deg)	6,9
Orbit Altitude	(km)	600
Orbit Inclination	(deg)	87,7

- A constellation composed of 1269 satellites:
- Each satellite covers a UE on a coverage of elevation (EL) min of 45°.
- One satellite at least in visibility for the UE and two during satellite handover period
- The earth surface is covered by 290850 cells [92]
- Each satellite in the C & Q/V band covers a surface on the earth of diameter 1050 km composed of 499 cells as in **Figure 4-1**
- Each satellite is composed of an active antenna able to generate multiple beams over this coverage (maximum of 100 beams/499 beams).

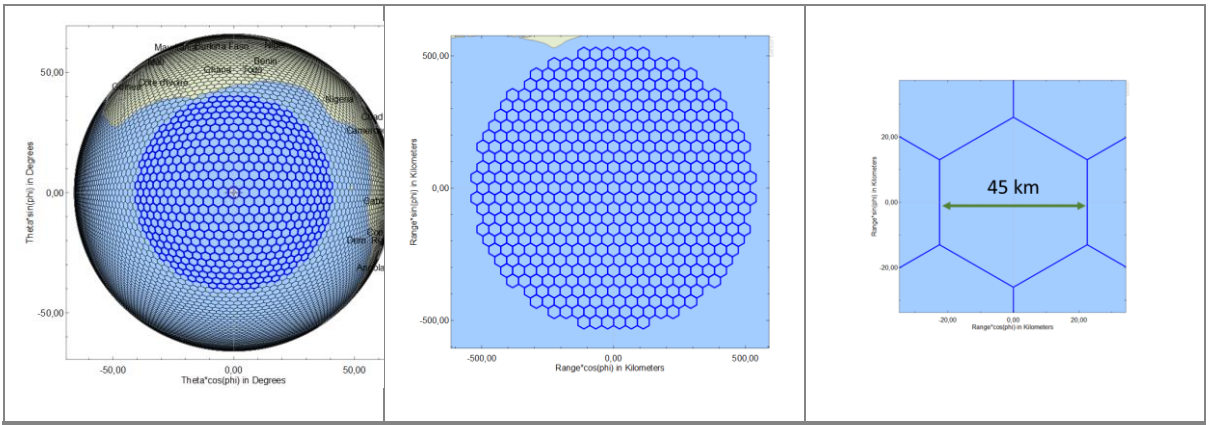

a) Full earth coverage (black) Min EL 45° (blue)	b) Satellite coverage Min EL 45° (blue)	c) Cell size 45 Km

FIGURE 4-1. *SATELLITE COVERAGE (BLUE), EARTH COVERAGE (BLACK)*

4.1.3 Antenna Definition in C Band

The antenna is a Direct Radiating Array (DRA) type antenna composed of 1056 Radiating Elements (REs) at Rx/Tx, in a lattice of 0.742 λ at 4 GHz (55.65 mm) and 0.65 λ at 3.5 GHz. The geometry of the antenna is a flat panel composed of blocks of 16 RE Rx/Tx arranged as described in **Figure 4**-2 below:

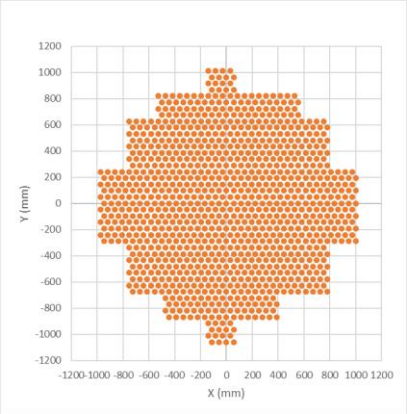	bande_C_1056_RE_0742 ++++ mm elem001 -111,3 -1060,2749 elem002 -55,65 -1060,2749
Flat panel antenna of 1056 RE Hexagonal lattice	**File Format**: 55,65 mm of lattice (0.742 λ at 4 GHz)Id X(mm) Y(mm) 0.65 λ at 3.5 GHz

FIGURE 4-2. ANTENNA GEOMETRY DESCRIPTION

The radiating element characteristic (pattern) is given below:

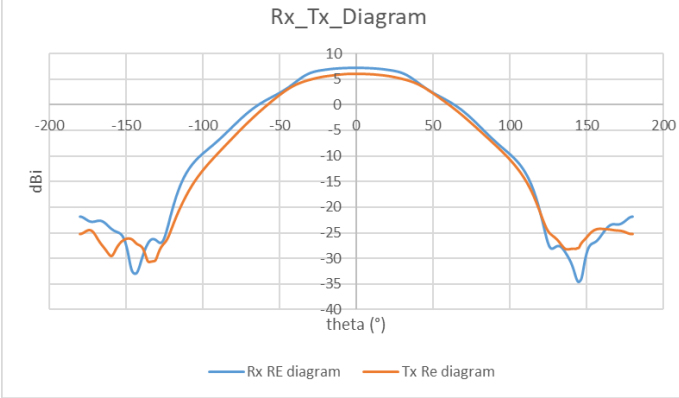

RE radiating element (Rx/Tx)

FIGURE 4-3. RADIATION PATTERN

The radiating element bandwidth is 3.4-3.5 GHz (Tx) and 3.9-4 GHz (Rx) and is illustrated in **Figure 4-3**. The 3dB beamwidth in Tx is 90° and in Rx is 81°, which are typical values for a 0.65 λ and 0.742 λ radiating element size, respectively.

4.1.3.1 Antenna Numerology in C Band

Frequency band and numerology are recalled in **Figure 4-4**:

Bandwidth of the antenna in Rx and Tx is 100 MHz.

ID	Frequency Range				Used Frequency		Channel Bandwidth		PRB						PRACH
	Uplink Sat Rx / UE Tx		Downlink Sat Tx / UE Rx		Uplink Sat Rx / UE Tx	Downlink Sat Tx / UE Rx	Uplink Sat Rx / UE Tx	Downlink Sat Tx / UE Rx	Uplink Sat Rx / UE Tx	Downlink Sat Tx / UE Rx	Number of carriers	SCS bandwidth	PRB bandwidth	Nummber of PRB	PRACH bandwidth
	Fmin (GHz)	Fmax(GHz)	Fmin (GHz)	Fmax(GHz)	GHz	GHz	MHz	MHz	kHz	kHz	-	kHz	kHz	-	kHz
C2	3,4	3,5	3,9	4	3,9	3,4	100	100	360	360	12	30	360	273	3600

FIGURE 4-4. NUMEROLOGY C BAND MIN FREQUENCY 3.4 GHZ AND MIN UPLINK FREQUENCY 3.9 GHZ

The numerology taken is issued from table 5.3.21 for FR1 of document [93]

4.1.3.2 Antenna Beams Management

Several beams could be overlapped on the same cells (at a level of 1 Physical Resource Block (PRB)). The maximum power is evaluated on the basis of 100 active beams over 499 cells occupying the full bandwidth. Nevertheless, the selection of the active beams shall be made with an optimization of the C/I in relation with the frequency allocation or with respect to a fixed target of C/I. Thus, according to the target, a best scheme or a better strategy could be decided and applied:

- Dynamically calculating and selecting the beams in a beam hopping frame that reduces the aggregated C/I.
- Fixed scheme or locally partially colored frame with full frequency allocation to be optimized according to beam hopping frame.

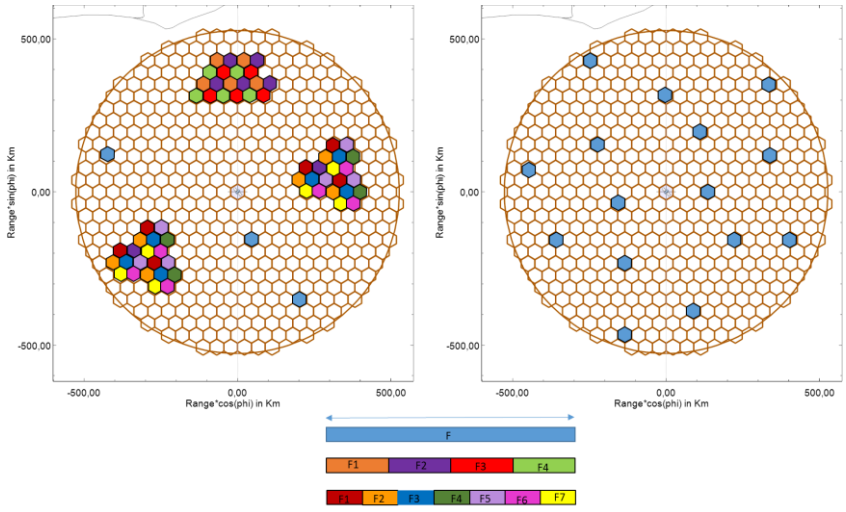

FIGURE 4-5. DYNAMIC COLORATION ACCORDING TO BEAM HOPPING FRAME AND ACTIVE BEAMS

Several studies concerning antenna beam management have been done in literature. In the present case, some new algorithms based on AI/RIC could be investigated.

Moreover, the cells' fixed coverage is ensured by a LEO satellite constellation which moves with time. During the displacement, the laws and beam pointing are refreshed and when the satellite is out of view of the coverage, the handover to the adjacent satellite shall be ensured. Thus, to ensure this handover some cells are in the visibility of two satellites during 10s (see **Figure 4-6** and for details in [92]):

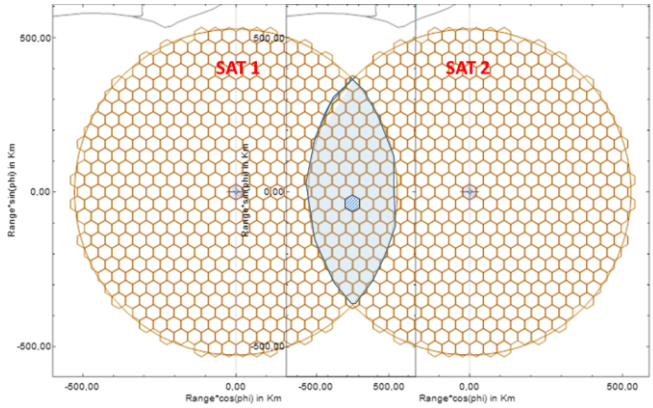

FIGURE 4-6. HANDOVER AREA: 2 SATELLITES IN VISIBILITY FOR THE UE

The antenna is able to generate multiple beams based on a full Digital Beamforming Network (DBFN) (i.e., no theoretical limitation in the number of beams): only the computation capacity and the memory storage capacity shall be sized accordingly. For a first evaluation, the number of active beams is limited to 100 with a maximum Radio Frequency (RF) power of 2200 W.

4.1.3.3 Antenna Beamforming in C Band

The earth surface is decomposed into cells (290850) ensured by a constellation of satellites. Each satellite is able to cover a maximum of 499 cells (field of view). In average, the number of cells for coverage purposes is almost 230 cells per satellite. The worst case is at the equator due to coverage overlapping of the satellite with elevation (see [92]).

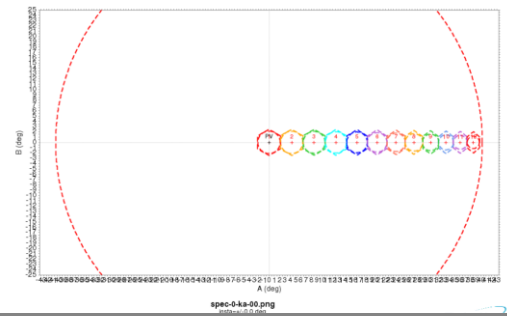

N° beam	1	2	3	4	5	6	7	8	9	10	11	12
beam position (°)	0.000	4.282	8.510	12.634	16.596	20.404	23.980	27.360	30.488	33.414	36.094	38.575

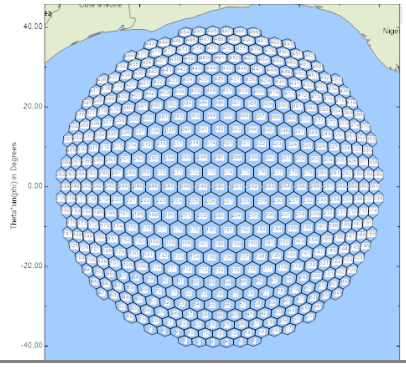

499 cells over a coverage of (Angular position) /numbering of cells

FIGURE 4-7. ANGULAR POSITION OF THE CELLS

The beamforming is realized on each cell according to their position in order to adapt the beam to the coverage. The optimization has been performed in amplitude and phase according to the cell angular size (solid angle) which varies according to the scan angle (see **Figure 4-7**). Amplitude dynamic goes up to 40 dB in Rx and is limited to 6dB in Tx in order to remain at the best functioning point of the amplifier. The active beam selection is designed to maintain the efficiency of each amplifier in the chain.

The complexity of beam shaping depends on the payload optimization (dissipation/consumption and cost), namely: phase only, amplitude and phase, on the target of performance and on the chosen mode of operation. The aim is to optimize the capacity according to the maximum available power by controlling the dissipation capacity of satellites in orbit. The RIC management shall define the best mode of operation to be used during the orbit of each satellite. The management of the interference and the level of C/I will allow to refine the performance of the satellite.

4.1.3.4 Resume of C-Band Antenna Satellite and UE (Handheld)

SATELLITE	Parameter	Unit	Value
	Satellite	-	LEO-600
	Altitude	km	600
	Band Name	-	C
	Nb spots total	-	499
	Cell diameter	km	45
TX (downlink)	Downlink Frequency	GHz	3,40
	Antenna Size	m	1,95
	Number of ER	-	1056
	Antenna gain (NADIR)	dBi	34,13
	Antenna gain (El 45°)	dBi	32,63
	Antenna gain (El 30°)	dBi	31,12
	EIRP density	dBW/MHz	28,00
	EIRP density attenuation	dB	0,00
	Effective EIRP density	dBW/MHz	28,00
RX (uplink)	Uplink Frequency	GHz	3,90
	Antenna gain (NADIR)	dBi	35,32
	Antenna gain (45°)	dBi	33,82
	G/T (NADIR)	dB/K	6,50
	G/T (45°)	dB/K	4,99
SCS PRB	SCS	kHz	30
	Downlink BW	MHz	100
	Nb Downlink PRBs	-	273
	Uplink BW	MHz	100
	Nb Uplink PRBs	-	273
C/I	Downlink (Sat TX)	dB	12
	Uplink (Sat RX)	dB	12

UE	Parameter	Unit	Value
	Band Name	-	C
RX (Downlink)	Downlink Frequency	(GHz)	3,40
	Antenna Size	(m)	0,05
	Number of ER	-	1
	Antenna Noise Figure (NF)	(dB)	9,00
	Antenna gain (NADIR)	(dBi)	2,28
	Antenna gain (45°)	(dBi)	0,78
	Antenna gain (30°)	(dBi)	-0,73
SCS & PRB definition	SCS	kHz	30
	Downlink BW	MHz	100
	Nb Downlink PRBs	-	273
	Uplink BW	MHz	100
	Nb Uplink PRBs	-	273
TX (uplink)	Uplink Frequency	(GHz)	3,90
	Antenna Size	(m)	0,05
	Number of ER	-	1
	Antenna gain (NADIR)	(dBi)	3,47
	Antenna gain (45°)	(dBi)	1,97
	Antenna transmit power	dBW	-7
	Antenna transmit power	W	0,20

Satellite synthesis (Value at the center of the cell)	UE synthesis

FIGURE 4-8. RESUME OF C BAND ANTENNA SATELLITE AND UE

4.1.3.5 Beamforming Laws Example in C-Band:

As mentioned previously, different beamforming schemes could be adapted depending on the performance. Several beamforming schemes can be dynamically adopted depending on performance requirements and constraints (dissipation & available power and the C/I) as example given in **Figure 4-9**

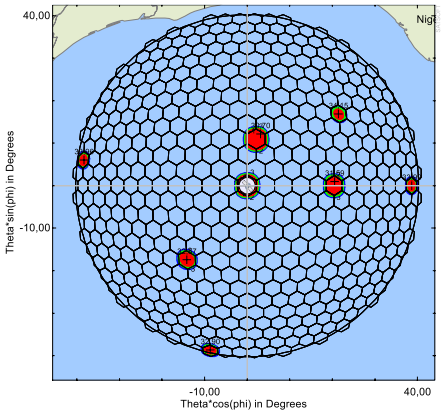

FIGURE 4-9. EXAMPLE OF BEAMS OVER THE COVERAGE (12 DB DYNAMIQUE BEAMFORMING) (-1DB, -2DB,-3DB)

The selection of the active beams could be done according to C/I computed with a set of beams,

The use of deep learning and AI may allow to optimize the data rate according to the needs. Several studies are in investigation in order to manage the efficiency of the global system (NTN+TN) by minimizing interference [23]-[30].

Gain and Losses

The RF chain (RE losses is 2dB) in Tx and Rx.

The Tx power per chain is 2W for a total RF power of 2200 W. This power is limited by the dissipation capacity of the satellite. These values are taken in coherence with the efficiency of the power amplifier and the antenna dissipation capacity.

4.1.4 Antenna Definition in Q/V Band

The antenna in Q and V band are DRA type antennas. These are the two different antennas, either Tx or Rx. The lattice for Q and V band DRA antenna is illustrated in **Figure 4-10**

Each antenna is composed of 7 flat panels and each panel is composed of 512 REs in a lattice of 0.741 λ for both Tx and Rx to be able to cover a minimum Elevation angle of 45°.

	Frequency	λ	lattice	lattice
	GHz	mm	λ	mm
Tx	40	7,5	0,741	5,5575
Rx	50	6	0,741	4,446

FIGURE 4-10. LATTICE FOR Q AND V BAND DRA ANTENNA

The 7 panels are identical and allow each one to generate 4 beams simultaneously.

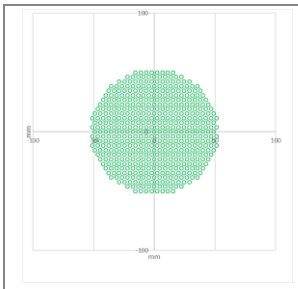	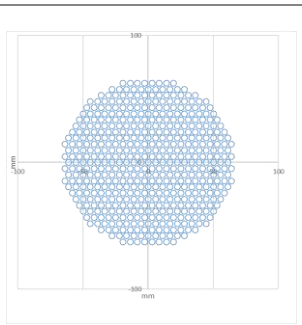
Panel of 512 REs (Rx)	Panel of 512 REs (Tx)
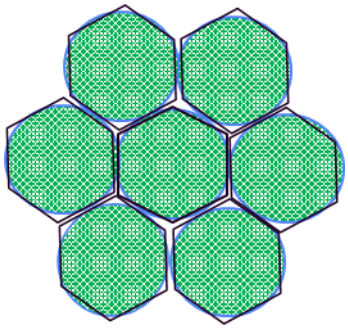	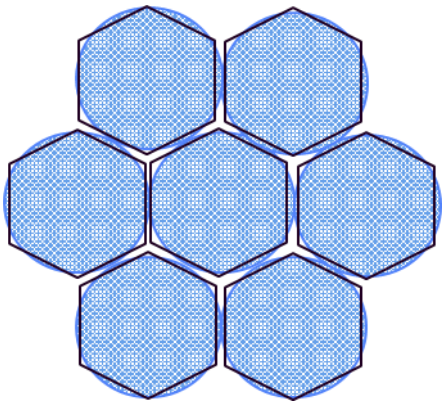
Rx antenna 3584 RE	Tx antenna 3584 RE

FIGURE 4-11. *RX AND TX ANTENNA*

Each panel could have a slight orientation in order to optimize the beam forming performance but, in that case, the power exchange capacity could have some restrictions and not be fully flexible. An analysis will have to be carried out as part of the optimization process if the orientation of the panels is chosen. The balance between performance improvement and decrease in flexibility shall be evaluated. By default, it is assumed that the panels are all arranged on a flat surface.

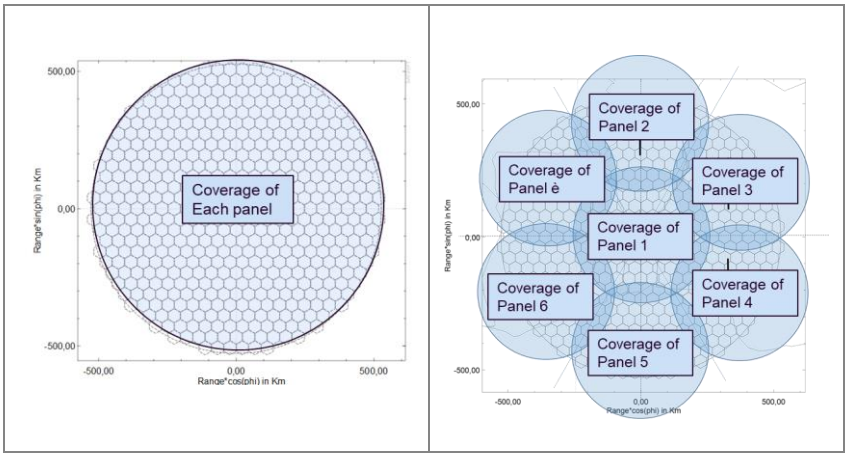

All the 7 panels on a flat surface: Identical beamforming capacity over the coverage	Each panel slightly oriented: each panel generates beams only in a sub-domain.

FIGURE 4-12. 2 WAYS OF BEAM FORMING TO COVER THE COVERAGE

4.1.4.1 Antenna numerology in Q/V band

The antenna bandwidth in Q band and in V band is 400 MHz. The antenna numerology in Q/V band is given in **Figure 4-13**.

	Frequency Range				Used Frequency		Channel Bandwidth		PRB						PRACH
ID	Uplink Sat Rx / UE Tx		Downlink Sat Tx / UE Rx		Uplink Sat Rx / UE Tx	Downlink Sat Tx / UE Rx	Uplink Sat Rx / UE Tx	Downlink Sat Tx / UE Rx	Uplink Sat Rx / UE Tx	Downlink Sat Tx / UE Rx	Number of carriers	SCS bandwidth	PRB bandwidth	Number of PRB	PRACH bandwidth
	Fmin (GHz)	Fmax(GHz)	Fmin (GHz)	Fmax(GHz)	GHz	GHz	MHz	MHz	kHz	kHz	-	kHz	kHz	-	kHz
Q_V2	47,2	50,4	37,5	40,5	50	40	400	400	1440	1440	12	120	1440	264	14400

FIGURE 4-13. NUMEROLOGY USED FOR Q AND V BAND

This numerology is selected from table 5.3.2.2 (FR2-1) of document [93].

4.1.4.2 Beamforming Capabilities of the Satellite in Q/V band

The number of total beams is limited to 28 beams (instantaneously), with 4 beams per panel. The beamforming architecture envisaged is of the Analogue Beamforming Network (ABFN) type, with a limited number of beams (4) and multiple antennas to obtain a suitable number of beams.

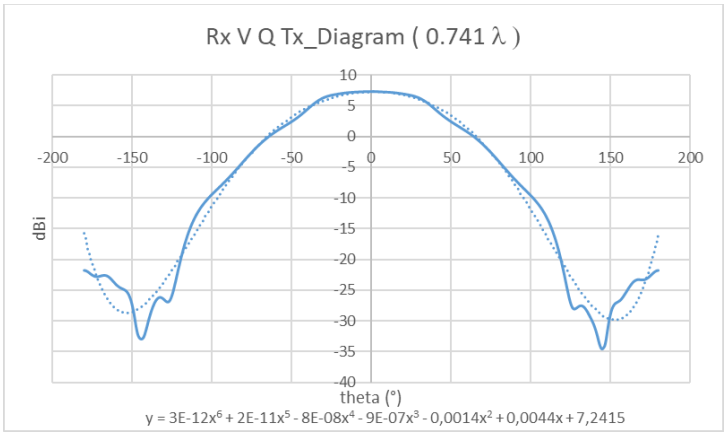

FIGURE 4-14. RADIATING ELEMENT MODEL FOR SATELLITE ANTENNA

The characteristics of the radiating element for a first hypothesis are given in **Figure 4-14**. The radiation element has an aperture efficiency of 90% and a 3-dB beamwidth of 81°. The efficiency will be adjusted according to the technology chosen and the compactness achieved. The ohmic losses are estimated to 2 dB.

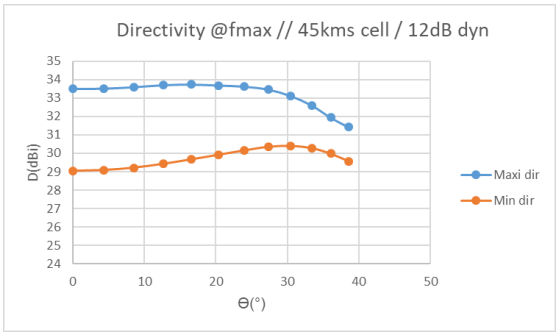

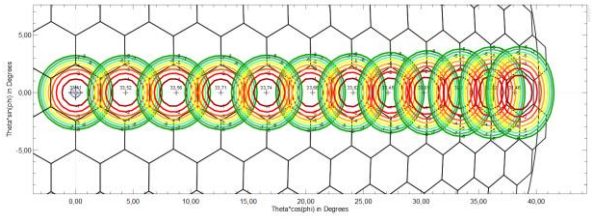

Directivity: Beamforming A/Phase 12 dB (Rx and Tx)	Beams view (Rx and Tx)

FIGURE 4-15. BEAMFORMING IN TX & RX

4.1.4.3 Terminal in Q/V band

The terminal is composed of two functioning antennas (DRA), one in Rx and the second one in Tx. Each one is able to generate a steering beam at a minimum elevation angle of 45°. Each antenna is composed of 379 REs. This definition is subject to evolve with the work of task 3.4 [92] within the 6G-NTN project. But for the first estimates, these values, which still need to be consolidated, are used for the evaluations (see [90] and [91] for different types of terminals, depending on their use and the equipment on which they will be mounted.

4.1.4.4 Resume of Satellite and UE terminal in Q/V Band

SATELLITE	Parameter	Unit	Value
	Satellite	-	LEO-600
	Altitude	km	600
	Band Name	-	Q-V
	Nb spots total	-	499
	Nb active spots during 1ms timeslot	-	4 or 8
	Cell size	km	45
TX (downlink)	Downlink Frequency	GHz	40,00
	Antenna Size	m	0,13
	Number of ER	-	512
	Antenna gain (NADIR)	dBi	33,00
	Antenna gain (El 45°)	dBi	31,49
	Antenna gain (El 30°)	dBi	29,99
	EIRP density	dBW/MHz	18,20
	EIRP density attenuation	dB	0,00
	Effective EIRP density	dBW/MHz	18,20
RX (uplink)	Uplink Frequency	GHz	50,00
	Antenna Size	m	0,1
	Number of ER	-	512
	Antenna Temperature	K	240,00
	Equivalent Temperature	K	767,33
	Antenna gain (NADIR)	dBi	32,40
	Antenna gain (45°)	dBi	30,89
	G/T (NADIR)	dB/K	3,55
	G/T (45°)	dB/K	2,04
SCS PRB	SCS	kHz	120
	Downlink BW	MHz	400
	Nb Downlink PRBs	-	264
	Uplink BW	MHz	400
	Nb Uplink PRBs	-	264

UE	Parameter	Unit	Value
	Band Name	-	Q-V
RX (downlink)	Downlink Frequency	GHz	40,00
	Antenna gain (NADIR)	dBi	31,59
	Antenna gain (45°)	dBi	30,09
	G/T (NADIR)	dB/K	3,06
	G/T (45°)	dB/K	1,56
SCS PRB	SCS	kHz	120
	Downlink BW	MHz	400
	Nb Downlink PRBs	-	264
	Uplink BW	MHz	400
	Nb Uplink PRBs	-	264
TX (uplink)	Uplink Frequency	GHz	50,00
	Antenna gain (NADIR)	dBi	31,09
	Antenna gain (45°)	dBi	29,59
	Antenna transmit power	dBW	4
	Antenna transmit power	W	2,51

Satellite synthesis (Value at the center of the cell)	UE synthesis

FIGURE 4-16. RESUME OF THE CHARACTERISTICS OF THE SATELLITE AND UE IN Q/V BAND

4.1.5 Data for C-band and Q/V Band

- Satellite ephemeris (satellite position at one moment)
- Cell angular positions (satellite at nadir): 499 positions over a coverage of elevation of 45°
- C-band radiating element: Rx (0.742 λ) and Tx (0.65 λ) (field in theta/phi cuts)
- Beamforming law for C band: phase only and amplitude + phase (dyn 12 dB)
- Pattern diagrams in C band for Tx and Rx
- Antenna in C-band: X,Y position of the radiating elements
- Q/V band radiating element: 0.741 λ for both Tx and Rx
- Beamforming law for Q/V band: phase only and amplitude + phase (6dB and 12 dB)
- Pattern diagrams in Q/V band for Tx and Rx

After having all the system description and relevant information, the rest of the section is dedicated to Traffic Load in NTN and the datasets comprising user spatial distribution is provided. These details are directly extracted from deliverable D4.3 from the 6G-NTN project.

4.1.6 Traffic Load

In the context of traffic load in relation to the use cases, particularly PPDR and direct-to-smartphone, a realistic traffic pattern is provided here for the purpose of integration with the datasets to complete the input information, which is typically required for designing the AI-enabled controller. The data, which refers to user demand as user traffic profile (UTP), is a collection of KPIs whose values provide information about the desired emergent features of the other provided datasets. As an example, **Figure 4-17** outlines the set of KPIs for the direct-to-smartphone or PPDR (extracted from D2.3).

In this regard, a UTP encompasses KPIs such as latency, information on link availability and reliability, experienced user data rate and activity factor [95], among other performance targets. Their values are derived from the analysis of several direct-to-smartphone subcases. For instance, the UTP outlined in **Figure 4-17** relates to a use case whereby users are trekking in areas without continuous terrestrial coverage and wish to continue using their audio chat and video streaming services, both in outdoor and indoor conditions, with different quality of experience. This specific subcase notably highlights high user UL requirements, which can be seen via the high values on the uplink Experienced User Data Rate and Activity Factor. It completes a more general case in which the Activity Factor DL is significantly higher than UL.

Direct-to-Smartphone UE type		Experienced user Data Rate		Activity Factor		Monthly User Traffic		Busy Hour Usage Rate		Latency	Radio Link Availability	Reliability	Mean User Density	Area Traffic Capacity		User Distribution	UE Speed
		DL	UL	DL	UL	DL	UL	DL	UL					DL	UL		
	(Text)	Mbps		%		GB/Month		Kbps		ms	%	%	user/km^2	Kbps/km^2		(Text)	km/h
Outdoor	Handheld	2	10	5.0	5.0	167	33	100	500	< 30	99.9	99.999	5	500	2500	UEs distributed on trails	20
Light indoor	Handheld	0.01	0.01	5.0	5.0			0.5	0.5	< 50	99.9	99.99	5	2.5	2.5		

FIGURE 4-17. KPIS FOR THE DIRECT TO CELL OR PPDR USECASE

The description of KPIs is detailed as follows according to [95]

- **Experienced User Data Rate**: Represents the minimum data rate needed to achieve a target Quality of Experience (QoE).
- **Activity Factor**: Ratio of simultaneous active UEs to the total number of UEs.
- **Monthly User Traffic:** Monthly User Traffic is expressed in GB/user/month for both the downlink and uplink.
- **Busy Hour Usage Rate:** Represented as,

  Busy Hour Usage Rate DL = Experienced Data Rate DL * Activity Factor DL

  Busy Hour Usage Rate UL = Experienced Data Rate UL * Activity Factor UL

- **Mean User Density:** Represents the average user density over a defined area.
- **Area Traffic Capacity:** Total traffic throughput served per geographic area.

4.1.7 User Spatial Distribution

The user spatial distribution of a subset of use cases such as Maritime, PPDR and Direct to cell defined in deliverable D2.1 of the project, is provided in D4.3. These datasets are crafted to be employed to train AI networks for optimizing the resource management functions. In essence, the brief description about the nature of those datasets and corresponding attributes are provided below, while detailed insights can be found in D4.3 [2]

Maritime User Spatial Distribution:

One of the preeminent datasets for optimizing the resources for the maritime use case, a weeklong dataset with the resolution of one hour, is acquired from a reputable data provider (VesselFinder & VT Explorer) [96]. This dataset consists of realistic marine traffic information updated every one hour obtained from Automatic Identification System (AIS) over the entire Mediterranean Sea. The dataset attributes of maritime traffic are shown in **Figure 4-18**.

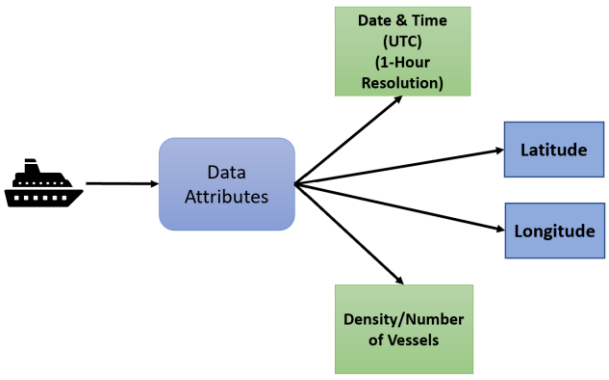

FIGURE 4-18. THE DATA ATTRIBUTES OF MARINE TRAFFIC DATASET ACQUIRED USING AIS

The dataset is stored in MATLAB files (.mat extension). The entire region of the Mediterranean Sea is converted into grids of haversian distance with 100 km x 100 km resolution. Each hour of the dataset contains two .mat files. The first one provides a matrix representing the central coordinates (longitude, latitude) of each grid while the second one provides the vessels density in each grid at any given hour.

PPDR User Spatial Distribution:

The PPDR-related open dataset is identified and provided in deliverable D4.3. This open dataset referred to as Ookla dataset, facilitates global fixed broadband and mobile network performance in the form of tiles. The fixed broadband refers to measurements taken from mobile devices with non-cellular type connection i.e., Wi-Fi or Ethernet, whereas the mobile network measurements are taken from mobile devices with cellular type connection, for instance, 4G LTE and 5G NR. The tiles are partitioned into zoom level 16 Web Mercator projection, measuring approximately 610.8 meters by 610.8 meters at the equator. The zoom level corresponds to the scale of terrestrial coverage. For instance, zoom level 0 corresponds to a single tile covering the entire globe while zoom level 1 divides the globe into 4 equal tiles. The dataset is provided in two formats: shape (SHP) files and Parquet files with each tile represented in World Geodetic System (WGS- EPSG:4326). The dataset spans from the period of Q1 2019 to the recently complete quarter Q2 2023 and is updated every quarter year (three months) [97]. Further details can be found in D4.3.

Direct to Smartphone User Spatial Distribution

The Ookla and along with Meta AI datasets for direct-to-smartphone use case provide useful information for the design of radio network management functions. However, to accurately manage the resources, it is essential to also know per user terminal demand for these use cases, which has been provided in subsection 4.1.6 as ´´Traffic Load´´. The given Meta AI dataset provides information about population density along with the geocoordinates while Ookla's dataset provides information about fixed and network mobile indicators. Combining both datasets provides insights about the approximate overall user demand. This spatial distribution can help to optimize the algorithms in such a way that the system capacity fulfills the approximate requested demand. The dataset attributes are shown in **Figure 4-19**

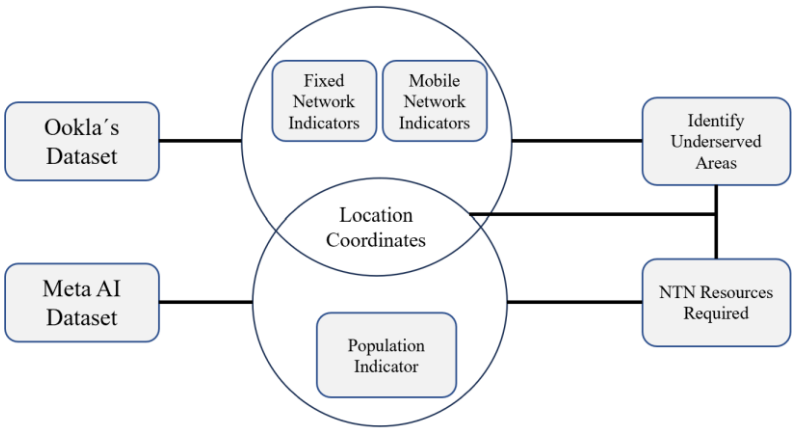

FIGURE 4-19. *THE MECHANISM OF ACQURING USER DISTRIBUTION FOR DIRECT TO SMARTPHONE USECASE*

Disclaimer: The detailed description about these datasets can be found in Deliverable D4.3 **[2]**

5 OPTIMIZATION TECHNIQUES

This section provides the proposed AI/ML optimization algorithms for each resource network function, as well as some insights on initial outcomes. The detailed optimized outcomes analysis will be provided in the final report in D4.6.

5.1 TRAFFIC OFF-LOADING

5.1.1 System Description

The system model considered for the traffic off-loading optimization technique is presented in this section. We consider a rural area served by a uniform deployment of terrestrial 6G Base Stations (BS). As recommended in 3GPP TR 38.901, for the considered Rural Macro (RMa) scenario we assume a hexagonal grid layout of $N_{BS} = 19$ macro sites deployed at an Inter-Site Distance (ISD) of 5000 m. Each macro site has a height h_{BS} of 35 m and three sectors per site. All BSs reuse the same terrestrial frequency band B_{TN}. The same rural area is assumed to be served by a 6G NTN beam on an orthogonal band B_{NTN} of the same width.

The users are uniformly distributed in the reference area and generate uplink traffic assuming a full buffer model, meaning that every user in the network is continuously active, generating data traffic at the maximum possible rate. The number of UEs in the coverage area is configured to ensure that the requested user traffic exceeds the terrestrial system capacity, meaning that, at a specific instant of time, only a subset UE_S of users is served while users UE_W are waiting to be served. Additionally, all the radio resources of each BS are continuously assigned to the served users. In this network function, the radio resources are considered to have already been scheduled to the users assuming that: i) in the radio resource scheduling phase the served UEs are assigned the same amount of radio resources, and ii) each UE is allocated to the BS that has the strongest received power. The allocation of a user to the corresponding BS is represented by the set $U_A = \{u_A^1, \dots, u_A^j, \dots, u_A^{N_u}\}$, N_u being the cardinality of $UE_W \cup UE_S$, and $u_A^j = \{1, \dots, N_{BS}\}$.

In this context, part of the exceeding load of the TN is assumed to be offloaded to the NTN. The traffic offloading can happen in two ways:

1. Part of the users UE_W, that are waiting to be served by the TN, are served by the NTN on the orthogonal band B_{NTN}. In this case, the NTN serves users that are not assigned to any TN radio resource and, thus, the TN scheduling process is not impacted by the NTN service. The system throughput T_{TOT} (TN+NTN) is expressed as:

$$T_{TOT} = \sum_{BS} B_{TN} log_2(1 + SINR_{BS}) + T_{NTN} \quad (5.1)$$

   With $SINR_{BS}$ being the Signal to Interference plus Noise Ratio of the specific BS, and T_{NTN} being the throughput of the NTN service on the band B_{NTN}.

2. The network function is free to select the UEs to be served by the NTN not only among the subset UE_W, but also among the subset UE_S that is already served by the TN. If a UE connected to BS_k is offloaded to the NTN, then, a UE that belongs to UE_W and that is in the coverage area of BS_k is connected to BS_k in the same radio resources of the previous UE.

5.1.2 Problem Formulation

Leveraging on a broad and centralized view on the network, the traffic off-loading network function aims at increasing the system throughput compared to the legacy UE allocation described in case 1. To this regard, the network function can optimize the system throughput by selecting which UEs to offload from the TN to the NTN, aiming to maximize the SINR at the base stations. We define the optimization problem as the selection of W_A that satisfies the objective function P, where $W_A = \{w_A^1, \dots, w_A^j, \dots, w_A^{N_u}\}, w_A^j \in \{0,1\}$ is a set that identifies the allocation of the user j to the NTN.

$$P = \max_{W_A} \sum_{BS} B_{TN} log_2(1 + SINR_{BS}) + T_{NTN} \quad (5.2)$$

$$C1: \sum_{j=1}^{N_u} w_A^j \leq C_{ntn}$$

$$C2: \sum_{j} w_A^j = \sum_{j} s_U^j, \qquad j|UE_j \in BS_k$$

The constraint in C1 denotes that the number of UEs that are offloaded must be lower or equal to the capacity C_{ntn} of the NTN. The constraint in C2 imposes that the number of UEs that are offloaded from the base station BS_k to NTN must be equal to the number of new UEs that connect to BS_k after the offloading operation. Indeed, $S_U = \{s_U^1, \dots, s_U^j, \dots, s_U^{N_u}\}, s_U^j \in \{0,1\}$ is a set that identifies the connection of a user UE_j to the TN after the offloading of the set W_A.

5.1.3 Optimization Framework

The optimization technique selected to implement this network function is based on Deep Q-Learning (DQL). DQL is an advanced Reinforcement Learning algorithm that leverages the power of deep neural networks to solve problems with high-dimensional state spaces, such as the traffic off-loading network function that is being evaluated. This approach extends the classic Q-Learning algorithm by using a neural network to approximate the Q-value function, which predicts the expected cumulative reward for taking a given action in a given state and following the optimal policy thereafter.

DQL has been selected for this network function because its learning process involves an agent interacting with an environment and does not require large datasets. The agent perceives the environment's state and takes actions that affect the state, receiving rewards as feedback. The state space $\mathcal{S}$ represents all possible situations the agent can encounter. The action space $\mathcal{A}$ includes all possible actions the agent can take. These actions might be discrete or continuous. The reward function $R(s,a)$ provides feedback from the environment, signaling how good or bad the action taken by the agent was in a specific state. This reward is used to guide the learning process, pushing the agent towards actions that maximize cumulative rewards. The Q-function $Q(s,a)$ estimates the expected cumulative reward of taking action a in state s and following the optimal policy thereafter. The policy π is the strategy the agent uses to decide its actions based on the current state.

The DQL framework is leveraged in this optimization function to address the high dimensionality of the considered environment. Specifically, in this first implementation, the DQL has a state space $\mathcal{S}$ composed by: i) the allocation of the UEs to the base stations U_A, ii) the signal strength of each UE, received from the base station they are allocated to ($SS = \{ss^1|_{BS_k}, \dots, ss^j|_{BS_k}, \dots, ss^{N_u}|_{BS_k}\}, with\ \mathrm{k}|\mathrm{k} = 1,2,\dots,N_{BS}$). As a second step, it is foreseen to evolve from the full-buffer traffic model and to consider a more detailed one. In this case, also

the traffic state of each UE could be considered in the state space. The action space $\mathcal{A}$ is the set W_A that identifies the allocation of the UEs to the NTN. The reward is computed to reflect the optimization objective of maximizing the system throughput, as the throughput gain obtained by applying the selected action:

$$R(s_n, a) = \sum_{BS} B_{TN} log_2\left(1 + SINR_{BS}^{S_n}\right) - \sum_{BS} B_{TN} log_2\left(1 + SINR_{BS}^{S_{n+1}|a}\right) \quad (5.3)$$

5.1.4 Network Function Simulation

The simulation reflects the system description implementing the optimization framework and defining the scenario with which the optimizer interacts. As described in section **5.1.1**, for the considered RMa scenario we assume a hexagonal grid layout of 19 macro sites with three sectors per site. In the complete scenario, the network function would need to optimize the off-loading of all the UEs in the satellite coverage area considering the radio resources they are allocated to. Since full-buffer traffic model is assumed and since the UEs are assigned with the same amount of radio resources, the problem is symmetric in the radio resources space. This means that it is possible to focus the optimization problem on a single radio resource without losing generality. For this reason, for the group UE_S, only N_{BS} users are considered, one for each base station. Similarly, other N_{BS} users are selected within UE_W such that each UE is associated to a different base station. The first group is represented by the red markers in **Figure 5-1**, while the second group is represented by the blue markers. At each iteration of the simulation the two groups of users are dropped in a random position that reflects the UE-BS allocation. Taking as example the base station 1 in the center of the area, the served UE (red) and the waiting UE (blue) are randomly deployed in the coverage area of BS_1 marked by the red polygon. As mentioned above, the DQL decides the optimal UE to be offloaded based on the state space $\mathcal{S}$. The radio resource of the offloaded UE is allocated to the waiting UE present in the same BS coverage area.

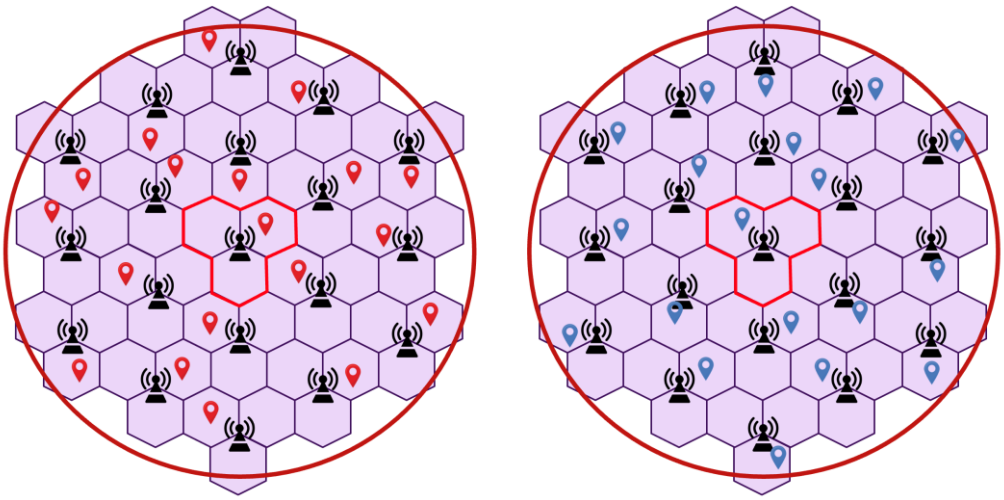

FIGURE 5-1: ALLOCATION OF SERVED (RED) AND WAITING (BLUE) USER EQUPMENT

The simulation reflects the configuration parameters from 3GPP TR38.901 regarding the scenario and the path loss model. The relevant information about the base station antenna model is reported in **Table 6.** 3GPP BS ANTENNA MODEL [38.921] from 3GPP TR 38.921 [38.921]. For the UE antenna a gain of 0 dB is considered in line with Rep. ITU-R M.2412-0. Additionally, a BS receiver noise figure of 5 dB and a thermal noise level of -174 dBm/Hz are considered. [ITU-R M.2412-0].

TABLE 6. 3GPP BS ANTENNA MODEL [38.921]

A_m (dB)	**30**
SLA_v (dB)	30
φ_{3dB} (deg.)	90
θ_{3dB} (deg.)	90
$G_{E,max}$ (dBi)	5.5
L_E (dB)	2.0
(M, N)	(16, 8)
Number of supported polarizations, P	2
d_h (m)	0.5λ
d_v (m)	0.5λ
Horizontal coverage range (deg.)	+/- 60
Vertical coverage range (deg.)	**90 to 120**

The path loss model for the rural macro area selected from TR 38.901 is expressed as:

$$PL_{\text{RMa-LOS}} = \begin{cases} PL_1 & 10\text{m} \le d_{2D} \le d_{BP} \\ PL_2 & d_{BP} \le d_{2D} \le 10\text{km} \end{cases}$$

$$PL_1 = 20\log_{10}(40\pi d_{3D} f_c / 3) + \min(0.03h^{1.72}, 10)\log_{10}(d_{3D}) - \min(0.044h^{1.72}, 14.77) + 0.002\log_{10}(h)d_{3D}$$

$$PL_2 = PL_1(d_{BP}) + 40\log_{10}(d_{3D} / d_{BP}) \quad (5.4)$$

Where $h = 5\ m$, $W = 20m$, and the UE are considered to be always in line of sight.

Initial results are reported in **Figure 5-2**, **Figure 5-3** and **Figure 5-4**. **Figure 5-2** shows the cumulative density function of the system spectral efficiency after the optimal allocation of the user to the NTN. The system spectral efficiency is computed as the mean of the spectral efficiency of each BS. **Figure 5-3** shows the performance increase in terms of percentual spectral efficiency after the optimization. **Figure 5-4** shows the cumulative density function of the spectral efficiency of each BS in the scenario after the optimization. It provides additional insights on the local BS performances showing that, although the system spectral efficiency increase is promising, there are cases in which the spectral efficiency of a BS could be not acceptable. This will be taken into account in the next deliverable together with more detailed simulation results.

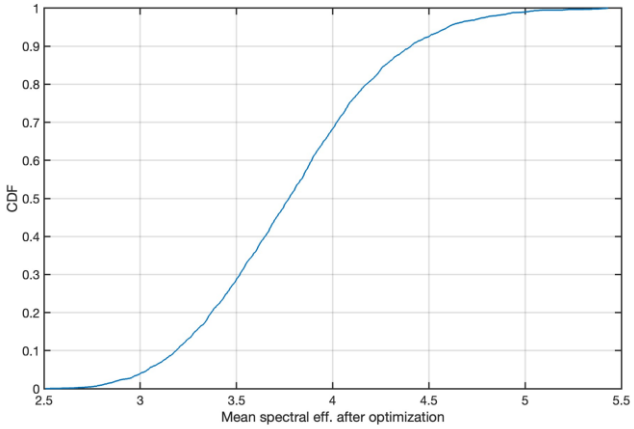

FIGURE 5-2: CDF OF THE MEAN SYSTEM SPECTRAL EFFICIENCY AFTER OPTIMIZATION.

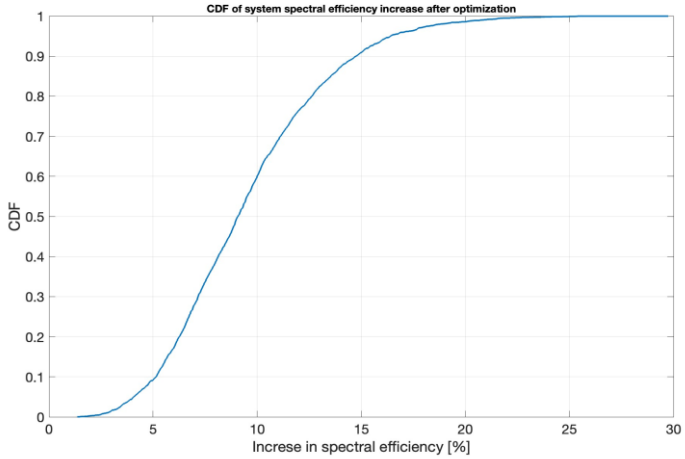

FIGURE 5-3: CDF OF SYSTEM SPECTRAL EFFICIENCY PERCENTUAL INCREASE AFTER OPTIMIZATION

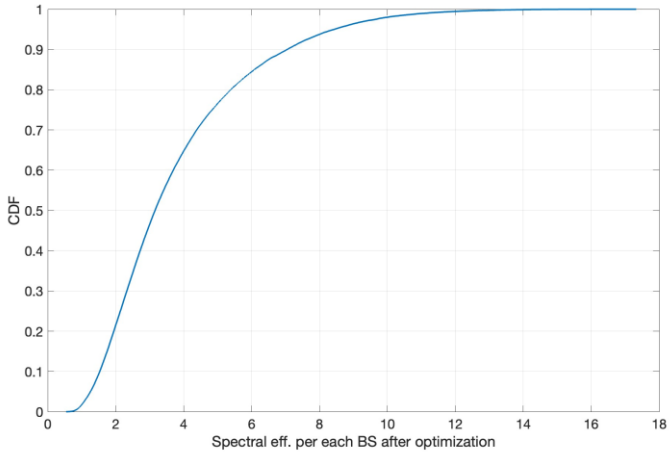

FIGURE 5-4:CDF OF THE SPECTRAL EFFICIENCY OF THE BASE STATIONS AFTER OPTIMIZATION.

5.2 FRACTIONAL FREQUENCY REUSE

5.2.1 System Description

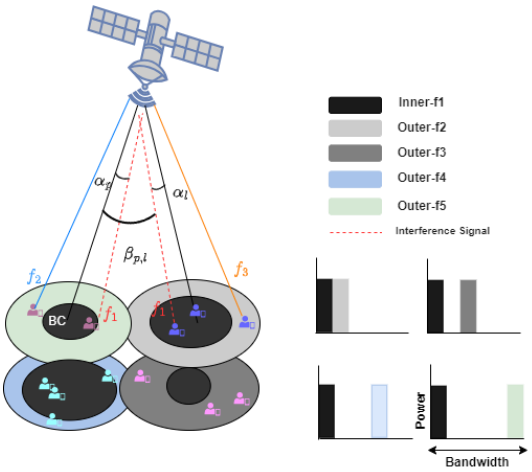

FIGURE 5-5. FFR FRAMEWORK WITH DYNAMIC INNER TO OUTER RATIO

Before indulging in the FFR technique, it is vital to comprehend the multi-beam satellite system following the FFR model which is essential to create an environment for AI/ML algorithms. For this purpose, consider a global model of multi-beam satellite system with B beams and beam $b, b = 1, \dots, B$ which is further split into local model for FFR as K outer beams and $\exists\, N$ inner beams inside, where $N = K$ at any time t. Each outer beam $k, k = 1, \dots, K$ and inner beam n, $n = 1, \dots, N$ is serving the heterogenous non-uniform user traffic (UT) U, $u = 1, \dots, U$ with geocoordinates $(x, y)_u$ and, $\forall K$ the area of any beam n follows $A_n(\theta_n) \subseteq A_k(\theta_k)$, where A_n and A_k is inner and outer beam area, and can be defined by the function of inner and outer beamwidths θ_n and θ_k, respectively. In this way, any user from UT is further distinguished as ith and jth user located in desired outer beam and inner beam and identified as beam $k(i)$ and $n(j)$, respectively. Each outer and inner beam is allocated with Bw_k and Bw_n bandwidth resources while the transmission power resources to outer and inner beam is P_k and P_n, respectively. Hence, considering a global beam model, a general received signal r_u at any user u in any beam B, can be represented as,

$$\mathbf{r}_u = \mathbf{h}_{\mathrm{u}}{}^{\mathrm{H}}\mathbf{s} \tag{5.5}$$

where H is Hermitian transpose, $\boldsymbol{s}$ is the transmitted signal and defined as $\boldsymbol{s} = \boldsymbol{W}\boldsymbol{x}$, where $\boldsymbol{x} \in \mathbb{C}^{U\times 1}$ are transmitted symbols and $\boldsymbol{W} \in \mathbb{C}^{B\times U}$ the beamforming matrix, $\boldsymbol{h_u} \in \mathbb{C}^{K\times 1}$ is the channel vector associated with any user u. Concatenating all the channel vectors corresponding to all the UT, the above CSI parameter can be rewritten as,

$$\boldsymbol{r}_u = \boldsymbol{H}\boldsymbol{s} \tag{5.6}$$

where $\boldsymbol{H} \in \mathbb{C}^{U\times B}$ now represents the system channel matrix. For better understanding, the channel matrix $\boldsymbol{H}$ is further split as $\boldsymbol{H} = \boldsymbol{D}\boldsymbol{F}$, where the real matrix $\boldsymbol{F}$ is determined $\boldsymbol{D}$ represents the phase-slant due to different propagation path between the users. Moreover, interpreting **Figure 5-5**, α is an azimuth angle of a desired user terminal u relative to the beam center ξ of desired beam $b(u)$ and used to calculate the relative beam gain while β is an azimuth angle of interfering user terminal relative to the desired ξ. This angle provides the relative beam gain

from interfering user to desired ξ. Considering this, any (u, b) entry of the matrix $\boldsymbol{H}$ can be given as,

$$h_{u,b} = \frac{\sqrt{G_{trans(u,b)} G_{r(u,b)} G_{tx(u,b)}}}{\left(4\pi \frac{d_{u,b}}{\lambda}\right)\sqrt{\kappa B_w}} \tag{5.7}$$

where $G_{trans(u,b)}$ and $G_{r(u,b)}$ represent the transmission gain and receiving gain to $\mathrm{u_{th}}$ user in any beam b, respectively, while $G_{tx(u,b)}$ is the gain defined by transmission radiation pattern at the $\mathrm{u_{th}}$ user location, $d_{u,b}$ is the distance between satellite antenna and the user u located in beam b, λ is the wavelength and κ is the Boltzmann constant.

If the user u is located in the desired beam $b(u)$ then $g_{(u,b(u))} = \left|h_{u,b(u)}\right|^2$ represents the channel gain that the user is experiencing in its desired beam. The users in adjacent beams may utilize the common frequency bands, therefore, the signal received by any user should also include the interference caused by the other users using the same frequency sub-bands in other beams. Hence, the SINR of the global model for any user u in its desired beam $b(u)$ can be formulated as,

$$SINR_{u,b(u)}^{global} = \frac{P_{b(u)} g_{(u,b(u))}}{\sum_{b=1,b\neq b(u)}^{B} P_{(u,b)} g_{(u,b)} + N_o} \tag{5.8}$$

where $P_{b(u)}$ and $P_{(u,b)}$ is the transmitted power allocated to desired beam and all other interfering co-frequency beams, respectively, and $\mathrm{N_0}$ is white Gaussian noise.

After defining the SINR expression for the global model, the discussion indulges into splitting the expressions for the local model implicitly representing the FFR system description. This helps to formulate the optimization problem statement. Nevertheless, prior to do so, it is essential to identify which FFR framework is to be considered in this network function since a variety of static and dynamic FFR schemes have been used in literature, as discussed in Section **3.2.1**. Also, as it is typically the case in FFR, each satellite beam is partitioned into two areas, A_n and A_k and the users in both areas should be served with distinct frequency resources. Therefore, two potential FFR schemes have been identified for the purpose of mapping into multi-beam satellite system that include traditional Strict FFR (S-FFR), along with introducing the modified version of S-FFR as Partially Strict FFR (PS-FFR).

S-FFR: Recalling from Section **2.3.2** , in S-FFR, the $A_n\ (\theta_n)$ utilizes FR of 1 meaning that the users in inner beam area of each beam assign with the common frequency sub-band. Meanwhile the FR of 4 is utilized for $A_k(\theta_k)$ which allows the users in each adjacent 4 beams utilize the disjoint frequency sub-bands δ. This stringent requirement needs to be in place since the SINR in $A_k(\theta_k)$ is more prone to co-channel interference than $A_n\ (\theta_n)$. This disjoint sub-bands make $A_k(\theta_k)$ resilient to co-channel interference. Hence S-FFR requires in total sub-bands $4+1$ such that $A_k(\theta_k)$ for adjacent 4 beams follow $\delta_k \cap \delta_x = \emptyset$ for $k \neq x$ where $k, x = 1, \ldots 4$. Hence, the local model SINR for S-FFR is reformulated as,

$$SINR_{u,b(u)}^{\mathrm{S-FFR}} = \begin{cases} SINR_{i,n(i)}^{n} = \frac{P_n g_{(i,n(i))}}{\sum_{n=1,n\neq n(i)}^{N} P_n g_{(i,n)} + N_0} \\ SINR_{j,k(j)}^{k} = \frac{P_k g_{(i,k(i))}}{\sum_{k=1,k\neq k(j)}^{K} P_k g_{(j,k)} + N_0} \end{cases} \tag{5.9}$$

PS-FFR: analogous to S-FFR, PS-FFR utilizes FR 4 in $A_k(\theta_k)$ but it does not exert FR 1 in $A_n\ (\theta_n)$ as is the case in S-FFR. Moreover, unlike Soft Frequency Reuse (SFR) that utilizes the entire bandwidth by reusing all the adjacent frequencies in the inner beam area, thereby resulting in more interference cases in both areas, PS-FFR offers the users in $A_n\ (\theta_n)$ to utilize

the sub-bands similar to one of the adjacent $A_k(\theta_k)$. This allows to use the bandwidth more aggressively than in S-FFR since it requires to split the total bandwidth per beam into 4 frequency sub-bands rather than $4+1$. Hence, the SINR relation for PS-FFR in the local model is reformulated as,

$$SINR_{u,b(u)}^{\mathrm{PS-FFR}} = \begin{cases} SINR_{i,n(i)}^{n} = \frac{P_n g_{(i,n(i))}}{\sum_{n=1,n\neq n(i),f(n)=f(n(i))}^{N} P_n g_{(i,n)} + \sum_{k=1,f(k)=f(n(i))}^{K} P_k g_{(j,k)} + N_0} \\ SINR_{j,k(j)}^{k} = \frac{P_k g_{(j,k(j))}}{\sum_{k=1,k\neq k(i),f(k)=f(k(j))}^{K} P_k g_{(i,k)} + \sum_{n=1,f(n)=f(k(j)}^{N} P_n g_{(i,n)} + N_0} \end{cases} \quad (5.10)$$

where f(.) is a beam frequency mapping formula that assigns each beam to a specific set of frequency resources.

Offered Capacity:

Following the SINR relation formulated for both S-FFR and PS-FFR, the average offered capacity per beam b is derived as,

$$C_b = \begin{cases} \frac{1}{|T_n|}\left(\sum_{i\epsilon T_n} Bw_n log_2(1+SINR_{i,n(i)})\right) \\ \frac{1}{|T_k|}\left(\sum_{j\epsilon T_k} Bw_k log_2(1+SINR_{k,k(j)})\right) \end{cases} \quad (5.11)$$

where $|T|$ is the cardinality of a set T which provides the total number of users being served in a desired beam area. The average total offered system capacity can be given as,

$$C_{tot} = \sum_{b=1}^{B} C_b \quad (5.12)$$

Since the system description in terms of both global and local models is readily defined, the problem formulation follows. Nevertheless, prior to that, it is pivotal to identify the factors that may impact the overall system throughput. This would explicitly assist in defining the optimization problem. To do so, the aforementioned FFR schemes are simulated over different inner to outer beamwidth ratios (IORs) φ and different bandwidth allocation to $A_k(\theta_k)$ and $A_n(\theta_n)$ for a simple scenario, i.e., a uniform traffic distribution. The simulation outcomes for such a scenario are depicted in **Figure 5-6.**

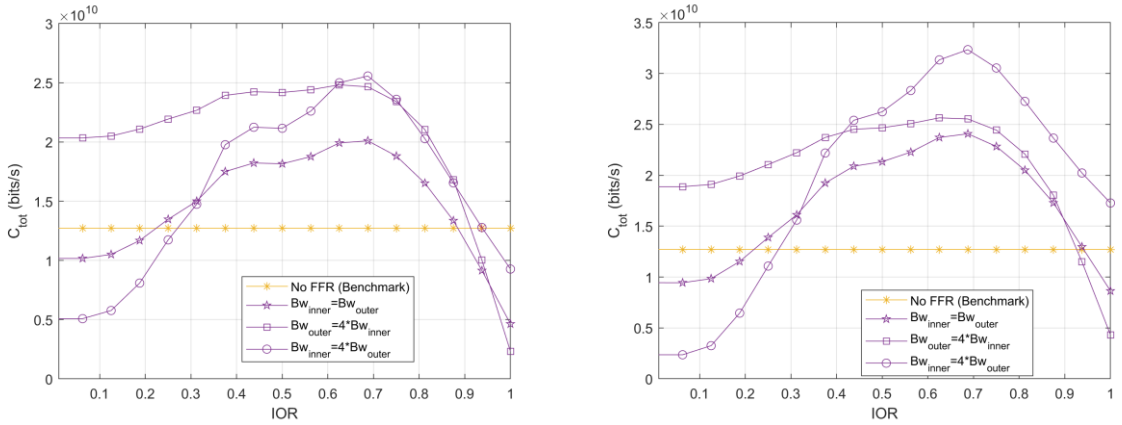

FIGURE 5-6. TOTAL SYSTEM THROUGHPUT CTOT AS A FUNCTION OF IOR AND BANDWIDTH FOR S-FFR (LEFT), PS-FFR (RIGHT).

5.2.2 Problem Formulation

Based on **Figure 5-6**, the throughput performance is explicitly impacted by the inner to outer beamwidth ratio φ, as well as the bandwidth allocation to $A_k(\theta_k)$ and $A_n\,(\theta_n)$, considering that all beam in a system is implementing an identical φ value over time. However, this should not be the case for heterogeneous UT, and neither using an identical φ value would be an optimal solution particularly when traffic is dynamic. Therefore, each beam has to be parametrized by dynamic values of φ. Moreover, in relation to **Figure 5-6** and the parameters in equation 5.9, 5.10, 5.11 impacting the objective function, the joint optimization $\{\varphi, [^{Bw_k}_{Bw_n}], [^{P_k}_{P_n}]\}$ is NP-hard. The overall problem formulation can be summarized as follows,

$$\underset{\varphi,Bw,P\ \forall k,n}{maximize}\ C_{tot} = \sum_{b=1}^{B} C_b$$

$$\begin{aligned}
\textit{subject to}\quad & C_1\colon 0 < \theta_n < \theta_k \ \ \forall n,\ n \epsilon N \quad \forall k,\ k \epsilon K \qquad (5.13)\\
& C_2^{S-FFR}\colon Bw_n + Bw_k \le 2\tfrac{Bw_b}{4+1} \quad \forall n,\ n \epsilon N \quad \forall k,\ k \epsilon K\\
& C_3^{PS-FFR}\colon Bw_n + Bw_k \le 2\tfrac{Bw_b}{4} \ \ \forall n,\ n \epsilon N \quad \forall k,\ k \epsilon K\\
& C_4 :\ P_n \ \le P_{max} \qquad \forall n,\ n \epsilon N\\
& C_5 :\ P_k \ \le P_{max} \qquad \forall k,\ k \epsilon K
\end{aligned}$$

In this problem, the search variables are $\varphi, Bw, P \ \ \forall k, n$ over the total throughput optimization. Constraints C_1 represents two conditions: 1) θ_n must be greater than 0 and 2) θ_n must less than θ_k. On the one hand, failing to fulfill constraint 1 leads to representing the full FR system with FR 4 . On the other hand, not satisfying constraint 2 results in no FR system and, thereby, all beams will occupy same frequency resources. C_2^{S-FFR} dedicates to S-FFR where the total bandwidth resources per beam partitioned 5 sub-bandwidths since A_n entitled to use FR 1 and A_k sets to use FR 4. Therefore, out of 5 sub-bands, only one sub-band can be allocated to each A_n and A_k per beam b. C_3^{PS-FFR}depicts the same situation for PS-FFR as given in S-FFR instead the total bandwidth resources per beam split into 4. This is due to the fact, A_n is not occupying the disjoint frequency resources but utilizing the same resources from one of the adjacent A_k. C_4 and C_5 is about the allocated power to inner and outer beam n and k respectively, should not exceed maximum available power resources.

5.2.3 Optimization Framework

In order to solve this joint optimization problem, the idea herein is to investigate the Deep Reinforcement Learning (DRL) based Deep Q Learning (DQL) framework. The motivation for selecting DRL for optimization task is that, unlike other learning frameworks which require large and fixed datasets for learning, a RL agent learns by interacting within an environment. On the other hand, since the state and action space in this network function are considered discrete, DQL is an appropriate choice for such a joint optimization task.

Typically, in DQL, an agent receives state s_t from state space $\mathbb{S}$ and performs an action a_t from action space $\mathbb{A}$. After executing action a_t, the agent receives a reward r_t and moves to the next new state s_{t+1}. The agent continues the process until reaching the terminal state. To execute an action, the agent follows a policy $\pi(a_t|s_t)$ for mapping from given state s_t to action a_t as shown in **Figure 5-7**. The ultimate objective of the agent here is to maximize the total accumulated reward. In Q learning, there exists action value functions typically expressed as $Q_\pi(s,a)$ and $Q^*(s,a)$, where the former depicts the expected return for selecting action a in

state s, while the latter represents an optimal action value function i.e. $Q^*(s,a) = max_\pi Q_\pi(s,a)$ by following any policy for state s and action a. Meanwhile, in DQL, a Deep Neural Network (DNN) is used to approximate the optimal action value function. Considering this, an internal optimization problem in DQL is to identify an appropriate DNN that could maximally approximate this optimal action value function. The workflow is illustrated in **Figure 5-7**

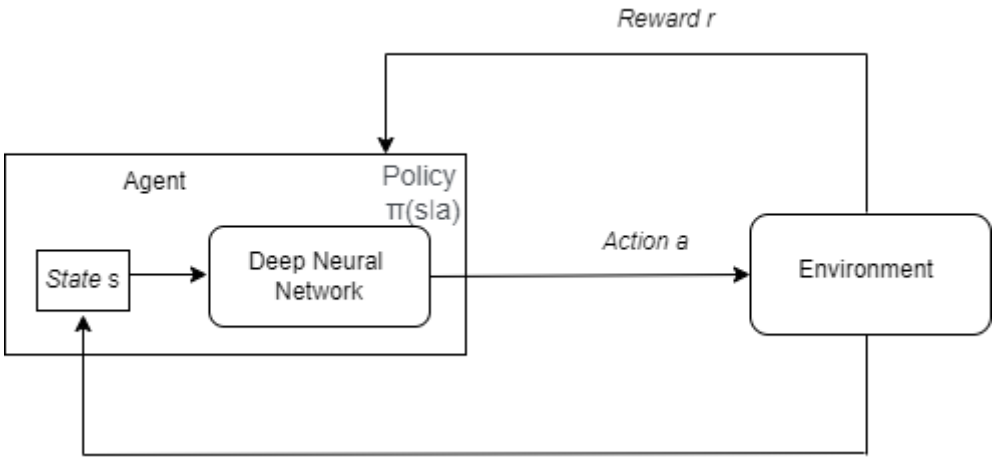

FIGURE 5-7. *HIGH LEVEL INTENDED DQL WORKFLOW FOR FFR NETWORK FUNCTION*

To map this DQL framework into the problem of FFR defined above, the idea is to keep the dimensionality of the state space vector $\mathbb{S}$ as low as possible to avoid increasing the system complexity. Considering the initial insights, the DQL model uses the cardinality of user distribution $|U_n|\ and\ |U_k|$ within $A_n(\tau_{\theta_n})$ and $A_k(\tau_{\theta_n})$ at time t as *state*, where τ_{θ_n} is a distance-based threshold calculated by inner beamwidth θ_n which characterizes if user $u \epsilon A_n\ or\ A_k$. The action space $\mathbb{A}$ is intended to be the discrete values of $\{\varphi, [^{Bw_k}_{Bw_n}], [^{P_k}_{P_n}]\}$. Meanwhile, the system throughput is to be considered as a reward. The FFR problem defined herein is a centralized training problem, which means that the action of changing inner beamwidths for one beam will impact the overall system performance. Therefore, one alternative is to consider all combinations of discrete inner beamwidths.

However, this work is being simulated in progress and the corresponding outcomes will be part of the next deliverable D4.6. Hence, the system state space vector $\mathbb{S}$ is subject to change to find the best possible state vector parameters.

5.3 TRAFFIC PREDICTION AND NTN RADIO OPTIMIZATION

5.3.1 System Description

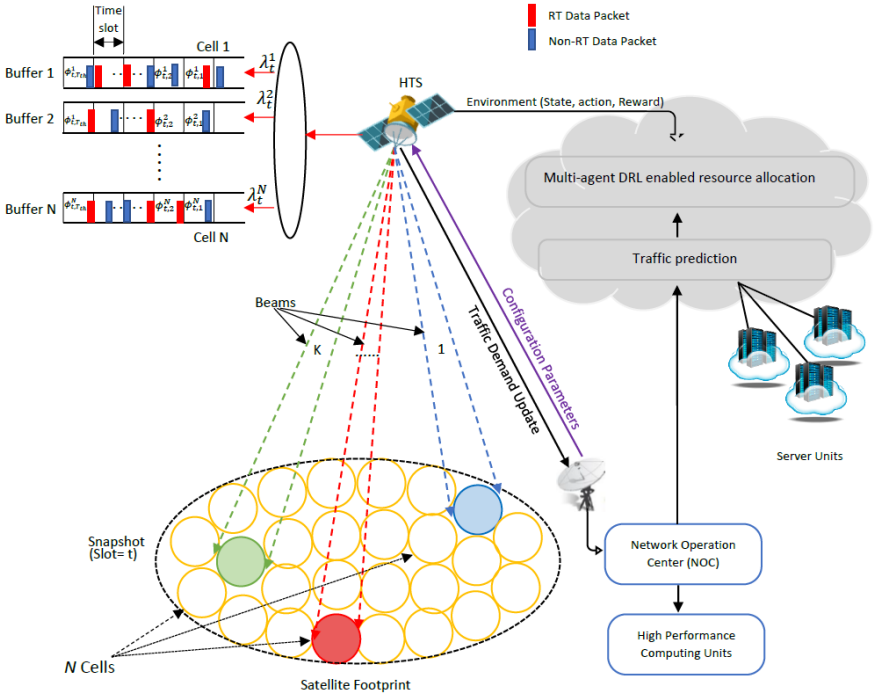

FIGURE 5-8. SYSTEM MODEL FOR TRAFFIC PREDICTION

The system model is presented in **Figure 5-8**. We considered a multi-beam satellite that can provide B beams to cover N cells, and B < N, in a time division multiplexing approach. The beams, the target cells and the U users are denoted $\mathrm{B} = \{\mathrm{b}|\mathrm{b} = 1, 2, \ldots, \mathrm{B}\}$, $\mathrm{N} = \{\mathrm{n}|\mathrm{n} = 1, 2, \ldots, \mathrm{N}\}$ and $\mathrm{U} = \{\mathrm{u}|\mathrm{u} = 1, 2, \ldots, \mathrm{U}\}$, respectively. Based on the geographical location and the traffic behavior of the users, the satellite provides N queues to store the arriving traffic of each cell that can be represented by $\Phi_t = \{\Phi_t^1, \ldots, \Phi_t^n, \ldots, \Phi_t^N\}$ and Φ_t^n represents the amount of packets arriving at cell n and time slot t. We assume that all the arrived packets are equal in size. Moreover, the stored data in the satellite buffer for each cell n can be classified based on the nature of the packets as either real time (RT) or non-real time (non-RT) data. Specifically, the RT data is denoted $\Phi_{1,t} = \{\Phi_{1,t}^1, \ldots, \Phi_{1,t}^n, \ldots, \Phi_{1,t}^N\}$ and the non-RT data is represented by $\Phi_{2,t} = \{\Phi_{2,t}^1, \ldots, \Phi_{2,t}^n, \ldots, \Phi_{2,t}^N\}$, i.e., such quantities represent the amount of RT and non-RT data at cell n at time slot t, respectively. The amount of traffic at time step t is denoted $\Lambda_t = \{\lambda_t^1, \ldots, \lambda_t^n, \ldots, \lambda_t^N\}$, i.e., λ_t^n is the amount of the traffic at cell n at time step t. Λ_t can be also divided into real time and non-real time types with $\Lambda_{1,t} = \{\lambda_{1,t}^1, \ldots, \lambda_{1,t}^n, \ldots, \lambda_{1,t}^N\}$ and $\Lambda_{2,t} = \{\lambda_{2,t}^1, \ldots, \lambda_{2,t}^n, \ldots, \lambda_{2,t}^N\}$, respectively. The satellite receives the traffic request from the UEs via the signaling beam, then, based on the amount and the nature of the arrival traffic, the payload parameters and channel conditions, the satellite has to define a beam hopping framework for beam selection, along with optimized flexible power and bandwidth resources for each beam to accommodate the requested data traffic. The beam hopping strategy defines which cell will be illuminated at a particular time step t, as the number of the cells is greater than the available number of the beams. Therefore, a beam indicator parameter $x_t^n \in \{0, 1\}$ is introduced to indicate if cell n is selected at time step t. Beam occupancy is further defined as

$\mathrm{X}_t = \{x_t^1, \ldots, x_t^n, \ldots, x_t^N\}$. In case the cell is not selected at the current time step t, its respective packets will wait in the satellite buffer for the next beam hopping. The delay for each packet in the cell n at time step t is denoted by l_t^n and the delay of each data packet is denoted by $\mathrm{L}_t = \{l_t^1, \ldots, l_t^n, \ldots, l_t^N\}$.

5.3.2 Problem Formulation

The objective herein is to provide a highly efficient radio resource management framework to support UEs with different traffic demands and QoS requirements by utilizing multi-dimensional communication resources in a flexible way. Accordingly, **we maximize the achievable throughput of non-RT services and ensure minimizing the delay for RT services while satisfying various resource constraints.** The throughput of the non-RT services is defined as the sum of the throughput of non-RT packets in all the selected cells to be illuminated, the delay of the RT services is defined as the average of instant packets delay. The multi-dimensional resources management (MDRM) problem is formulated as a trade-off between two objective functions P1 and P2. The non-RT data throughput maximization is defined by the objective function P1 while P2 represents delay minimization of RT data.

$$P_1 = \max_{p_{t_j}^n, B} \sum_{t_j} \sum_n \left(\Phi_{2,t_{j-1}}^n + \lambda_{2,t_j}^n - \Phi_{2,t_j}^n \right) \tag{5.14}$$

$$P_2 = \min_{p_{t_j}^n, B} \sum_{t_j} \sum_n \left(l_{t_j}^n \times \Phi_{1,t_j}^n \right)$$

$$opt.P = \alpha_1 P_1 + \alpha_2 P_2$$

$$s.t. \begin{cases} C1: \sum_{n=1}^{N} x_{t_j}^n \le B, x_{t_j}^n \in \{0,1\}, & \forall n, t_j \\ C2: 0 \le p_{t_j}^n \le p_{max}, & \forall n, t_j \\ C3: \sum_{n=1}^{N} x_{t_j}^n \times p_{t_j}^n \le p_{tot}, & \forall t_j \\ C4: \theta_n^{3dB} \ge {}^{70c}/_{fD}, & \forall n \\ C5: \theta_{u,n} \le \theta_n^{3dB}, & \forall u, n \\ C6: w_{u,n} = 0, if\ x_{t_j}^n = 0, & \forall u, n \\ C7: \alpha_1 + \alpha_2 = 1, \quad \alpha_1, \alpha_2 \in [0,1] \end{cases}$$

The constraint in C1 denotes that there are no more than B beams to cover the cell at the current time. The constraint in C2 and C3 means the transmitting power of any selected single beam and the total transmitting power of all the beams should not exceed the maximum beam power and the onboard power limitation, respectively. The term θ_n^{3dB} denotes the half-power beamwidth (HPBW) of the antenna and by introducing the constraint C4, we can control the coverage of the beam that illuminates the selected cell n. The constraint C5 guarantees that all UEs are within the coverage area of the beam that illuminates cell n. In constraint C6, it is clarified that all sub-channels of the beam are unavailable if the beam is inactive. The satellite bounds the time for storing each packet from time t in the satellite memory by T_{th} and $\tau \in [t, t + T_{th}]$, which means that for every packet arrived at time t, it will be dropped from the satellite memory if it passed the T_{th}. Φ_{2,t_j}^n is the amount of the remaining non-RT data of cell n at time t_j . Φ_{1,t_j}^n is the amount of remaining RT data at cell n and time t_j.

The optimization of the two objective functions hinges upon identifying the optimal values of α1 and α2. The first step of our algorithm is to refine these parameters based on RT call traffic and non-RT internet traffic predictions within the designated geographical service area. Then based on the optimized α1 and α2 in step 1, we will solve the resource optimization problem. A summarized procedure of our algorithm can be found in **Figure 5-9**

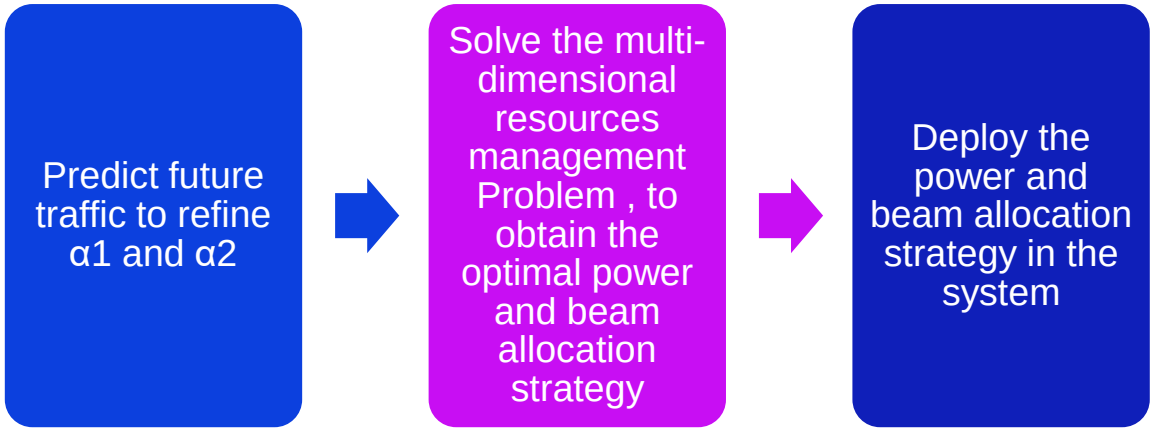

FIGURE 5-9. A SUMMARY OF THE PROCEDURE OF OUR ALGORITHM

5.3.3 Optimization Framework

The complex nature of cellular traffic patterns, influenced by multiple factors including user mobility patterns, arrival dynamics, and diverse user requirements, presents a huge challenge for conventional linear models. Consequently, the advent of deep learning methodologies has emerged as a transformative solution. Leveraging the inherent capacity of neural networks to recognize nonlinear patterns and features, deep learning methods exhibit superior adaptability in capturing the tangled dynamics of traffic patterns. One of the defining strengths of deep learning lies in its ability to exploit hierarchical representations through multiple layers, enabling the extraction of latent features and abstract patterns embedded within complex time series data. This attribute not only facilitates a more nuanced understanding of traffic dynamics but also augments prediction accuracy, thereby heralding a paradigm shift in the realm of network traffic analysis towards more robust and adaptable predictive frameworks.

The recent advancements in time series forecasting techniques have underscored the efficacy of prediction-based methodologies in furnishing detailed network traffic forecasts tailored for practical applications such as bandwidth management, resource allocation and resource provisioning. Specifically, we leverage a cutting-edge time series forecasting algorithm, namely Diviner, to project future 24-hour internet and call traffic volumes within the satellite service area.

By closely monitoring the trend variations in RT and Non-RT traffic volumes, we dynamically adjust the values of α1 and α2 to ensure alignment with the evolving traffic dynamics. This adaptive approach ensures that our optimization framework remains finely calibrated to the

fluctuating demands of the network, thereby enhancing its responsiveness and efficacy in addressing the dual objectives of call and internet traffic management.

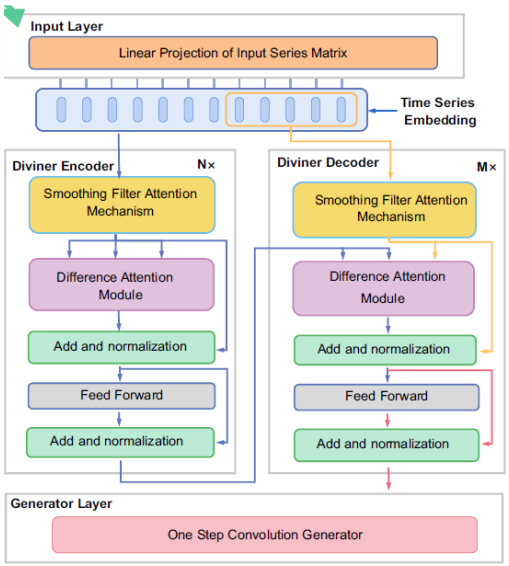

FIGURE 5-10 SCHEMATIC ILLUSTRATION FOR THE WORKFLOW OF DIVINER.

5.3.3.1 Traffic Prediction Algorithm: Diviner

The authors in [98], proposed a deep learning model called" Diviner" for improving the robustness and predictive accuracy of forecasts, particularly for long-term 5G network traffic by using a combination of deep learning and stochastic process theories. The authors incorporate deep stationary processes into neural networks to effectively capture multi-scale stable features within non-stationary time series data, ensuring precise long-term forecasts. To attain this goal, a smoothing filter attention mechanism as a scale converter and a difference attention module to discover the stable regularities were proposed. In the former, the feature scale adjustment is done through Nadaraya-Watson regression. in addition, this mechanism dynamically transforms non-stationary time series data by incorporating a learnable scale adjustment unit to adaptively adjust feature scales, shrinking or magnifying variations for different scales, and eliminates outliers. The difference attention module is introduced to capture stable regularities within non-stationary time series through the calculation of internal connections among stable shifted features to overcome uneven distributions and interference. It separates shifts from long term trends, captures temporal dependencies within the variation, and generates a non-stationary time series conforming to its covered regularities. The workflow of the Diviner framework is presented in **Figure 5-10**.

5.3.3.2 Traffic Prediction Realization: Dataset

As mentioned above, traffic prediction will be a game changer for automation and resource management processes for future networks. Seeking this goal, the traffic prediction algorithms need to be trained on a real dataset to be more accurate. In this context, we have found a big and public dataset of telecommunication activities in the cities of Milan and Trentino from [99]. This dataset encompasses time series data on aggregated cell phone activities, including short message service (SMS), call service, and internet connection events. These activities are either sent or received by users within a specific area in the city of Milan. The city of Milan is partitioned into a grid with dimensions H $\times$ W, where each square in the grid is termed a cell. The figures show the temporal and spatial dynamics of wireless traffic. In **Figure 5-11** (Left), we observe the fine dynamics of SMS and Call services traffic within a specific cellular network

cell. The figure illustrates the daily traffic patterns observed over the period of one week, revealing distinctive fluctuations in traffic volume between weekdays and weekends. Notably, there is a noticeable decrease in traffic volume during weekends compared to the bustling activity witnessed on working days. Furthermore, a notable discrepancy emerges between inbound and outbound traffic for SMS services compared to the inbound and outbound traffic of Call services. This variance underscores the intricate interplay between user behaviors, network utilization patterns, and service-specific dynamics within the cellular network ecosystem. Expanding on the analysis, **Figure 5-11** (right), showcases the spatial distribution of SMS traffic at a specific point in time. Notably, we observe an uneven distribution of SMS traffic across various cellular network cells due to the demographic landscape characterized by densely populated urban centers side-by-side with sparsely populated rural regions. Consequently, it's unsurprising to witness heightened SMS activity concentrated within city centers compared to more remote, rural areas.

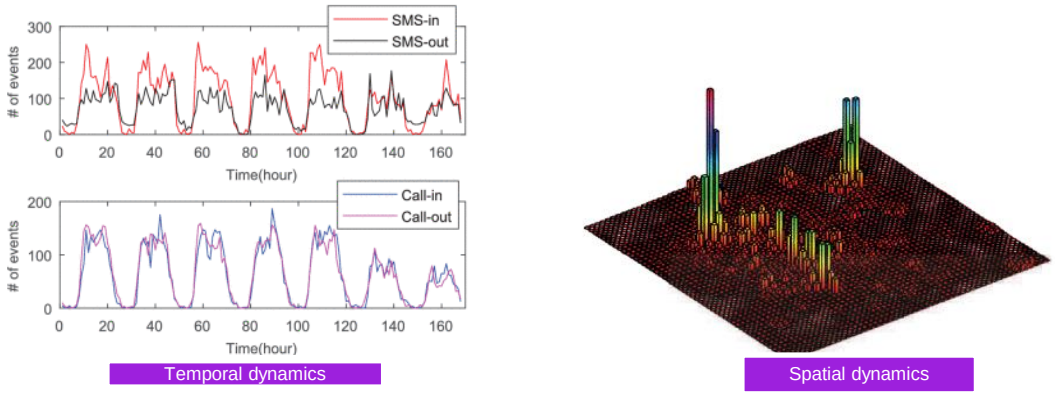

FIGURE 5-11: *SPATIAL AND TEMPORAL DISTRIBUTION OF THE CONSIDERED CELLULAR*

In our traffic prediction algorithm, we have defined the spatial dimensions as H = W = 4, to facilitate a more efficient analysis, resulting in a city area partitioned into a grid of 4×4 individual cells. The recorded traffic data spans from 00:00 on 11/01/2013 to 00:00 on 01/01/2014, with temporal Observations captured at hourly intervals. This comprehensive temporal coverage enables us to capture and analyze traffic patterns, providing valuable insights into the dynamics of urban traffic flow within the designated city area.

5.3.3.3 Traffic Prediction Results

Here, we present some of the results obtained from the traffic prediction algorithm for the call traffic for a random cell in the satellite serving area grid.

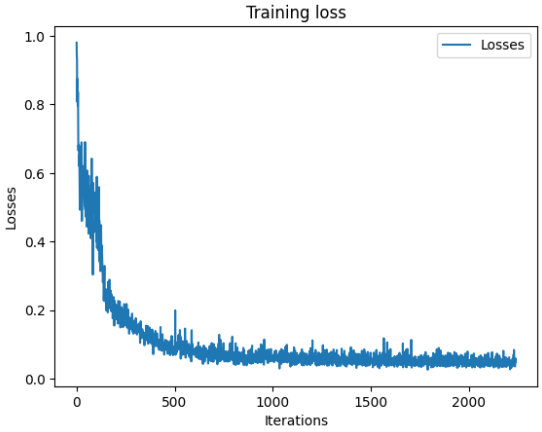

FIGURE 5-12: TRAINING LOSSES.

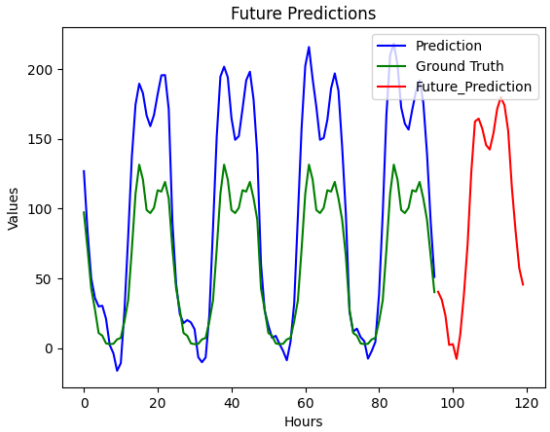

FIGURE 5-13: TRAFFIC FUTURE PREDICTION WITH TESTING RESULTS.

In **Figure 5-12**, we observe the Mean Square Error (MSE) losses experienced during the training phase. It's noteworthy that the training loss exhibits a consistent downward trend over time, indicative of the model's iterative learning process and progressive improvement in performance. Moving to **Figure 5-13**, we delve into the algorithm's predictive prowess by comparing the predicted traffic over the last 4 days (96 hours, denoted by the blue curve) against the ground truth, represented by the actual data (green curve). While the training loss demonstrates a declining trajectory, it's imperative to note the discrepancies between the predicted and actual traffic volumes. Although both the Mean Square Error (MSE) and Mean Absolute Error (MAE) exhibit low values during both training (train loss=0.049481, valid loss=0.101457) and testing phases (MSE: 0.299650, MAE: 0.4032453), indicating promising model performance, an observed gap persists between the predicted and actual traffic data.

This incoherence underscores the necessity for further parameter tuning to enhance predictive accuracy. However, it's important to highlight our primary interest in identifying the underlying trends within the traffic dynamics and quantifying the percentage change from one hour to the next. The adaptive adjustment of the α1, α2 values is performed by relying on the percentage of change in traffic volume. This dynamic adaptation mechanism will help the DRL Algorithm to accurately reflect the evolving traffic dynamics in the environment state, thereby optimizing the capabilities of the model.

5.4 LINK QUALITY PREDICTION

5.4.1 Qualitative Description of Initial Problem

The following is a brief qualitative account of the initial experiments that have been carried out for link-prediction in NTN. In this phase we shall focus on an elementary version of the main problem, described as follows: given a satellite's current ephemeris, predict the free-space pathloss (FSPL) to a ground UE at a future time by employing an AI/ML approach, rather than the conventional propagation-algorithm.

FSPL is a function of frequency, which relates to the effective aperture area of receive antenna, and LOS distance between transmitter and receiver, which relates to the power-density of radiated power in space. The standard formula for FSPL is given as:

$$FSPL(f,d) = \left(\frac{c}{4\pi f d}\right)^2, \quad (5.15)$$

where c is the speed of light in vacuum, f is the frequency of the radiowave, and d is the LOS separation distance between the transmit and receive antennas. When f and d are expressed in GHz and m, respectively, the foregoing is typically written in dB as follows:

$$FSPL(f,d) = -32.441772 - 20log_{10}f - 20log_{10}d \text{ [dB]}. \quad (5.16)$$

In the NTN system, since the distance to the satellite changes over time, even for a stationery UE, the foregoing expression needs to be qualified with a time variable:$FSPL(f,d) = FSPL\big(f,d(t)\big)$. We hence see that a knowledge of the LOS distance to the satellite at any time instant t is required by the UE to estimate $FSPL\big(f,d(t)\big)$. **Figure 5-14** below shows an example of the time-variation of $d(t)$ for a sample LEO-satellite orbit at a height of 650 km above the Earth's surface. In this example, the UE has a minimum elevation angle (MEA) of 25-degrees when it begins to sight the satellite at t=0 sec. The UE lies on the satellite's ground-track and tracks the satellite for about 300 seconds of coverage. Also shown for reference is the corresponding FSPL at 3GHz. A conventional approach to estimate $d(t)$ is to utilize the satellite-ephemeris to propagate and predict, using the laws of physics, the satellite's state (position and velocity) at any required time. Note that the satellite-ephemeris is not available at all times, hence the need to predict. This, when combined with the UE's position leads to estimates of $d(t)$. As noted previously, our aim, in this subproblem, is to achieve the same using an AI/ML approach.

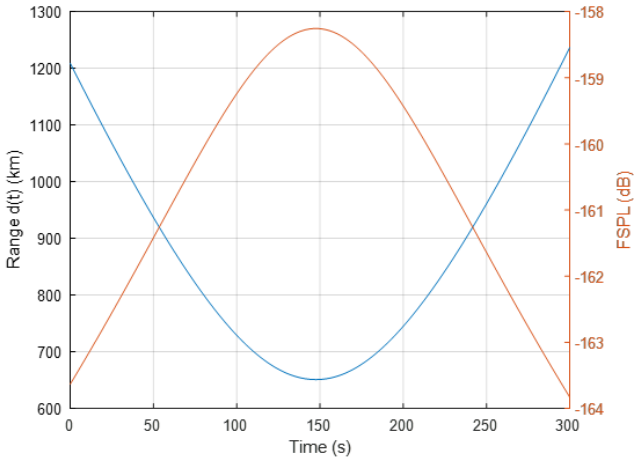

FIGURE 5-14. TIME-VARIATION OF D(T) FOR A SAMPLE LEO-SATELLITE ORBIT AT A HEIGHT OF 650 KM ABOVE THE EARTH'S SURFACE

We thus intend to study and characterize AI/ML approaches that can effectively serve as an alternative to the conventional approach. In notation, we seek to

$$\min_{x \in S} \; E \left| FSPL\big(f, d(t)\big)_x - FSPL\big(f, d(t)\big)_{conv} \right|, \qquad (5.17)$$

where S represents the class of all AI/ML-based algorithms, $FSPL\big(f, d(t)\big)_x$ is the prediction of FSPL result using an AI/ML procedure, $FSPL\big(f, d(t)\big)_{conv}$ is the same using the conventional propagation procedure, the operator E denotes the average of the operand taken over the tuple of UE's Earth-locations, LEO Satellite-orbits, and corresponding visibility-times.[1]

To this end, two AI/ML approaches were chosen for an initial study: (i) Polynomial regression and (ii) Deep neural network. The former represents a traditional machine-learning methodology whereas the latter exemplifies a more modern AI method [100] [101]. Training and evaluation datasets were obtained from basic conventional satellite-propagation algorithms (these models assume only the 2-body symmetrical gravitational force for propagation of the satellite state) by sampling from 8 different LEO-satellite orbits, and by randomizing the UE-position within 30km radius of a specific Earth-location.

Initial results on this front show that both the foregoing approaches tend to overfit the data (good performance on training-data and poor performance on evaluation-data) when only the satellite's position and associated epoch is considered as input to the algorithm. We are currently working on expanding the training dataset to include more diverse orbits, inclusion of velocity information as algorithm-input, incorporation of atmospheric loss models, RSRP prediction, exploration of advanced AI/ML approaches etc. A detailed account of the study shall be provided later in D4.6.

[1] We limit the parameters for averaging in this version of the elementary problem for tractability. In reality, the averaging must include atmospheric losses, UE's environmental factors, etc.

6 CONCLUSIONS

This deliverable, D4.2, comprised an initial comprehensive report on the task of designing the AI-enabled RAN intelligent controller (RIC). The objective herein revolved around covering the dynamic allocation of radio resources, in particular the Radio Resource Management (RRM), for integrated Terrestrial and Non-Terrestrial Networks (TN-NTN). This is in fact important to ensure Quality of Service (QoS) requirements and overall system optimization both in non-Real time (non-RT) and near-Real time (n-RT) scenarios and particularly in the presence of challenges, for instance, non-uniform user traffic demand and user density, and heterogenous and unpredictable channel conditions.

To this end, this initial report primarily focused on the prospective discussion of current 3GPP Artificial Intelligence/Machine Learning (AI/ML) activities, following the proposal of a baseline AI/ML RIC architecture which provides intuitions about the deployment of AI/ML server, explicitly responsible for handling the AI/ML functions for instance, model training, testing, inference and Life Cycle Management (LCM) etc. This AI/ML architecture proposal is based on the general ``Conventional Architecture`` defined in D3.5, and this report thereafter extends the discussion on providing the very initial AI/ML aspects of ``Distributed Architecture`` also proposed in D3.5.

In addition, highlighting another main contribution to D4.2, this deliverable puts forward the efforts of identifying four potential resource network functions: traffic off-loading, fractional frequency reuse, traffic prediction and link quality prediction. These identified network functions are intended to be optimized in resource allocation perspectives by investigating the advanced AI/ML algorithms, leveraging the dynamic traffic and channel characteristics. Moreover, it is envisaged that all four identified network functions will generally utilize the defined baseline AI/ML architecture for the deployment of AI/ML MEC/server. Therefore, each resource network function elucidated their own AI/ML MEC/server deployment preferences considering the optimal feasibility of resources allocation. Subsequently, the discussion led towards the comprehensive state of the art (SoTA) analysis, defining the problem statements and the Key Performance Indicators (KPIs) to be optimized to enhance the system performances, for each individual resource network function.

Moreover, given the fact that the training of AI/ML algorithms require NTN system parameters, training datasets and traffic loads etc., in this context, one of the sections of D4.2 provided the NTN system description aspects that include the user traffic loads, user spatial distribution and mission definition of the overall NTN system. The overall system description and traffic distribution draws from the work done in tasks T3.1 of WP3 and T4.2 of WP4, respectively.

Having all the required information to enable the resource optimization in these network functions, the last part of D4.2 is concluded by defining the AI/ML based optimization paradigm, which is explicitly dedicated to formulating the system framework, problem statement, initial insights of potentially selected optimization algorithms and some initial outcomes.

Future Work on AI-Enabled RIC

The following aspects (included but not limited to) are intended to be covered in the subsequent deliverable D4.6 on AI-Enable RIC (final report):

- A further detailed contribution on the working principles of the AI/ML architecture, particularly, the `` Distributed Architecture``.

- A complete analysis of designed optimization algorithms for the defined resource optimization problems along with the final optimized outcomes relevant to each resource network function.
- A possibility of defining and optimizing new resource network functions.

REFERENCES

[1] 6G-NTN Deliverable 2.1, “Use Case Definition”, v1.0.

[2] 6G-NTN Deliverable 4.3, “Open Datasets for 6G-NTN Data Driven Radio Access Networks”, v1.0.

[3] 6G-NTN Deliverable 3.5, “Report on 3D/Multilayered NTN Architecture”, v1.0.

[4] 3GPP TR 38.843, “Study on Artificial Intelligence (AI)/Machine Learning (ML) for NR ‘air interface,” V18.0., January 2024.

[5] 3GPP TR 37.817, “Study on Enhancement for Data Collection for NR and EN-DC,” V17.0.0, April 2022.

[6] 3GPP RP-220635, “Work Item Description on Artificial Intelligence (AI)/Machine Learning (ML) for NG-RAN”, Release 18 (accessed on February 2024)

[7] 3GPP TS 38.423, “5G; NG-RAN; Xn Application Protocol (XnAP)”, Release 17, V17.4.0, 2023-05.

[8] 3GPP TR 23.700-81, “Study on Enablers for Network Automation for 5G-phase 3”, Release 18.

[9] 3GPP SP-220071, “Study on 5G System Support for AI/ML-based Services”, Release 18.

[10] 3GPP TR 23.700-80, “Study on System Support for AI/ML-based Service”, Release 18.

[11] Novlan, T., Andrews, J. G., Sohn, I., Ganti, R. K., & Ghosh, A. (2010). Comparison of Fractional Frequency Reuse Approaches in the OFDMA Cellular Downlink. In 2010 IEEE Global Telecommunications Conference GLOBECOM 2010 (pp. 1-5). IEEE.

[12] Yoo, H.M., Rhee, J.S., Bang, S.Y. and Hong, E.K., 2022, October. Load balancing Algorithm Running on Open RAN RIC. In 2022 13th International Conference on Information and Communication Technology Convergence (ICTC) (pp. 1226-1228). IEEE.

[13] Dryjański, M., Kułacz, Ł. and Kliks, A., 2021. Toward Modular and Flexible Open RAN Implementations in 6G Networks: Traffic Steering Use Case and O-RAN xAPPs. *Sensors*, *21*(24), p.8173.

[14] Orhan, O., Swamy, V.N., Tetzlaff, T., Nassar, M., Nikopour, H. and Talwar, S., 2021, December. Connection management xAPP for O-RAN RIC: A Graph Neural Network and Reinforcement Learning Approach. In *2021 20th IEEE International Conference on Machine Learning and Applications (ICMLA)* (pp. 936-941). IEEE.

[15] Erdol, H., Wang, X., Li, P., Thomas, J.D., Piechocki, R., Oikonomou, G., Inacio, R., Ahmad, A., Briggs, K. and Kapoor, S., 2022, September. Federated Meta-Learning for Traffic Steering in O-RAN. In *2022 IEEE 96th Vehicular Technology Conference (VTC2022-Fall)* (pp. 1-7). IEEE.

[16] Lacava, A., Polese, M., Sivaraj, R., Soundrarajan, R., Bhati, B.S., Singh, T., Zugno, T., Cuomo, F. and Melodia, T., 2023. Programmable and Customized Intelligence for Traffic Steering in 5G Networks using Open RAN Architectures. *IEEE Transactions on*

Mobile Computing.

[17] Rashad, R. and Sudhir, S., 2022. Load Balancing Technique Based on Network Segmentation and Adaptive Sleep Scheduling for 5G-IoT Networks. 10.21203/rs.3.rs-825633/v1

[18] Addali, K. and Kadoch, M., 2019, May. Enhanced Mobility Load Balancing Algorithm for 5G Small Cell Networks. In *2019 IEEE Canadian conference of electrical and computer engineering (CCECE)* (pp. 1-5). IEEE.

[19] Addali, K.M., Melhem, S.Y.B., Khamayseh, Y., Zhang, Z. and Kadoch, M., 2019. Dynamic Mobility Load Balancing for 5G Small-cell Networks Based on Utility Functions. *IEEE Access*, *7*, pp.126998-127011.

[20] Saibharath, S., Mishra, S. and Hota, C., 2021. Swap-based Load Balancing for Fairness in Radio Access Networks. *IEEE Wireless Communications Letters*, *10*(11), pp.2412-2416.

[21] Ma, B., Yang, B., Zhu, Y. and Zhang, J., 2020. Context-aware Proactive 5G Load Balancing and Optimization for Urban Areas. *IEEE Access*, *8*, pp.8405-8417.

[22] Shahid, S.M., Seyoum, Y.T., Won, S.H. and Kwon, S., 2020. Load balancing for 5G Integrated Satellite-Terrestrial Networks. *IEEE Access*, *8*, pp.132144-132156.

[23] Lin, Z., Ni, Z., Kuang, L., Jiang, C. and Huang, Z., 2022. Multi-satellite Beam Hopping based on Load Balancing and Interference Avoidance for NGSO Satellite Communication Systems. *IEEE Transactions on Communications*, *71*(1), pp.282-295.

[24] Badini, N., Jaber, M., Marchese, M. and Patrone, F., 2023, May. Reinforcement Learning-Based Load Balancing Satellite Handover Using NS-3. In *ICC 2023-IEEE International Conference on Communications* (pp. 2595-2600). IEEE.

[25] Diógenes do Rego, I., & de Sousa Jr, V. A. (2021). Solution for Interference in Hotspot Scenarios Applying Q-Learning on FFR-Based ICIC Techniques. *Sensors*, *21*(23), 7899.

[26] Angeletti, P., & De Gaudenzi, R. (2021). Heuristic Radio Resource Management for Massive MIMO in Satellite Broadband Communication Networks. *IEEE Access*, *9*, 147164-147190.

[27] Meng, F., Chen, J., Ren, S., Guo, J., & Wu, J. (2011, November). Comparison of Frequency Reuse Schemes in OFDMA based Multi-beam Satellite Communications Systems. In *29th AIAA International Communications Satellite Systems Conference (ICSSC-2011)* (p. 8035).

[28] Ng, U. Y., Kyrgiazos, A., & Evans, B. (2014, September). Interference Coordination for the Return Link of a Multibeam Satellite System. In *2014 7th Advanced Satellite Multimedia Systems Conference and the 13th Signal Processing for Space Communications Workshop (ASMS/SPSC)* (pp. 366-373). IEEE.

[29] Zhang, W., Yang, W., Wang, Z., Li, D., & Guo, Q. (2020, July). Optimizing Frequency Reuse in Multibeam Satellite Communication Systems. In *International Conference in Communications, Signal Processing, and Systems* (pp. 1344-1349). Singapore: Springer Singapore.

[30] Leng, T., Wang, Y., Hu, D., Cui, G., & Wang, W. (2022). User-level Scheduling and

Resource Allocation for Multi-beam Satellite Systems with Full Frequency Reuse. *China Communications*, *19*(6), 179-192.

[31] Mohammadi, F. S., & Kwasinski, A. (2018, July). QoE-driven Integrated Heterogeneous Traffic Resource Allocation Based on Cooperative Learning for 5G Cognitive Radio Networks. In *2018 IEEE 5G World Forum (5GWF)* (pp. 244-249). IEEE.

[32] Kebedew, T. M., Ha, V. N., Lagunas, E., Tran, D. D., Grotz, J., & Chatzinotas, S. (2023, December). Reinforcement Learning for QoE-Oriented Flexible Bandwidth Allocation in Satellite Communication. In *2023 IEEE Globecom Workshops: Workshop on Cellular UAV and Satellite Communications*. IEEE, New York, United States.

[33] **Li**, R., Zhao, Z., Zheng, J., Mei, C., Cai, Y. and Zhang, H., 2017. The Learning and Prediction of Application-level Traffic Data in Cellular Networks. IEEE Transactions on Wireless Communications, 16(6), pp.3899-3912.

[34] Box, G., Jenkins, G., Reinsel, G. & Ljung, G. Time Series Analysis: Forecasting and Control (John Wiley & Sons, America, 2015).

[35] Moayedi, H. & Masnadi-Shirazi, M., ARIMA Model for Network Traffic Prediction and Anomaly Detection. in Proceedings of International Symposium on Information Technology, vol. 4, 1–6 (2008).

[36] Azari, A., Papapetrou, P., Denic, S. & Peters, G. Cellular Traffic Prediction and Classification: A Comparative Evaluation of LSTM and ARIMA. In Proceedings of International Conference on Discovery Science, 129-144 (2019).

[37] Tikunov, D. & Nishimura, T. Traffic Prediction for Mobile Network using Holt-Winter's Exponential Smoothing. In Proceedings of International Conference on Software, Telecommunications and Computer Networks, 1–5 (2007).

[38] Shu, Y., Yu, M., Yang, O., Liu, J. and Feng, H., 2005. Wireless Traffic Modeling and Prediction using Seasonal ARIMA Models. IEICE Transactions on Communications, 88(10), pp.3992-3999.

[39] Chen, X., Jin, Y., Qiang, S., Hu, W. and Jiang, K., 2015, June. Analyzing and Modeling Spatio-temporal Dependence of Cellular Traffic at City Scale. In 2015 IEEE international conference on communications (ICC) (pp. 3585-3591). IEEE.

[40] Li, R., Zhao, Z., Zhou, X., Palicot, J. and Zhang, H., 2014. The Prediction Analysis of Cellular Radio Access Network Traffic: From Entropy Theory to Networking Practice. IEEE Communications Magazine, 52(6), pp.234-240.

[41] Feng, H., Shu, Y., Wang, S. and Ma, M., 2006, June. SVM-based Models for Predicting WLAN Traffic. In 2006 IEEE International Conference on Communications (Vol. 2, pp. 597-602). IEEE.

[42] Shu, Y., Yu, M., Yang, O., Liu, J. and Feng, H., 2005. Wireless Traffic Modeling and Prediction using Seasonal ARIMA Models. IEEE Transactions on Communications, 88(10), pp.3992-3999.

[43] Wang, S., Zhang, X., Zhang, J., Feng, J., Wang, W. and Xin, K., 2015, September. An Approach for Spatial-Temporal Traffic Modeling in Mobile Cellular Networks. In 2015 27th International Teletraffic Congress (pp. 203-209). IEEE.

[44] Taylor, S. & Letham, B. Forecasting at scale. Am. Stat. **72**, 37–45 (2018).

[45] Salinas, D., Flunkert, V., Gasthaus, J. & Januschowski, T. DeepAR: Probabilistic Forecasting with Autoregressive Recurrent Networks. Int. J. Forecast. **36**, 1181–1191 (2020).

[46] Qin, Y., Song, D., Chen, H., Cheng, W., Jiang, G. and Cottrell, G. A Dual-stage Attention-based Recurrent Neural Network for Time Series Prediction. in Proceedings of International Joint Conference on Artificial Intelligence, 2627–2633 (2017).

[47] Qiu, C., Zhang, Y., Feng, Z., Zhang, P. and Cui, S., 2018. Spatio-temporal Wireless Traffic Prediction with Recurrent Neural Network. IEEE Wireless Communications Letters, 7(4), pp.554-557.

[48] Wang, J., Tang, J., Xu, Z., Wang, Y., Xue, G., Zhang, X. and Yang, D., 2017, May. Spatiotemporal modeling and prediction in cellular networks: A Big Data Enabled Deep Learning Approach. In IEEE INFOCOM 2017-IEEE conference on computer communications (pp. 1-9). IEEE.

[49] LeCun, Y., Bengio, Y. and Hinton, G., 2015. Deep Learning. Nature, 521(7553), pp.436-444.

[50] Zhang, C., Zhang, H., Yuan, D. and Zhang, M., 2018. Citywide Cellular Traffic Prediction based on Densely Connected Convolutional Neural Networks. IEEE Communications Letters, 22(8), pp.1656-1659.

[51] Zhou, H., Zhang, S., Peng, J., Zhang, S., Li, J., Xiong, H. and Informer, W.Z., Beyond Efficient Transformer for Long Sequence Time-series Forecasting. in *Proceedings of AAAI Conference on Artificial Intelligence* (2021).

[52] Kitaev,N., Kaiser,L. & Levskaya, A. Reformer: The Efficient Transformer. in Proceedings of International Conference on Learning Representations (2019).

[53] Li, S., Jin, X., Xuan, Y., Zhou, X., Chen, W., Wang, Y.X. and Yan, X., 2019. Enhancing the Locality and Breaking the Memory Bottleneck of Transformer on Time Series Forecasting. Advances in Neural Information Processing Systems, 32.

[54] Yang, Y., Geng, S., Zhang, B., Zhang, J., Wang, Z., Zhang, Y., & Doermann, D. (2023). Long term 5G Network Traffic Forecasting via Modeling Non-Stationarity with Deep Learning. *Communications Engineering*, *2*(1), 33.

[55] Senanayake, R., O'Callaghan, S. and Ramos, F., 2016, March. Predicting Spatio-Temporal Propagation of Seasonal Influenza using Variational Gaussian Process Regression. In Proceedings of the AAAI conference on artificial intelligence (Vol. 30, No. 1).

[56] Xu, Y., Yin, F., Xu, W., Lin, J. and Cui, S., 2019. Wireless Traffic Prediction with Scalable Gaussian Process: Framework, Algorithms, and Verification. IEEE Journal on Selected Areas in Communications, 37(6), pp.1291-1306.

[57] McMahan, B., Moore, E., Ramage, D., Hampson, S. and y Arcas, B.A., 2017, April. Communication-Efficient Learning of Deep networks From Decentralized Data. In Artificial intelligence and statistics (pp. 1273-1282). PMLR.

[58] Yang, Q., Liu, Y., Chen, T. and Tong, Y., 2019. Federated Machine Learning: Concept and Applications. ACM Transactions on Intelligent Systems and Technology (TIST), 10(2), pp.1-19.

[59] Zhang, C., Dang, S., Shihada, B. and Alouini, M.S., 2021, May. Dual Attention-based Federated Learning for Wireless Traffic Prediction. In IEEE INFOCOM 2021-IEEE conference on computer communications (pp. 1-10). IEEE.

[60] Perifanis, V., Pavlidis, N., Koutsiamanis, R.-A., & Efraimidis, P. S. (2023). Federated Learning for 5G Base Station Traffic Forecasting. Computer Networks, 235, 109950

[61] Lei, L., Lagunas, E., Yuan, Y., Kibria, M.G., Chatzinotas, S. and Ottersten, B., 2020, May. Deep Learning for Beam Hopping in Multibeam Satellite Systems. In *2020 IEEE 91st Vehicular Technology Conference (VTC2020-spring)* (pp. 1-5). IEEE.

[62] Lei, L.E.I., Lagunas, E., Yuan, Y., Kibria, M.G., Chatzinotas, S. and Ottersten, B., 2020. Beam Illumination Pattern Design in Satellite Networks: Learning and Optimization for Efficient Beam Hopping. *IEEE Access*, *8*, pp.136655-136667.

[63] Hu, X., Zhang, Y., Liao, X., Liu, Z., Wang, W. and Ghannouchi, F.M., 2020. Dynamic Beam Hopping Method based on Multi-objective Deep Reinforcement Learning for Next Generation Satellite Broadband Systems. *IEEE Transactions on Broadcasting*, *66*(3), pp.630-646.

[64] Lin, Z., Ni, Z., Kuang, L., Jiang, C. and Huang, Z., 2022. Dynamic Beam Pattern and Bandwidth Allocation based on Multi-agent Deep Reinforcement Learning for Beam Hopping Satellite Systems. *IEEE Transactions on Vehicular Technology*, *71*(4), pp.3917-3930..

[65] Vázquez, M.Á., Henarejos, P., Pappalardo, I., Grechi, E., Fort, J., Gil, J.C. and Lancellotti, R.M., 2021. Machine Learning for Satellite Communications Operations. *IEEE Communications Magazine*, *59*(2), pp.22-27.

[66] Ortiz Gómez, F.D.G., Martínez Rodríguez-Osorio, R., Salas Natera, M.A., Landeros Ayala, S., Tarchi, D. and Vanelli Coralli, A., 2019. On the Use of Neural Networks for Flexible Payload Management in VHTS systems.

[67] Ortiz-Gómez, F.G., Tarchi, D., Martinez, R., Vanelli-Coralli, A., Salas-Natera, M.A. and Landeros-Ayala, S., 2022. Supervised Machine Learning for Power and Bandwidth Management in very High Throughput Satellite Systems. International Journal of Satellite Communications and Networking, 40(6), pp.392-407.

[68] Ortiz-Gomez, F.G., Tarchi, D., Rodriguez-Osorio, R.M., Vanelli-Coralli, A., Salas-Natera, M.A. and Landeros-Ayala, S., 2020, October. Supervised Machine Learning For Power and Bandwidth Management in VHTS Systems. In 2020 10th Advanced Satellite Multimedia Systems Conference and the 16th Signal Processing for Space Communications Workshop (ASMS/SPSC) (pp. 1-7). IEEE.

[69] Ortiz Gómez, F.D.G., Martínez Rodríguez-Osorio, R., Salas Natera, M.A. and Landeros Ayala, S., 2019, “On the Use Machine Learning for Flexible Payload Management in VHTS Systems,” in Proceedings of 70th International Astronautical Congress 2019, pp. 1–6. [Online]. Available: https://oa.upm.es/64705/https://oa.upm.es/64705/

[70] Ortiz Gómez, F.D.G., Martínez Rodríguez-Osorio, R., Salas Natera, M.A., Landeros Ayala, S., Tarchi, D. and Vanelli Coralli, A., 2019, “On the Use of Neural Networks for Flexible Payload Management in VHTS Systems,” in 25th Ka Broadband Communication Conference, 2019, pp. 1–10.

[71] Ortiz-Gomez, F.G., Tarchi, D., Martínez, R., Vanelli-Coralli, A., Salas-Natera, M.A. and Landeros-Ayala, S., 2020. Convolutional Neural Networks for Flexible Payload Management in VHTS Systems. IEEE Systems Journal, 15(3), pp.4675-4686.

[72] Zhang, P., Wang, X., Ma, Z., Liu, S. and Song, J., 2020. An Online Power Allocation Algorithm Based on Deep Reinforcement Learning in Multibeam Satellite Systems. International journal of satellite communications and networking, 38(5), pp.450-461.

[73] Luis, J.J.G., Guerster, M., del Portillo, I., Crawley, E. and Cameron, B., 2019, June. Deep Reinforcement Learning for Continuous Power Allocation in Flexible High Throughput Satellites. In 2019 IEEE Cognitive Communications for Aerospace Applications Workshop (CCAAW) (pp. 1-4). IEEE.

[74] Luis, J.J.G., Pachler, N., Guerster, M., del Portillo, I., Crawley, E. and Cameron, B., 2020, March. Artificial Intelligence Algorithms for Power Allocation in High Throughput Satellites: A Comparison. In 2020 IEEE Aerospace Conference (pp. 1-15). IEEE.

[75] Ortiz-Gomez, F.G., Tarchi, D., Martínez, R., Vanelli-Coralli, A., Salas-Natera, M.A. and Landeros-Ayala, S., 2021. Cooperative Multi-agent Deep Reinforcement Learning for Resource Management in Full Flexible VHTS Systems. IEEE Transactions on Cognitive Communications and Networking, 8(1), pp.335-349.

[76] Vidal, F., Legay, H. and Goussetis, G., 2020, October. Joint Power, Frequency and Precoding Optimisation in a Satellite SDMA Communication System. In 2020 10th Advanced Satellite Multimedia Systems Conference and the 16th Signal Processing for Space Communications Workshop (ASMS/SPSC) (pp. 1-8). IEEE.

[77] Cocco, G., De Cola, T., Angelone, M., Katona, Z. and Erl, S., 2017. Radio Resource Management Optimization of Flexible Satellite Payloads for DVB-S2 Systems. *IEEE Transactions on Broadcasting*, *64*(2), pp.266-280.

[78] Wang, L., Liu, S., Wang, W. and Fan, Z., 2020. Dynamic Uplink Transmission Scheduling for Satellite Internet of Things Applications. *China Communications*, *17*(10), pp.241-248.

[79] Fourati, F. and Alouini, M.S., 2021. Artificial Intelligence for Satellite Communication: A Review. Intelligent and Converged Networks, 2(3), pp.213-243.

[80] Zhang, Y.; Wen, J.; Yang, G.; He, Z.; Wang, J., 2019. Path Loss Prediction Based on Machine Learning: Principle, Method, and Data Expansion. Applied Sciences, 9(9) , pp.1908.

[81] Ates, H.F., Hashir, S.M., Baykas, T. and Gunturk, B.K., 2019. Path Loss Exponent and Shadowing Factor Prediction from Satellite Images using Deep Learning. IEEE Access, 7, pp.101366-101375.

[82] Thrane, J., Zibar, D. and Christiansen, H.L., 2020. Model-aided Deep Learning Method for Path Loss Prediction in Mobile Communication Systems at 2.6 GHz. IEEE Access, 8, pp.7925-7936.

[83] Ahmadien, O., Ates, H.F., Baykas, T. and Gunturk, B.K., 2020. Predicting Path Loss Distribution of an Area from Satellite Images using Deep Learning. IEEE Access, 8, pp.64982-64991.

[84] Thrane, J., Artuso, M., Zibar, D. and Christiansen, H.L., 2018, August. Drive Test Minimization using Deep Learning with Bayesian Approximation. In 2018 IEEE 88th Vehicular Technology Conference (VTC-Fall) (pp. 1-5). IEEE.

[85] Song, X., Li, W., Liu, C., Wang, K., Hou, Y., Bao, Z. and Yuan, Y., 2021, October. AI-Enabled Quality Prediction of 5G Wireless Network in Smart Grid. In 2021 13th International Conference on Wireless Communications and Signal Processing (WCSP) (pp. 1-6). IEEE.

[86] Belgiovine, M., Sankhe, K., Bocanegra, C., Roy, D. and Chowdhury, K.R., 2021. Deep Learning at the Edge for Channel Estimation in Beyond-5G Massive MIMO. IEEE Wireless Communications, 28(2), pp.19-25.

[87] Dong, P., Zhang, H., Li, G.Y., Gaspar, I.S. and NaderiAlizadeh, N., 2019. Deep CNN-based Channel Estimation for mmWave Massive MIMO Systems. IEEE Journal of Selected Topics in Signal Processing, 13(5), pp.989-1000.

[88] Bai, L., Wang, C.X., Xu, Q., Ventouras, S. and Goussetis, G., 2019. Prediction of Channel Excess Attenuation for Satellite Communication Systems at Q-Band Using Artif i cial Neural Network. IEEE Antennas and Wireless Propagation Letters, 18(11), pp.2235-2239.

[89] Mahboob, S. and Liu, L., 2024. Revolutionizing Future Connectivity: A Contemporary Survey on AI-Empowered Satellite-based Non-Terrestrial Networks in 6G. IEEE Communications Surveys & Tutorials.

[90] 6G-NTN Deliverable 3.2, “Terminals”, v1.0.

[91] 6G-NTN Deliverable 3.3, “Software Defined Payload and its Scalability”, v1.0.

[92] 6G-NTN Deliverable 3.4, “vLEO Space Segment”, v1.0.

[93] 3GPP TR 38.811 V15.4.0, “Study on New Radio (NR) to Support Non-Terrestrial Networks,” Release 15, Sept. 2020.

[94] 6G-NTN Deliverable 2.5, “Policies and Regulatory”

[95] “Service requirements for the 5G system,” 3GPP Technical Specification TS22.261, stage 1 (Rel. 19), v19.3.0, June 2023.

[96] The FREE AIS vessel tracking platform (https://www.vesselfinder.com/).

[97] Speedtest by Ookla Global Fixed and Mobile Network Performance Maps was accessed from (https://registry.opendata.aws/speedtest-global-performance).

[98] Y. Yang, S. Geng, B. Zhang, J. Zhang, Z. Wang, Y. Zhang, and D. Doermann, “Long Term 5G Network Traffic Forecasting via Modeling Non-Stationarity with Deep Learning,” Communications Engineering, vol. 2, no. 1, p. 33, 2023.

[99] G. Barlacchi, M. D. Nadai, R. Larcher, A. Casella, C. Chitic, G. Torrisi, F. Antonelli, A. Vespignani, A. Pentland, and B. Lepri, “A Multi-Source Dataset of Urban Life in the City of Milan and the Province of Trentino,” Scientific Data, vol. 2, p. 150055, 10 2015.

[100] Wikipedia contributors, "Polynomial Regression," *Wikipedia, The Free Encyclopedia,* https://en.wikipedia.org/w/index.php?title=Polynomial_regression&oldid=1210627454 (accessed June 1, 2024).

[101] Wikipedia contributors, "Deep Learning," *Wikipedia, The Free Encyclopedia,* https://en.wikipedia.org/w/index.php?title=Deep_learning&oldid=1225866800 (accessed June

1, 2024).